

**Design and Analysis of Cooperative Spatial Multiplexing System in
Wireless Relay Networks**

by

Andreas Darmawan

A dissertation submitted to the graduate faculty
in partial fulfillment of the requirements for the degree of
DOCTOR OF PHILOSOPHY

Major: Electrical Engineering

Major Professor:
Hiroyuki Morikawa

The University of Tokyo

Tokyo, Japan

2007

Copyright © Andreas Darmawan, 2007. All rights reserved.

School of Engineering
The University of Tokyo

This is to certify that the doctoral dissertation of
Andreas Darmawan
has met the dissertation requirements of The University of Tokyo

Major Professor

“To my mother, who is always watching, guiding, and loving me even from a place far beyond this life. Her memories live forever in our hearts.”

TABLE OF CONTENTS

LIST OF TABLES	viii
LIST OF FIGURES	ix
LIST OF ACRONYMS	xii
ABSTRACT	xiv
CHAPTER 1. INTRODUCTION	1
1.1 Problem Statement	1
1.2 Motivation	2
1.3 Dissertation Organization	4
CHAPTER 2. BACKGROUND THEORY	5
2.1 Cooperative Communications	5
2.2 Multiplexing and Multiple Access	6
2.3 Spatial Multiplexing	7
2.3.1 V-BLAST	8
2.4 Fading in Mobile Radio Propagation	12
CHAPTER 3. COOPERATIVE WIRELESS MIMO COMMUNICATIONS:	
UPLINK TRANSMISSION	14
3.1 Amplify-and-Forward System	15
3.1.1 System Model and Assumptions: Source-Relay Link	16
3.1.2 System Model and Assumptions: Relay-Destination Link	18
3.2 Decode-and-Forward System	19
3.2.1 System Model and Assumptions: Source-Relay Link	21

3.2.2	System Model and Assumptions: Relay-Destination Link	21
3.3	Numerical Results and Discussions	23
3.4	Conclusions	25
CHAPTER 4. COOPERATIVE WIRELESS MIMO COMMUNICATIONS:		
	DOWNLINK TRANSMISSION	28
4.1	Amplify-and-Forward System	29
4.1.1	Classical Relay Case	30
4.1.2	Space-Time Coding Relay	31
4.1.3	Practical Issues	33
4.2	Decode-and-Forward System	34
4.2.1	Classical Relay Case	34
4.2.2	Space-time Coding Relay	35
4.2.3	Practical Issue	36
4.3	Numerical Results and Discussions	38
4.4	Conclusions	45
CHAPTER 5. THEORETICAL PERFORMANCE ANALYSIS OF UPLINK		
	AND DOWNLINK COOPERATIVE SPATIAL MULTIPLEXING SYS-	
	TEMS	46
5.1	Outage Probability Analysis	47
5.1.1	Uplink Amplify-and-Forward	47
5.1.2	Uplink Decode-and-Forward	52
5.1.3	Downlink Amplify-and-Forward	54
5.1.4	Downlink Decode-and-Forward	55
5.2	Theoretical Bit-error Rate Analysis	57
5.2.1	Uplink Amplify-and-Forward	58
5.2.2	Uplink Decode-and-Forward	59
5.2.3	Downlink Amplify-and-Forward	60
5.2.4	Downlink Decode-and-Forward	61

5.3	Numerical Results and Discussions	62
5.4	Conclusions	66
CHAPTER 6. THEORETICAL CAPACITY OF COOPERATIVE SPA-		
TIAL MULTIPLEXING SYSTEM		70
6.1	Uplink Amplify-and-Forward	71
6.2	Uplink Decode-and-Forward	72
6.3	Downlink Amplify-and-Forward	73
6.4	Downlink Decode-and-Forward	73
6.5	Numerical Results and Discussions	75
6.6	Conclusions	77
CHAPTER 7. OPTIMAL POWER ALLOCATION SCHEME FOR COOP-		
ERATIVE SPATIAL MULTIPLEXING SYSTEMS		80
7.1	Uplink Amplify-and-Forward	81
7.2	Uplink Decode-and-Forward	83
7.3	Downlink Amplify-and-Forward	84
7.4	Downlink Decode-and-Forward	86
7.5	Numerical Results and Discussions	87
7.6	Conclusions	92
CHAPTER 8. CONCLUDING REMARKS		99
8.1	General Conclusion	99
8.2	Real-world Implementation	100
8.3	Future Works	102
APPENDIX A. ADDITIONAL MATERIALS		103
A.1	Derivation of Decoding Scheme for Practical Space-time Coded Downlink Amplify- and-Forward Cooperative Spatial Multiplexing	103
A.2	Theoretical BER Analysis of Uplink Amplify-and-Forward Cooperative Spatial Multiplexing	104
A.3	Derivation of CDF of the Harmonic Mean of Two Exponential RVs	106

BIBLIOGRAPHY	108
ACKNOWLEDGEMENTS	112

LIST OF TABLES

Table 4.1	Space-time coding transmission sequence	32
Table 4.2	Practical space-time coding transmission sequence	34
Table 4.3	Transmission sequence in practical space-time DF system	37

LIST OF FIGURES

Figure 2.1	Simple cooperative diversity scheme	6
Figure 2.2	V-BLAST system diagram	8
Figure 3.1	Cooperative spatial multiplexing system	15
Figure 3.2	Cooperative spatial multiplexing system: Amplify-and-Forward scheme.	16
Figure 3.3	Cooperative spatial multiplexing system: Decode-and-Forward scheme.	20
Figure 3.4	Cooperative spatial multiplexing system: relay diagram	20
Figure 3.5	BER comparison of AF-CSM system and other systems.	24
Figure 3.6	Power allocation trend of AF-CSM, source-relay distance = 0.5.	25
Figure 3.7	BER of AF-CSM with different relay distances & power allocation scheme.	26
Figure 3.8	Recommended power allocation for AF-CSM, SNR=40 dB.	27
Figure 4.1	Downlink 2x2 AF and DF Cooperative Spatial Multiplexing systems. .	29
Figure 4.2	BER performance of downlink AF & DF CSM systems for different relay locations, $E_b/N_0 = 10$ dB.	39
Figure 4.3	BER performance of downlink AF-CSM with two and four relays. . . .	40
Figure 4.4	BER performance of downlink AF-CSM systems.	41
Figure 4.5	BER performance of downlink DF-CSM systems.	42
Figure 4.6	BER performance of ideal downlink AF-CSM and DF-CSM systems. .	43
Figure 4.7	BER performance of practical downlink AF-CSM and DF-CSM systems.	44
Figure 5.1	Comparison of exact (3.15) and approximate (5.10) relay amplifying factors.	49
Figure 5.2	Comparison of exact (5.11) and approximate (5.12) SNR.	50

Figure 5.3	Geometrical representation of received vector signal & its rotation for $M = N = 2$ CSM.	51
Figure 5.4	Theoretical Outage Probability of Uplink AF and DF-CSM.	63
Figure 5.5	Theoretical BER of Uplink AF-CSM.	64
Figure 5.6	Theoretical BER of Uplink DF-CSM.	65
Figure 5.7	Theoretical Outage Probability of Downlink AF and DF-CSM.	66
Figure 5.8	Theoretical BER of Downlink AF and DF-CSM.	67
Figure 5.9	Relay location vs. BER performance, SNR = 10dB.	68
Figure 5.10	Theoretical BER of Downlink AF and DF-CSM, various SNR & source-relay distances.	69
Figure 6.1	Outage capacity of uplink CSM systems, $c_{th} = 2$ bits/s/Hz.	76
Figure 6.2	Outage capacity of uplink CSM systems, $E_b/N_0 = 10$ dB.	77
Figure 6.3	Outage capacity of downlink CSM systems, $c_{th} = 2$ bits/s/Hz.	78
Figure 6.4	Outage capacity of downlink CSM systems, $E_b/N_0 = 10$ dB.	79
Figure 7.1	BER performance of AF uplink systems with uniform and optimal power allocation schemes.	88
Figure 7.2	BER performance of AF uplink systems with uniform and optimal power allocation schemes.	89
Figure 7.3	BER performance of DF uplink systems with uniform and optimal power allocation schemes.	90
Figure 7.4	BER performance of AF & DF downlink systems with uniform and optimal power allocation schemes.	91
Figure 7.5	Optimal power allocation scheme for CSM systems.	93
Figure 7.6	Relay location vs. BER performance, SNR = 0dB.	94
Figure 7.7	Relay location vs. BER performance, SNR = 10dB.	95
Figure 7.8	Relay location vs. BER performance.	96

Figure 7.9	Outage capacity performance of uplink CSM with optimal power allocation.	97
Figure 7.10	Outage capacity performance of downlink CSM with optimal power allocation.	98

LIST OF ACRONYMS

AF	Amplify-and-Forward
BER	Bit Error Rate
AWGN	Additive White Gaussian Noise
BPSK	Binary Phase Shift Keying
BS	Base Station
CCDF	Complementary Cumulative Distribution Function
CDF	Cumulative Distribution Function
CDMA	Code Division Multiple Access
CSI	Channel State Information
CSM	Cooperative Spatial Multiplexing
dB	Decibel
DF	Decode-and-Forward
DL	Downlink
DSP	Digital Signal Processing
EIRP	Effective Isotropic Radiated Power
FDMA	Frequency Division Multiple Access
ICI	Inter-channel Interference
LLR	Log-Likelihood Ratio
MC	Monte-Carlo
MISO	Multiple-Input-Single-Output
MIMO	Multiple-Input-Multiple-Output
SISO	Single-Input-Single-Output

SIMO	Single-Input-Multiple-Output
SNR	Signal-to-Noise Ratio
TDM	Time Division Multiplexing
PDMA	Polarization Division Multiple Access
PDF	Probability Density Function
QAM	Quadrature Amplitude Modulation
QPSK	Quadrature Phase Shift Keying
RF	Radio Frequency
RV	Random Variable
SDMA	Space Division Multiple Access
SIC	Successive Interference Cancellation
STC	Space-Time Coding
TDM	Time Division Multiplex
TDMA	Time Division Multiple Access
UL	Uplink
VLSI	Very Large System Integration
V-BLAST	Vertical Bell Laboratories Layered Space-Time

ABSTRACT

This dissertation presents and proposes a comprehensive concept of a particular type of cooperative communications called cooperative spatial multiplexing system. The main advantage of the system is that it allows for the realization of MIMO performance in single-antenna wireless terminals environment. This also means that the proposed systems will be superior to the currently existing SISO and MIMO schemes, especially in low-SNR conditions.

Transmission schemes for uplink/downlink amplify-and-forward and decode-and-forward relaying were investigated and proposed. In the amplify-and-forward scheme, non-regenerative relays are employed such that they only amplify and forward different portion of the received signal at a reduced data rate to the receiver (destination). While in decode-and-forward scheme, the regenerative relays actually decode the received signal before forwarding it to the destination sink. MIMO communication is established for relays to destination data transmission. For downlink transmission, the relays may opt to forward the data to the destination by utilizing simple TDM transmission or Alamouti's space-time coding. The combination of transmitter, relays, and receiver forms a virtual MIMO system in single-antenna wireless terminals environment. Symbol decoding at the destination sink is done by SNR (Signal-to-Noise Ratio) based detection ordering schemes, along with successive interference cancelation process.

Theoretical analysis on the performance of the different above-mentioned transmission schemes based on Gram-Schmidt orthogonalization process is also presented. The analysis focuses on the outage probability and average BER performance of the system under Rayleigh fading environment. Closed-form solutions for $1 \times 2 \times 2$ uplink and $2 \times 2 \times 1$ downlink systems employing coherent BPSK modulation are presented. The theoretical analysis results are then confirmed with Monte-Carlo simulations in order to prove their validity and accuracy. Our

analysis of Shannon capacity will give a deeper insight into the performance of the CSM system, as it shows the maximum error-free transmission rate possible. We further derived the optimal and semi-optimal transmit power allocation schemes for the different systems by applying Lagrange multiplier optimization to the outage probability expressions. This allows the system to allocate power optimally between the source and relaying terminals, such that the outage probability and BER will be minimized for the given link conditions. Hence, as a result, performance improvements over the classical uniform power distribution scheme are expected.

CHAPTER 1. INTRODUCTION

The continuous research towards the ultimate standard for global communications system was started the day Shannon published his infamous work, "A Mathematical Theory of Communication" [1], and it is still far from over. The more human exploits and understands the nature, the more advance technology evolves with a very rapid rate. The trend for the last two decades in communication system has been the re-utilization of limitedly available communication resources which is better known as the multiple access techniques. Some of the more popular multiple access techniques employed in the current communication systems include FDMA, TDMA, and CDMA.

1.1 Problem Statement

Future wireless communication environments are highly resource-constrained, offering a limited and tightly regulated spectrum. The energy supply on wireless terminals is usually very limited and must be properly conserved to gain the longest operational time possible. A promising approach to overcome such limitations is the use of multiple antennas both to transmit and receive information, also known as *multiple-input multiple-output* (MIMO) system, which can provide a diversity gain as well as a multiplexing gain at no extra bandwidth or power consumption [2]-[6]. Though attractive, this option requires co-located antenna elements with antenna spacing of tens of wavelengths at the base station and up to a wavelength at the terminal. In many practical scenarios, space limitations at the terminal site make antenna spacing critical; a physical constraint that significantly limits the applicability of antenna arrays.

Recently, a lot of research has been done on various spatial multiplexing schemes to exploit

multipath fading, realizing high data rates over the rich-scattering wireless channel. According to [10], if exploited properly using the appropriate processing technique, theoretically, a rich-multipath scattering is capable of approaching 90% of Shannon capacity. Along with all of the innovations, there are always issues arising during the actual realizations of the theories. In the case of spatial multiplexing it is more of a physical limitation issue because it requires M transmit antennas and N receive antennas, with $N \geq M$. In real world implementation, especially in mobile wireless communications, utilizing more than one antenna in a mobile unit is not practical for several reasons such as ergonomics and antenna separation issues.

To overcome these issues, we propose several new systems which allow the use of spatial multiplexing in a mobile wireless system by exploring the cooperative communications concept [7]. The word "cooperative" carries the meaning of user-cooperation, in which each user utilizes other wireless terminals as relays to forward information from the transmitting source to the receiving destination. Practically, other users in is scattered all around the area and the issue of which terminals should be selected as relays is an important one. As we will see later in the following chapters, due to the path loss effect, the locations of the relays affect the overall performance of the proposed system quite significantly.

Since power is not a cheap resource, it has to be limited and distributed efficiently among the source and relays. One of the goals of this work, other than to prove that spatial multiplexing cooperative diversity is realizable, is to find the optimum power allocation which minimizes the overall bit-error-rate (BER) performance of the systems with the relays located at different distances from the source. For this purpose, we simulated the proposed system with relays located at various locations under different power allocation schemes.

1.2 Motivation

Both Laneman's and Alamouti's schemes in [7] and [21], together with the ever-advancing Digital Signal Processing (DSP) processing power really opened up a whole new perspective in exploring different methods to achieve diversity gain; we could see the trend from the number of recently published papers on the topic. Something that was thought impossible to be realized

in the last decade, could be made possible with the help of the latest VLSI technology.

Building on these schemes, the idea of cooperative MIMO communications system was established. [11], [12], and [13] explore the algorithms and system capacity performance in which all the communicating terminals are equipped with multiple-antennas. [27], [28], [29], and [30] presented the basic foundation of a more practical cooperative MIMO system called the *cooperative spatial multiplexing (CSM)* for uplink transmission, where the source and relays employ only single-antenna transceivers. Here, a transmitting source forms *virtual antenna array* [3] from a collection of distributed antennas belonging to different wireless terminals and utilizes them as relays. The source then transmits identical signal to the relays. Each relay processes only intended portion of the received signal and forward it to the receiver (destination) simultaneously at a reduced data rate. The receiver, equipped with multiple antenna arrays (such as used in base stations), nulls and cancels the interference from several relays, and detects the original symbols transmitted from the source.

Aside from technical motivation, in the daily life, information has become an inseparable entity from human activities as can be seen from the increasing demand of high-speed internet, and it has changed the pace and lifestyle of human being. For the people on the move, this flow of information can not stop because they may miss a crucial moment if their job is related to real-time market update, for example. As for the trendy and fashion people, video conference and video-on-demand in their cellular phones will be a must in the near future, because the use of latest technology and trends could increase their social status among their friends. All of those conditions and features require the availability of very high bandwidth and data rate in the wireless system itself. Unfortunately, bandwidth is very expensive and the harsh environment of urban landscape, which induces all sorts of noise and interference, makes it very difficult to maintain and achieve the high data rate for future systems. Due to this reason, inventors are doing extensive research in maximizing the capacity and squeezing every extra bits/second they can gain from the available resources.

1.3 Dissertation Organization

Chapter 2 reviews several important theories, techniques, and previous works which help to the establishment of the different schemes discussed in the dissertation. In Chapter 3 and Chapter 4, we propose several new amplify-and-forward and decode-and-forward cooperative spatial multiplexing schemes, including the system models and underlying assumptions for both uplink and downlink transmissions, respectively. The performance of the proposed schemes are evaluated in MATLAB using different parameters such as different modulating schemes, detection ordering techniques, power constraints, number of transmit and receive antennas.

Having established the different system models, in Chapter 5, we present the theoretical analysis on the outage probability and bit-error-rate performance for each of the system discussed in Chapter 3 and 4. In order to prove the validity and accuracy of the underlying analysis, the main results are then compared with Monte-Carlo simulations using MATLAB software. The theoretical analysis will be carried further in Chapter 6 as we will also analyze the Shannon capacity performance for various CSM systems, and see where they stand in comparison with SISO and MIMO V-BLAST systems.

In Chapter 7, we proposed both optimal and semi-optimal transmit power allocation schemes for the different systems by applying Lagrange multiplier optimization to the outage probability expressions. This allows the system to allocate power optimally between the source and relaying terminals, such that the outage probability and BER will be minimized for the given link conditions. Thus as a result, performance improvement over the classical uniform power distribution scheme are expected.

In Chapter 8, we summarize our work and give some general observations on the proposed cooperative spatial multiplexing schemes, while also discuss the issues which may hinder the deployment of the system. In general, we conclude that our research objectives have been met. Some future work recommendations for further system improvements and development are also proposed and discussed.

CHAPTER 2. BACKGROUND THEORY

2.1 Cooperative Communications

A series of papers has suggested a new form of diversity obtained from virtual antenna arrays consisting of a collection of distributed antennas belonging to different wireless terminals [7]-[15], in order to overcome the physical constraint (multi-antenna placement) issue of the MIMO system. These types of communications are known as *cooperative communications*, in which the source broadcasts its data to both intermediate terminals (i.e. relays) and the destination. The key principle of cooperative communications is that transmitted signals can be received and processed by any node. Nodes can act as relays and help other nodes, either individually or in groups. Consequently, nodes can create additional paths for a source-destination pair to increase diversity against fading and interference, and allow spatial multiplexing between other nodes.

Earliest work on cooperative communications started with a simple relay transmission system which was introduced back in 1971 by van der Meulen in [16] and studied further by Sato [17]. Cover and Gammal then pioneered the first information theoretical analysis of the relay channel in [18]. In these early contributions, the transmission between the source and target terminals is assisted by a relaying terminal, creating a simple source-relay-destination configuration system. [18] derived the maximum achievable communication rate in various communication scenarios, including the cases with and without feedback to either the source or relaying terminals, or both. Furthermore, it shows that the capacity of a relayed transmission exceeds that of a direct link, which lays the foundation to further researches in the field.

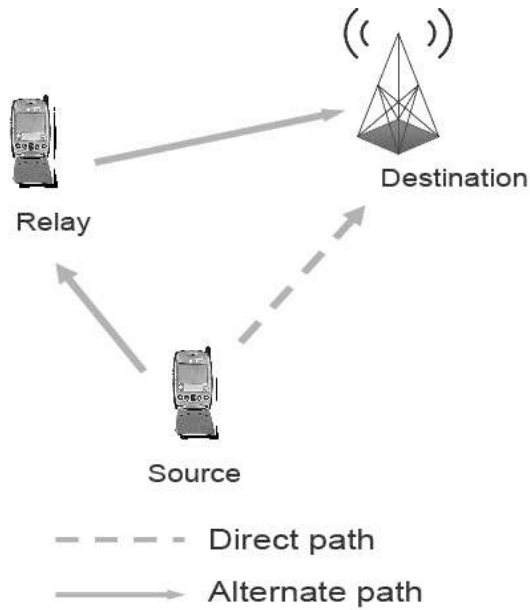


Figure 2.1 Simple cooperative diversity scheme

2.2 Multiplexing and Multiple Access

The sharing of a fixed communications resource is often referred to as "multiplexing" and "multiple access", and both terms carry a subtle difference. According to [20], in multiplexing, the user's requirements or plans for communications resource sharing are fixed, or slowly changing at the most. While in multiple access, normally a resource, e.g. satellite, is remotely shared.

Increasing the total data rate of a communications resource can be done in three basic methods :

- Increasing the transmitter's effective isotropic radiated power (EIRP) or reducing system losses (E_b/N_0 is increased)
- Increasing the available bandwidth
- Allocating the communications resource more efficiently

Due to the high cost of approach 1 and 2, people are opting to go with method 3, which is the domain of communications multiple access. The basic goal of multiple access techniques

is to distribute effectively the available resource between multiple users, sharing a common frequency spectrum, at a variety of bit rates and duty cycles. The commonly used multiple access techniques are:

- Frequency Division Multiple Access (FDMA) - Multiple users of the system are assigned narrow slices of the frequency spectrum. The total number of users equals the total number of frequency bands. The first generation analog system AMPS (Advanced Mobile Phone System) employs the FDMA technique.
- Time Division Multiple Access (TDMA) - Multiple users operate in M different time slices on N frequency bands, resulting in $M \times N$ total number of users in the system. The second generation interim standard (IS-54) employs TDMA into its system.
- Code Division Multiple Access (CDMA) - Each user is assigned a unique orthogonal code that separates the different users. The same frequency band is simultaneously used by the multiple users, which leads to high spectral efficiency. CDMA was employed in Qualcomm's IS-95, which was adopted as the digital cellular standard for the second generation system.
- Space Division Multiple Access (SDMA) - Radio signals are separated by spot beam antennas pointing in different directions. It allows for reuse of the same frequency band.
- Polarization Division Multiple Access (PDMA) - Orthogonal polarizations are used to separate signals, allowing for reuse of the same frequency band. [22]

2.3 Spatial Multiplexing

A standard method for achieving spatial diversity to combat fading without expanding the bandwidth of the transmitted signal is to use multiple antennas at the receiver and/or at the transmitter side.

These multiple antennas techniques can also be used to create multiple spatial channels and provide increase in data rate as a result. Generally speaking, with M transmit antennas

and N receive antennas, with $N \geq M$, an M -fold increase in the data rate could be achieved, while simultaneously providing N th-order reception diversity to combat fading for each of the M transmitted signals. Interchannel Interference (ICI) among the spatial channels will exist, since there is no orthogonal structure imposed on the signals at the M transmitting antennas [19].

Several types of spatial multiplexing systems take advantage of the sufficiently rich-multipath scattering wireless channel in order to realize high data rates over the channel by exploiting it using the appropriate processing. Examples of such system are the V-BLAST and our own proposed cooperative spatial multiplexing scheme.

2.3.1 V-BLAST

Vertical Bell Laboratories Layered Space-Time, or more commonly known as V-BLAST, is an example of a system for realizing very high data rates over rich-scattering wireless channel. The V-BLAST system, pictured in Figure 2.2, performs spatial multiplexing by sending many independent signals through multiple independent transmit antennas.

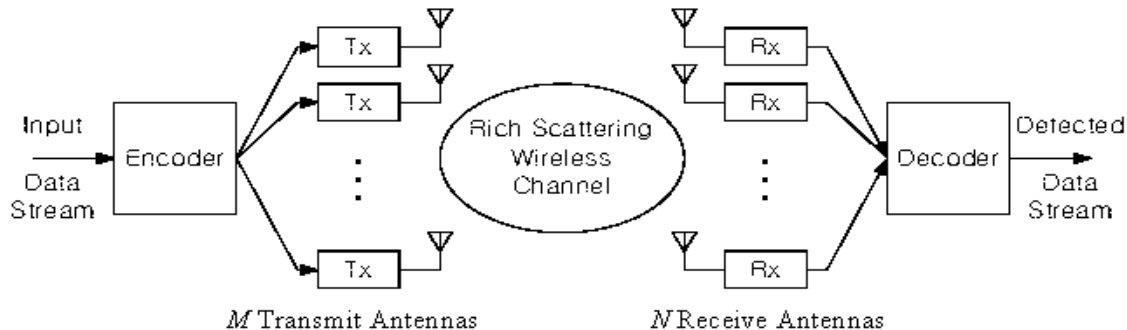


Figure 2.2 V-BLAST system diagram

More specifically, a single user's data stream is split into M multiple sub-streams, which will be encoded into independent symbols and then routed to its respective transmitter for simultaneous transmission in the same frequency band. The N receivers are individual, conventional receivers, which operate co-channel, each receiving the signals radiated from the M transmit antennas ($M \leq N$).

Combination of ordering, nulling and cancelling used in V-BLAST is a widely-used recursive decoding method in spatial multiplexing systems. The order in which the received sub-streams are detected and cancelled affects the overall performance of the system. Detection ordering for V-BLAST based on maximum signal-to-noise ratio (SNR) was introduced in [10], where the sub-stream with the maximum SNR is detected and its contribution from the received signal is cancelled. Following the symbol cancellation the corresponding channel matrix will be zeroed, and the same process is repeated for the remaining undetected symbols.

Another new effective ordering method called LLR-based Ordering, which gives significantly better BER performance compared to SNR method, is proposed in [25] where the sub-stream is detected and cancelled based on its maximum log-likelihood ratio (LLR). It was shown that by implementing LLR ordering, a 4x4 V-BLAST with LLR ordering will perform as good as an 8x8 SNR-ordering system. So generally speaking, the LLR-based ordering implementation reduces the system's complexity significantly, resulting in extra communications resource that may be allocated for other necessities.

2.3.1.1 V-BLAST Mathematical Model

Let the received signal at the receiving antenna be:

$$\mathbf{y} = \mathbf{H}\mathbf{x} + \mathbf{n} \quad (2.1)$$

where $\mathbf{x} = [x_1, x_2, \dots, x_M]^T$ is the transmitted signal, $\mathbf{y} = [y_1, y_2, \dots, y_N]^T$ is the received signal, and $\mathbf{n} = [n_1, n_2, \dots, n_N]^T$ is the i.i.d. complex Gaussian noise vector with zero mean and variance $N_0/2$ per-dimension. The channel matrix \mathbf{H} is an i.i.d. zero-mean and unit-variance elements, complex Gaussian $M \times N$ matrix given by:

$$\mathbf{H} = [\mathbf{h}_1, \mathbf{h}_2, \dots, \mathbf{h}_M] \quad (2.2)$$

$$= \begin{bmatrix} h_{11} & h_{12} & \cdots & h_{1M} \\ h_{21} & h_{22} & \cdots & h_{2M} \\ \vdots & \cdots & \ddots & \vdots \\ h_{N1} & h_{N2} & \cdots & h_{NM} \end{bmatrix} \quad (2.3)$$

Linear Combinatorial Nulling

Also known as adaptive antenna array (AAA), nulling is a technique in which each sub-stream is considered as the desired signal while the remainder are regarded as interferers. The nulling matrix is defined as:

$$\mathbf{W} = (\mathbf{H}^H \mathbf{H})^{-1} \mathbf{H}^H \quad (2.4)$$

$$= [\mathbf{w}_1, \mathbf{w}_2, \dots, \mathbf{w}_M]^T \quad (2.5)$$

where \mathbf{w}_i is a $1 \times N$ nulling vector.

Let the pre-detection received symbol be $\mathbf{y}^{(0)} = \mathbf{y}$, and pre-detection channel matrix be $\mathbf{H}^{(0)} = \mathbf{H}$, then the nulling will take place as:

$$\mathbf{W}\mathbf{y}^{(0)} = \underbrace{\mathbf{W}\mathbf{H}^{(0)}}_{=I} \mathbf{x} + \mathbf{W}\mathbf{n} \quad (2.6)$$

So, for the i^{th} transmit antenna:

$$y_i = \mathbf{w}_i \mathbf{y}^{(0)} = x_i + \mathbf{w}_i \mathbf{n} \quad (2.7)$$

As the result of the nulling, we obtained a symbol plus noise scalar quantity y_i , where $\mathbf{w}_i \mathbf{n}$ is a zero-mean and variance $\|\mathbf{w}_i\|^2 N_0/2$ per-dimension complex Gaussian random variable. In BPSK signaling, for a signal plus Gaussian noise model, the optimum detection will be the *maximum-likelihood* detection with threshold 0. Then we will get \hat{x}_i by hard decoding y_i with $Q(y_i) = +\sqrt{E_s}$ if $y \geq 0$ and $Q(y_i) = -\sqrt{E_s}$ if $y < 0$.

Symbol Cancellation

By assuming that $\hat{x}_i = x_i$, x_i is cancelled from received $\mathbf{y}^{(0)}$, then modified received vector $\mathbf{y}^{(1)}$ and modified channel matrix $\mathbf{H}^{(1)}$ are generated:

$$\mathbf{y}^{(1)} = \mathbf{y}^{(0)} - \hat{x}_i \mathbf{h}_i \quad (2.8)$$

And,

$$\mathbf{H}^{(1)} = [\mathbf{h}_1, \mathbf{h}_2, \dots, \mathbf{h}_M] \quad (2.9)$$

$$(2.10)$$

$\mathbf{H}^{(1)}$ contains the i^{th} transmit antenna elements that has been zeroed (cancelled). When symbol cancellation is employed, the order in which the components of \mathbf{x} are detected also determines the overall performance of the system.

SNR-based ordering

From [24], the signal-to-noise ratio (SNR) of x_i is given by:

$$SNR_i = \frac{|x_i|^2}{E[\|\mathbf{w}_i \mathbf{n}\|^2]} \quad (2.11)$$

$$= \frac{E_s}{\|\mathbf{w}_i\|^2 N_0} \quad (2.12)$$

In SNR-based ordering, the component of \mathbf{x} which minimizes the norm $\|\mathbf{w}_i\|^2$ is detected and cancelled first; minimizing $\|\mathbf{w}_i\|^2$ is equivalent to maximizing the SNR quotient in Eq. 2.12.

LLR-based ordering

The work in [25] proposed an LLR-based ordering for V-BLAST system and showed that the technique was indeed superior to ordering based on SNR. Assuming x_i is equally probable, the LLR is defined as:

$$\Lambda_i = \ln \frac{P(x_i = +\sqrt{E_s} | y_i)}{P(x_i = -\sqrt{E_s} | y_i)} \quad (2.13)$$

$$= \frac{4\sqrt{E_s} \operatorname{Re}\{y_i\}}{N_0 \|\mathbf{w}_i\|^2} \quad (2.14)$$

The sign of Λ_i gives the hard decision value, while the magnitude of Λ_i describes the reliability of the hard decision. According to [25], the ordering scheme is to detect first the component of \mathbf{x} that provides the largest $|\Lambda_i|$ given by

$$|\Lambda_i| = \frac{4\sqrt{E_s} |x_i + \operatorname{Re}\{\mathbf{w}_i \mathbf{n}\}|}{N_0 \|\mathbf{w}_i\|^2} \quad (2.15)$$

Exploiting the noise term $\mathbf{w}_i \mathbf{n}$ by selecting the component of \mathbf{x} with the signs of x_i and $\mathbf{w}_i \mathbf{n}$ being identical, gives a larger LLR magnitude or equivalently, higher reliability. The result of this algorithm is that the performance will be governed by the peak channel condition.

Proven the effectiveness in AWGN model and relatively low in implementation complexity, the nulling, cancelling, and SNR & LLR-based ordering will be the decoding method of choice in our proposed cooperative spatial multiplexing scheme signal detection process.

2.4 Fading in Mobile Radio Propagation

This thesis work takes into account the signal performance degradation factors, such as fading and noise, in the system model. When the effects of fading is manifested, the modeling and design of the system becomes much more complex than those whose only source of performance degradation is AWGN.

[20] clearly explains that in mobile communications system, fading is divided into two categories: large-scale and small-scale fading. Large-scale fading represents the average signal power attenuation or path loss due to motion over large areas, and is usually affected by the environment contours (hills, forests, buildings, etc) between the transmitter and receiver.

Small-scale fading is a phenomenon where there is a significant changes in signal amplitude and phase as a result of small changes in the spatial separation between the transmitter and receiver. It is realized in two different occurrence: time-spreading of the signal (signal dispersion) and time-variance of the channel. Since the received signal's envelope can be described by a Rayleigh pdf, if there is a large number of multiple reflective paths and no line-of-sight signal component present, small-scale fading is also known as Rayleigh fading.

In a mobile radio application, The free space path loss is defined as:

$$\bar{L}_s(d) = \left(\frac{4\pi d}{\lambda} \right)^2 \quad (2.16)$$

where λ is the wavelength of the propagating signal. Free space means that the region between the transmitter and receiver is free of radio frequency (RF) absorbing or reflecting objects.

The mean path loss of large-scale fading, $\bar{L}_p(d)$, is a function of distance d between the transmitter and receiver, and is defined by:

$$\bar{L}_p(d)(dB) = L_s(d_0) + 10n \log(d/d_0) \quad (2.17)$$

where d_0 is a point located in the far field of the antenna, and $L_s(d_0)$ is the free space path loss at the reference distance obtained through actual measurements or approximated by Eq. 2.16. Typical values for d_0 is 1 m for indoor channels, 100 m for microcells, and 1km for large cells. Most textbooks on electromagnetics, e.g. [23], explain the default calculate d_0 based on

the antenna properties, should a more accurate value for d_0 is required. Another issue to be considered from Eq. 2.16, we see that the free space path loss depends on the wavelength of the carrier frequency, λ , thus it is frequency-dependent. So, the higher the carrier frequency, the higher the path loss will be.

Analyzing 2.17 further and defining $\bar{L}_p(d)$ as the ratio of power transmitted to power received, we derive:

$$\frac{E_r}{N_0} = \frac{E_t}{N_0} \frac{1}{L_s(d_0)} \left(\frac{d}{d_0} \right)^{-m} \quad (2.18)$$

with E_r/N_0 and E_t/N_0 being the received SNR and transmitted SNR, respectively. The value of exponent m will depend on the frequency, antenna heights, and propagation environment. The range for m is typically between $2 \leq m \leq 4$, with 2 being the value of m in free space and 4 in a harsh environment [7],[20]. The harsher the environment condition gets, the bigger the m value needs to be employed for a more accurate representation of the path loss model.

CHAPTER 3. COOPERATIVE WIRELESS MIMO COMMUNICATIONS: UPLINK TRANSMISSION

In a conventional single-input single-output (SISO) wireless transmission system, information is being sent directly from a source to the destination, and is affected by path loss and fading in the channel between. The model of a direct transmission system for each time slot k is given by:

$$y = h_{s,d}x + n \quad (3.1)$$

where y is the received signal at the destination, $h_{s,d}$ is the channel gain between the source and destination, x is the transmitted signal, and n is the noise induced at the receiver.

This method of transmission suffers greatly from large and small-scale fading causing the decrease detection reliability as the source-destination distance becomes farther apart. The farther the signal has to propagate, the more energy needs to be allocated in every symbol transmitted in order to overcome the channel degradation. Thus, it is only good for short distance wireless communications, especially when power availability is very limited.

A step-up from the direct transmission system would be the conventional spatial multiplexing system, e.g. V-BLAST. In V-BLAST, the rich-multipath scattering wireless channel is exploited by sending independent data sub-streams over the multipath. Unfortunately, this technique requires both the source and the destination to employ multiple transmit and receive antennas at their terminals, respectively. So for future mobile communications applications, the multiple antennas requirement at the source becomes a physical limitation to the applicability of the system. In this chapter, we address this issue in our proposed scheme by only employing one transmit antenna at the source (mobile unit), while still being able to perform spatial multiplexing.

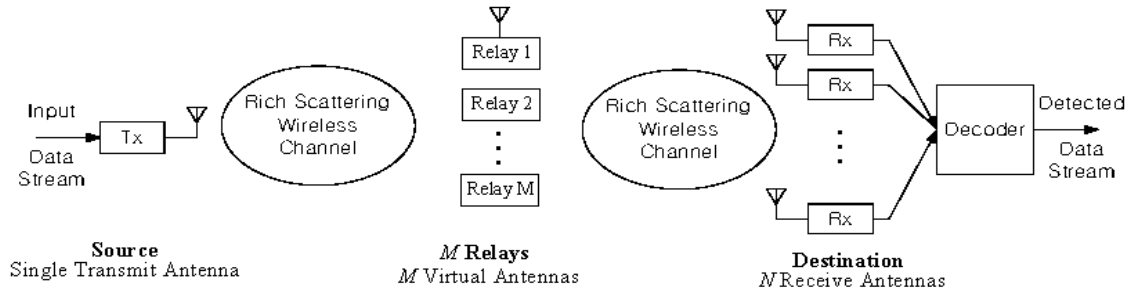


Figure 3.1 Cooperative spatial multiplexing system

Since the proposed scheme does not require multiple antennas at the source, in a practical application, it could be implemented as the uplink of a mobile communications system, where data is being transmitted from a mobile user 1 to the base station. Unlike the current conventional cellular system, our scheme allows mobile user 1 to broadcast its data stream to other mobile users within the same broadcast cell. Some chosen neighboring mobiles will serve as the relays to decode the received data symbol from user 1 and transmit its estimation to the base station with the power allocated at each relay P_r .

3.1 Amplify-and-Forward System

In this section we introduce the *amplify-and-forward* (AF) cooperative spatial multiplexing (CSM) scheme (Fig. 3.2) in which the transmitter (source), equipped with a single antenna, forms *virtual antenna array* [3] from a collection of distributed antennas belonging to different single-antenna wireless terminals and utilizes them as analog non-regenerative relays [30]. The source then transmits identical signal to the relays, utilizing them as non-regenerative relays. Each relay amplifies and forwards only a selected portion of the received signal with gain factor β to the receiver (destination) at a reduced data rate, in order to exploit the MIMO capacity. A very important assumption is that the relays are perfectly synchronized, such that they cut and retransmit simultaneously only the intended portion of the received signal. The receiver, equipped with multiple antenna arrays, nulls and cancels the interference from several relays, and detects the original symbols transmitted from the source. This combination of transmitter, relays, and receiver forges a virtual MIMO system and realizes its performance

in single-antenna wireless terminals environment.

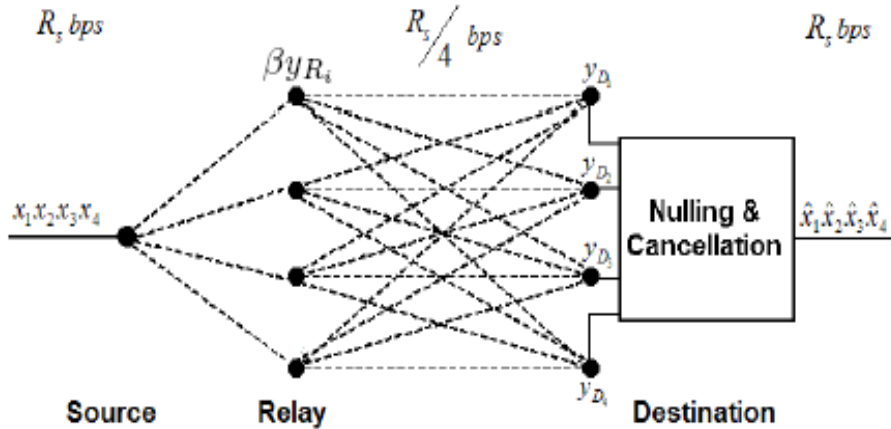


Figure 3.2 Cooperative spatial multiplexing system: Amplify-and-Forward scheme.

In the time slot t , the source, equipped with one antenna, transmits data $x_1 x_2 \dots x_N$ to N relays R_1, R_2, \dots, R_N with a transmission power P_s at a rate of R_s bits/sec (bps).

3.1.1 System Model and Assumptions: Source-Relay Link

In baseband transmission model, the received signal plus noise, y_{R_i} , at relay R_i (also equipped with single antenna) is given by

$$y_{R_i} = h_{R_i,S} x_i + n_{R_i} \quad (3.2)$$

where $h_{R_i,S}$ is the channel gain between the source and relay R_i , $x_i \in \{+\sqrt{E_s}, -\sqrt{E_s}\}$ is the transmitted symbol from the source, and n_{R_i} is the complex Gaussian noise with mean zero and variance $N_0/2$ per-dimension. We assume that $h_{R_i,S}$ is rich-scattering complex Gaussian-distributed with mean zero and variance $E[|h_{R_i,S}|^2] = G d_{R_i,S}^{-m}$, where $d_{R_i,S}$ is the distance between the source and relay R_i , and m is the path loss exponent, typically $2 \leq m \leq 4$ [26]. The constant G captures the effects of antenna gain and carrier frequency and is given by $\left(\frac{4\pi d_0}{\lambda}\right)^{-m}$, with λ being the wavelength of the propagating signal, and d_0 is the reference distance (a point in the far field of the antenna) [26].

During the next phase, N number of relays are selected for the data symbol amplification and forwarding. These are the relays, within the same cell which satisfy $d_{R_i,S}$ and d_{D_j,R_i} to be less than $d_{D_j,S}$, the distance between source and destination, with the one-dimensional geometrical assumption:

$$d_{D_j,S} = d_{R_i,S} + d_{D_j,R_i} \quad (3.3)$$

where $d_{R_i,S}$ and d_{D_j,R_i} are the source-relay and relay-destination distances, respectively. This means all relays are assumed to be at equal distances from the source, and relay R_i ($1 \leq i \leq N$) only transmits the $(tN + i)^{th}$ bit from the corresponding received x_i , in each time slot $t \geq 0$. Each relay R_i then amplifies the received signal y_{R_i} with an amplification factor β to satisfy the relay transmit power of P_r , before forwarding it to the destination. During the forwarding stage, the data rate is reduced to R_s/N bits/sec in order to exploit the capacity of MIMO transmission. Furthermore, we assume that all the relays are perfectly synchronized and transmit the corresponding amplified signal *simultaneously* to the destination. The algorithm on how to select the N relays is beyond the scope of this paper and shall be exploited further in other works.

Then R_i amplifies only selected portion of the received signal plus noise βy_{R_i} , and simultaneously forwards it to the destination with a transmission power P_r , in the time slot $t + 1$ at a rate of R_s/N bits/sec. Therefore, the energy per bit at the source E_s is P_s/R_s and that at the relay E_r is NP_r/R_s . Fig. 3.2 shows a special case of $N = 4$, where the dark circle and dotted lines represent the antenna and wireless links, respectively. Imposing this orthogonal transmit diversity bound [14], the data rate in CSM must be twice of the SISO in order to achieve the same spectral efficiency.

The total transmission power in the system $P_s + NP_r$ is held at a fixed value P , such that

$$P = P_s + NP_r \quad (3.4)$$

Increasing P_s will increase the reliability of source-relay link, and conversely, less power allocation at the relays, causing the detection at the destination less reliable. On the other hand, decreasing P_s will allow more power to be allocated at the relays at the expense of the

source-relay link quality. Thus, we expect that there exists an optimal pair of P_s and P_r that minimizes the probability of error at the final destination, which also depends on the location of the relays.

3.1.2 System Model and Assumptions: Relay-Destination Link

The receiver (or destination), equipped with $M(\geq N)$ antennas, detects data $x_1x_2\dots x_N$ coherently using the V-BLAST successive interference cancelation algorithm: nulling, cancelation, and ordering. This proposed scheme differs from the V-BLAST scheme in [5] in terms that there exists a collection of antenna array, i.e. the relays, such that the wireless link between the source and the relays experiences fading, noise, and interference.

The received signal y_{D_j} at the j^{th} receive antenna at the destination is given by

$$y_{D_j} = \sum_{i=1}^N g_{D_j,R_i} \beta_i y_{R_i} + n_{D_j} \quad j = 1, 2, \dots, M \quad (3.5)$$

where g_{D_j,R_i} is the channel gain between the relay R_i and destination D_j , $\beta_i y_{R_i}$ is the β -amplified received signal plus noise at relay R_i of x_i , and n_{D_j} is the complex Gaussian noise with mean zero and variance $N_0/2$ per-dimension. We assume that g_{D_j,R_i} is complex Gaussian distributed with mean zero and variance $E[|g_{D_j,R_i}|^2] = Gd_{D_j,R_i}^{-m}$. Here, d_{D_j,R_i} is the distance between relay R_i and destination D , and $M(\geq N)$ is the number of receive antennas at the destination.

Then, the received vector at the destination $\mathbf{y}_D = [y_{D_1}, y_{D_2}, \dots, y_{D_M}]^T$ can be expressed by

$$\mathbf{y}_D = \mathbf{G}\mathbf{x} + \mathbf{N}_D \quad (3.6)$$

where

$$G_{j,i} = \beta_i g_{D_j,R_i} h_{R_i,S} \quad (3.7)$$

$$N_{D_j} = \beta_i g_{D_j,R_i} n_{R_i} + n_{D_j} \quad (3.8)$$

$$\mathbf{x} = [x_1, x_2, \dots, x_N]^T \quad (3.9)$$

$$\hat{\mathbf{x}} = [\hat{x}_1, \hat{x}_2, \dots, \hat{x}_M]^T \quad (3.10)$$

and

$$\mathbf{N}_D = [N_{D_1}, N_{D_2}, \dots, N_{D_M}]^T \quad (3.11)$$

$$i = 1, 2, \dots, N \quad (3.12)$$

$$j = 1, 2, \dots, M \quad (3.13)$$

Defining the relay transmit power in each relay i as P_r :

$$\begin{aligned} P_r &= \overline{\beta_i^2 y_{R_i}^2} \\ &= \beta_i^2 \left[\overline{|h_{R_i,S}|^2} P_s + N_0 \right] \end{aligned} \quad (3.14)$$

we then obtain the amplification factor β_i as:

$$\beta_i = \sqrt{\frac{P_r}{\left[\overline{|h_{R_i,S}|^2} P_s + N_0 \right]}} \quad (3.15)$$

Note that the relay amplifying gain β varies according to the channel fading coefficient $h_{R_i,S}$ and that noise from the source-relay link will also be amplified by β . When the source-relay link condition suffers from severe interferences, this condition will propagate to the destination and affects the final symbol decoding result.

After the destination receives from the relays the β -amplified, channel-attenuated, noise-corrupted multipath signals (\mathbf{y}_D) at the antennas, successive interference cancelation process (defined in Chapter 2) follows.

The V-BLAST and SISO systems has an advantage over the CSM scheme due to the fact that it has only one wireless link (source-destination), while CSM has two (source-relays and relays-destination). This implies that the transmitted signal in CSM system experiences degradation, i.e. fading, noise, and other interferences, twice.

3.2 Decode-and-Forward System

This section discusses in brief the decode-and-forward cooperative spatial multiplexing scheme [28]. Here, a group of relays, formed by a collection of distributed antennas of other wireless terminals' located between the source and destination, serves as a mean to

estimate/decode the signal received from the source and forward the estimated data to the destination with relay transmit power P_r , as depicted in Figure. 3.3 and Figure. 3.4. The relays cooperate with the source in the data transmission process and become *virtual* antennas of the source to accommodate the data spatial multiplexing. The existence of these relays resulted in two wireless links between the source and destination, namely the *Source-Relay* and *Relay-Destination* links. We call this scheme *Decode-and-Transmit* to reflect the actual purpose of the relays in the data transmission. Another advantage of this scheme is that the signal does not have to propagate as far as it has to in a direct transmission system, thus minimizing the path loss fading effect.

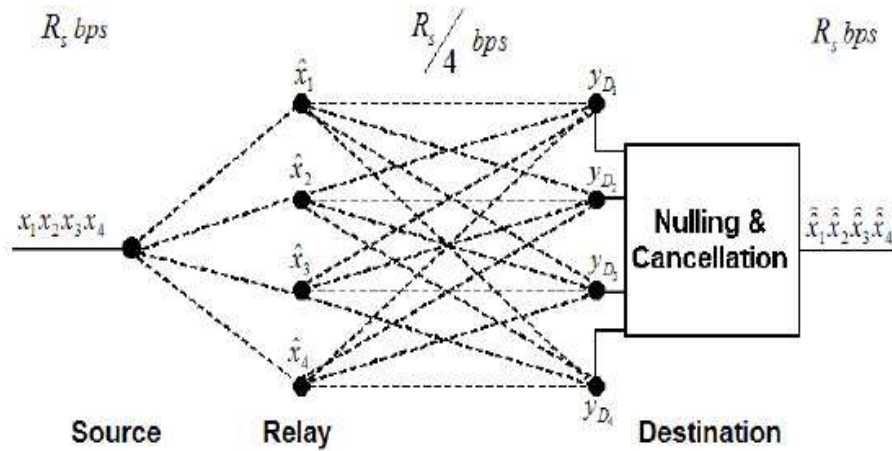


Figure 3.3 Cooperative spatial multiplexing system: Decode-and-Forward scheme.

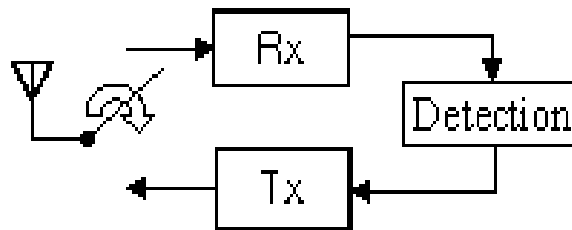


Figure 3.4 Cooperative spatial multiplexing system: relay diagram

3.2.1 System Model and Assumptions: Source-Relay Link

This particular link is connecting the single antenna source to the relays through a wireless binary symmetric channel (BSC) suffering the effects of path loss and fading. At each time slot k , the source is transmitting $x_1x_2\dots x_M\dots$ at a rate of R_s bits/sec to the M selected relays. Each potential relay receives

$$y_{R_i} = h_{R_i,S}x_i + n_{R_i} \quad (3.16)$$

where y_{R_i} is the received signal at relay R_i ($1 \leq i \leq M$), $h_{R_i,S}$ is the channel gain between the source and the relay R_i , x_i is the transmitted signal of source's taking values $+\sqrt{E_s}$ or $-\sqrt{E_s}$ with equal probability, and n_{R_i} , representing the noise and interference at relay R_i , is a complex Gaussian random variable with mean zero and variance $N_0/2$ per-dimension. The main purpose of existence of each relay R_i is to make a hard data decision based on y_{R_i} , yielding \hat{x}_{R_i} to be transmitted in the second phase of the cooperative spatial multiplexing scheme.

We assume that $\overline{|h_{R_i,S}|^2} = G \left(\frac{d_{S,R_i}}{d_0} \right)^{-m}$, where d_{s,R_i} is the distance between source and relay R_i , d_0 is the reference distance, free space path loss G (Eq. 2.16) at d_0 captures the effects of antenna gain and carrier wavelength, and m is the path loss exponent with typical values of $2 \leq m \leq 4$ [20]. Statistically, we model $h_{R_i,s}$ as independent, zero-mean complex Gaussian random variables with variances $G \left(\frac{d_{S,R_i}}{d_0} \right)^{-m}$, so that $|h_{R_i,S}|$ are Rayleigh distributed and the phases $\angle h_{R_i,S}$ are uniformly distributed on $[0, 2\pi)$.

Furthermore, the whole system is assumed to operate in real time, which means that the effect of time delay is neglected. All channels and links in the system are as well assumed to be independent of one another.

3.2.2 System Model and Assumptions: Relay-Destination Link

For the second phase of the transmission, M relays are selected from L available relays for the data forwarding. Each relay R_i estimates and transmits, with a data rate of R_s/M bits/sec and power P_r , the $(kM + i)^{th}$ symbols received from the source in each time slot $k \geq 0$.

The destination with N independent receive antennas ($N \geq M$) will then receive

$$y_{D_j} = \sum_{i=1}^M h_{D_j, R_i} \hat{x}_{R_i} + z_{D_j} \quad 1 \leq i \leq M, \quad 1 \leq j \leq N \quad (3.17)$$

where y_{D_j} is the received signal at destination D_j , h_{D_j, R_i} is the channel gain between the relay and the destination D_j , \hat{x}_{R_i} is the relay-estimated signals transmitted at $+\sqrt{E_r}$ or $-\sqrt{E_r}$ with equal probability. Finally, z_{D_j} , representing the noise and interference at destination D_j , is a mutually independent complex Gaussian random variable with mean zero and variance $N_0/2$ per-dimension. In this relay-destination link, h_{D_j, R_i} is modelled as independent zero-mean complex Gaussian random variables with variances $G \left(\frac{d_{R_i, D_j}}{d_0} \right)^{-m}$ with G being the free space path loss at d_0 , such that $|h_{D_j, R_i}|$ are Rayleigh distributed and the phases $\angle h_{D_j, R_i}$ are uniformly distributed on $[0, 2\pi)$.

Similar to the V-BLAST system, the received signal at the destination is sorted based on SNR and LLR-based ordering, followed by the nulling and cancellation process. In the case of the LLR-based ordering, since we want to base the signal detection on the original signal x_{R_i} , instead of the relay-estimated \hat{x}_i , we set up the LLR for the nulling's zero forcing output z_i to take into account the reliability factor of relay R_i which is defined by the first quotient in Eq. 3.18. Then the LLR of z_i for the original transmitted signal x_i will be given by

$$\Lambda(z_i) = \frac{e^{|\Lambda(y_{R_i})|} - 1}{e^{|\Lambda(y_{R_i})|} + 1} \frac{4\sqrt{E_r} \operatorname{Re}\{z_i\}}{N_0 \|\mathbf{w}_i\|^2} \quad (3.18)$$

where

$$\Lambda(y_{R_i}) = \frac{4\sqrt{E_s}}{N_0} \operatorname{Re}\{h_{R_i, s}^* y_{R_i}\} \quad (3.19)$$

is the LLR of relay R_i .

We assume that the total transmit power of the system, $P_s + MP_r$, is held at a fixed value P such that

$$P = P_s + MP_r \quad (3.20)$$

where P is the total power of the system, P_s is the source transmit power, P_r is the transmit power of each relay, and M is the number of relays. When more power is allocated on the

source, the reliability of the relay estimation increases. But on the other hand, less power is being allocated on the relays, decreasing the detection reliability at the destination. Based on this reason, it is important to find an optimal pair of P_s and P_r such that the detections at the relays and destination are reliable enough to keep the overall system BER at minimum.

3.3 Numerical Results and Discussions

In this section we present simulation results of AF-CSM system utilizing two relays and two antennas at the destination ($M = N = 2$). Modulation of choice is BPSK signaling with backward coherent detections both at the relays and destination, i.e. a terminal knows perfectly the channel state information of the link preceding it. Random data is generated to form the transmitted signal in the Monte Carlo simulation over a population of scenarios. We assume that the channel is flat-fading time-invariant during the transmission of one symbol period. In all graphs, SNR is parameterized by E_b/N_0 , which is the total transmit energy per-bit per-noise spectral density, given by $(E_s + E_r)/N_0$. E_s and E_r are chosen to minimize the BER subject to $(E_s + E_r) = E_b$ or equivalently $P_s + NP_r = P$.

Fig. 3.5 shows the BER performance of AF-CSM with the SNR-based ordering. Here, with the power constraint imposed, $P_s = P_r = P/(N + 1)$, and normalized source-relay distance of 0.5 (graph legend "AF-CSM"), the AF-CSM performance is inferior to the other systems. Keeping the same parameters and applying the suitable power allocation scheme, the performance gap is much reduced, surpassing the SISO system.

The power allocation trend to achieve the lowest BER for relays located at normalized distance 0.5 from the source for the AF-CSM is shown in Fig. 3.6. Here we observe that despite the available transmit SNR, most of the power is always allocated to the source (P_s), indicating that the source-relay broadcast link is the weaker link in AF-CSM. The application of source-channel coding (e.g. turbo coding, error-correction, etc) here might improve robustness against noise and interference for a better overall performance of the system.

Fig. 3.7 shows the BER performance of AF-CSM with various normalized source-relays distances with transmit power allocated optimally to achieve the lowest BER possible. We

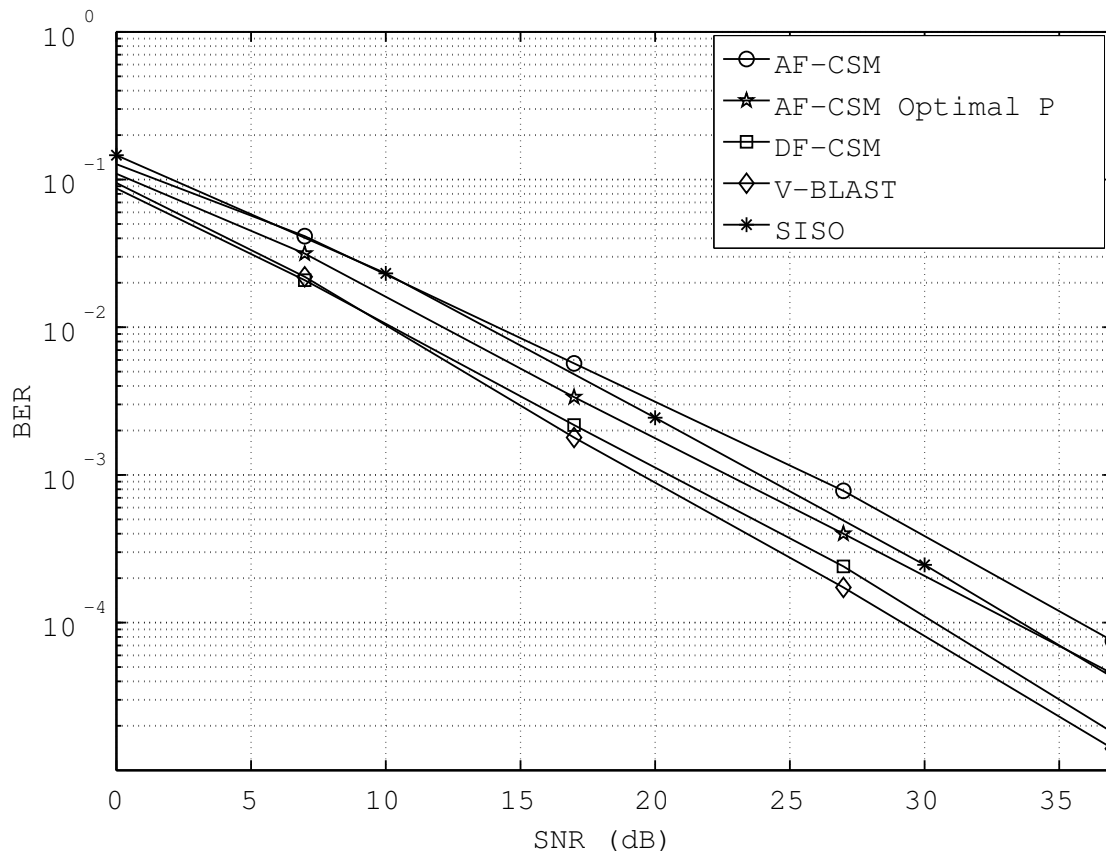


Figure 3.5 BER comparison of AF-CSM system and other systems.

observe that as the source-relays distance gets smaller, the performance of the system increases, surpassing that of V-BLAST's. This confers with our discussion above that the source-relay link is the weakest in the system. Hence, it is much recommended to select relays which are in close proximity to the source in order to increase the source-relay link quality.

Fig. 3.8 depicts the optimal normalized P_s and P_r versus the source-relay distance $d_{R_i,S}$, subject to $P_s + NP_r = P$. Based on the result, we conclude that for optimal power allocation, P_s or P_r should be increased or decreased, respectively, as the $d_{R_i,S}$ increases to maintain high reliability of channel estimation at the relays and minimize the BER at the destination.

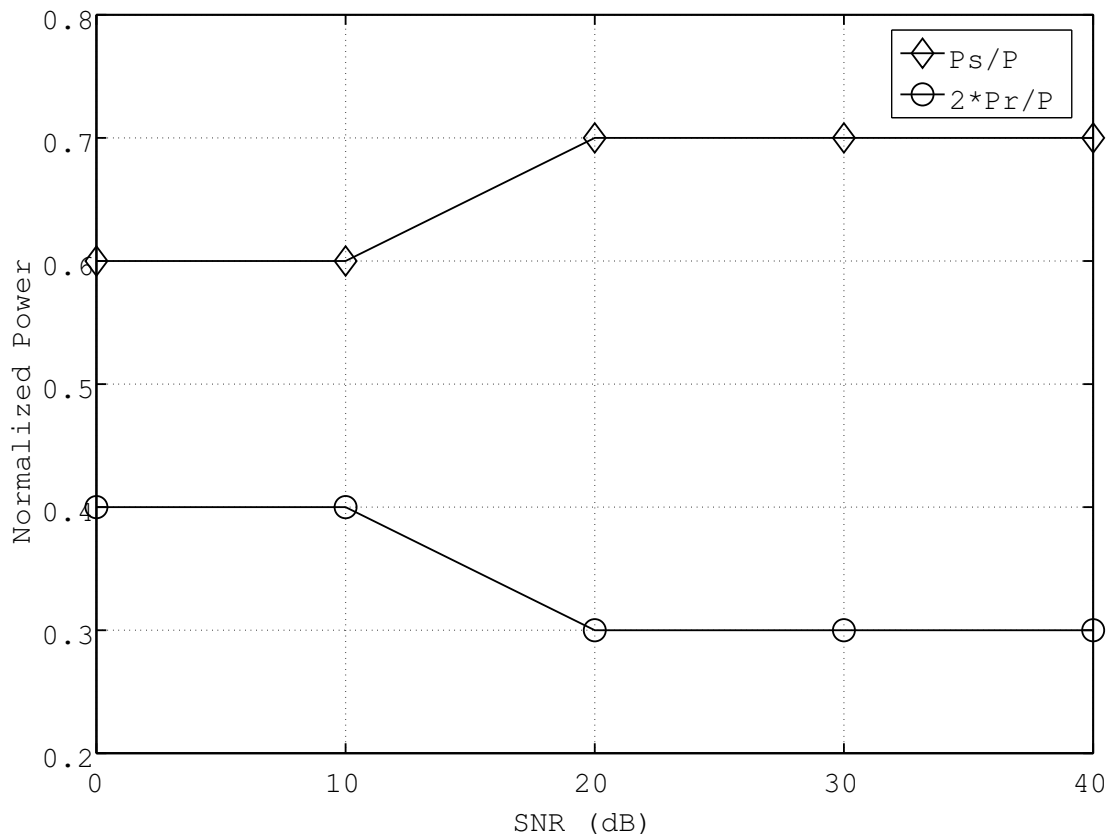


Figure 3.6 Power allocation trend of AF-CSM, source-relay distance = 0.5.

3.4 Conclusions

We introduced the implementation of amplify-and-forward scheme in cooperative spatial multiplexing system, and investigated its behavior under different parameters. The performance of AF-CSM is weighed against single-input-single-output (SISO), conventional spatial multiplexing (V-BLAST), as well as decode-and-transmit CSM systems. The proposed system combines the best of both worlds: MIMO system-like performance in the practical single antenna system environment, with no additional power consumptions and bandwidth at all. Its relative low-complexity at the relays, where the received signal from the source is only amplified by a factor β and forwarded (i.e. no decoding process, less computational burden compared to DF) to the destination, combined with optimal power allocation and relay selec-

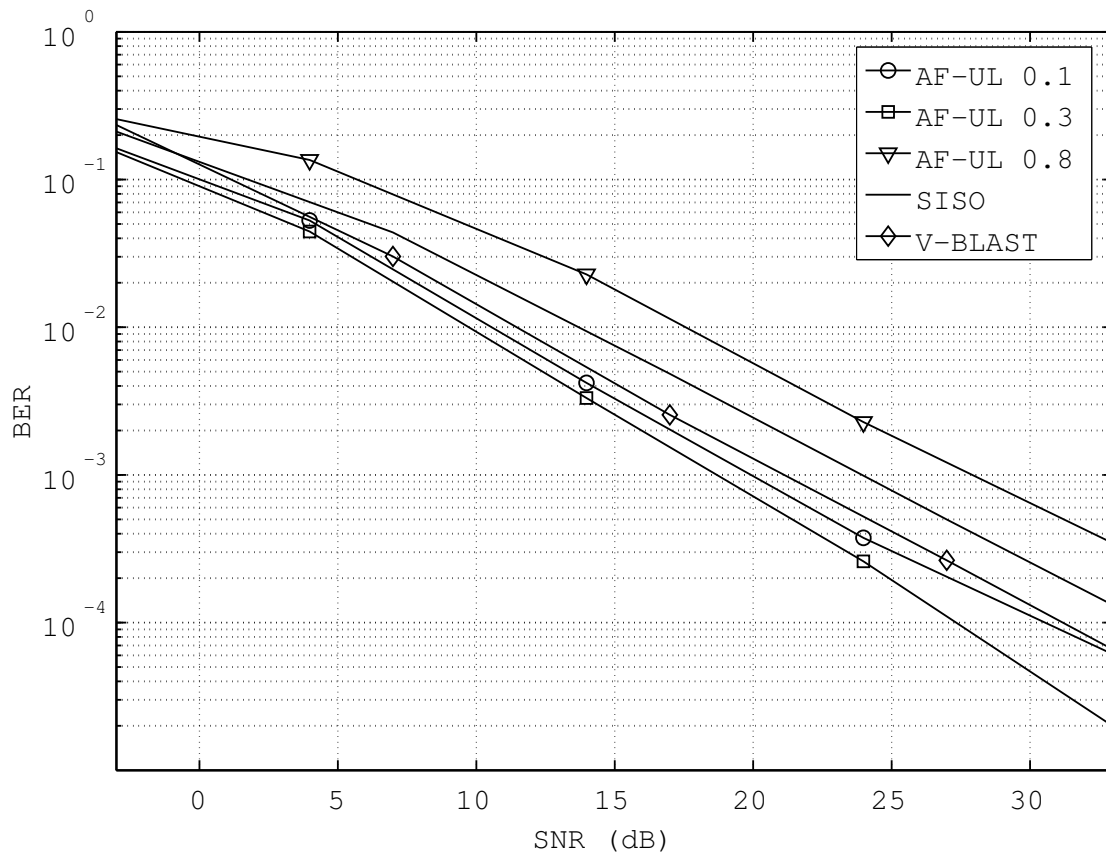


Figure 3.7 BER of AF-CSM with different relay distances & power allocation scheme.

tion schemes, allows it to surpass the performance of V-BLAST in which the impractical use of multiple antennas at the transceivers is unavoidable. Also, with total system power being distributed between the source and relays, individual terminals in CSM scheme require less power to complete data transmission compared to the current SISO and MIMO where all the system transmit power is allocated only to one terminal.

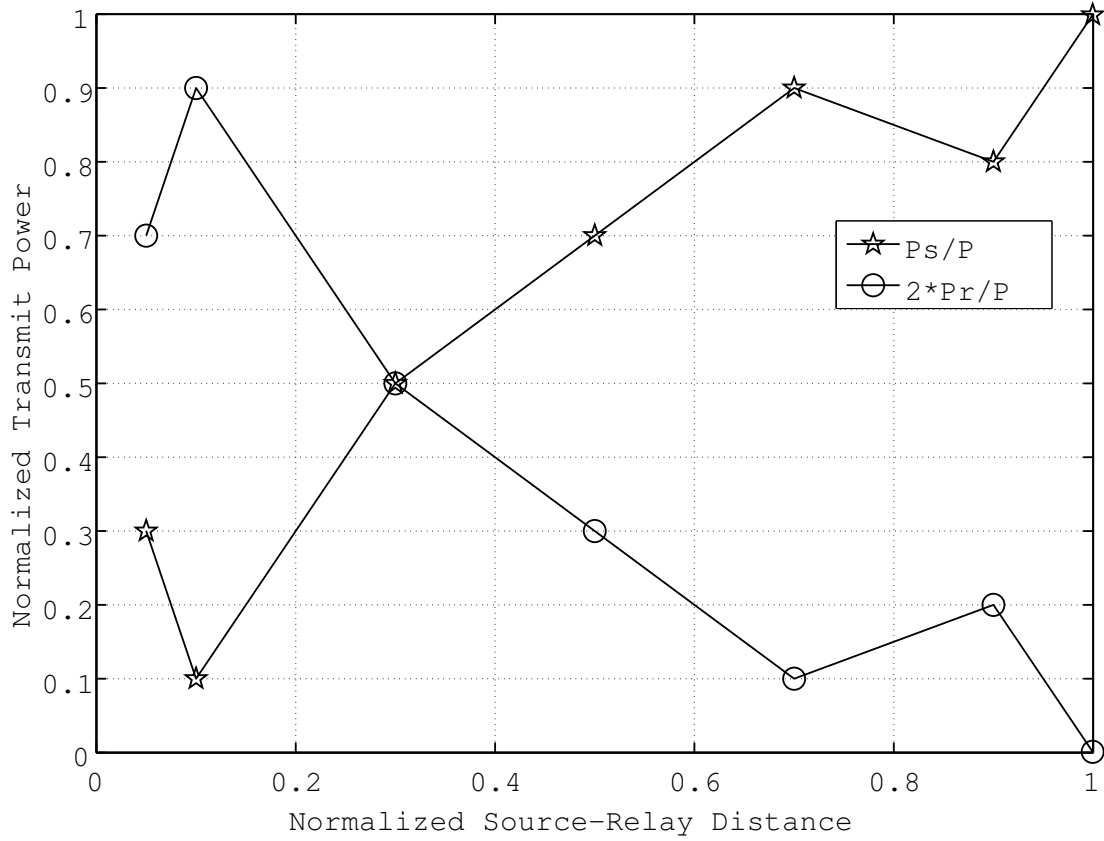


Figure 3.8 Recommended power allocation for AF-CSM, SNR=40 dB.

CHAPTER 4. COOPERATIVE WIRELESS MIMO COMMUNICATIONS: DOWNLINK TRANSMISSION

In this chapter, we propose the downlink CSM system for both amplify-and-forward (AF) and decode-and-forward (DF) transmission schemes depicted in Fig. 4.1, in which non-regenerative and regenerative relays are employed respectively in each scheme. Compared with the uplink system, different data symbols are transmitted simultaneously from a source (such as base-station or router, equipped with multiple antennas) to a single-antenna user terminal acting as the destination receiver. The transmission is assisted by several single-antenna relaying terminals, whose task is to receive and process source-transmitted symbols before forwarding them to the user terminal, while at the same time creating receive diversity effect for the single-antenna equipped destination receiver. Overall, the whole source-relay-destination transmission scheme allows the realization of downlink MIMO system in single-antenna terminals environment. Furthermore, Alamouti space-time coding transmit diversity scheme is implemented in the relay to destination transmission, taking advantage of the multiple relays to destination structure which resembles a multiple-input-single-output (MISO) system. Some will logically question the need of relaying system in downlink transmission since the base-station is virtually power-unlimited, thus transmission power can be adjusted accordingly even in the worst channel condition. Unfortunately, wireless transmission power is limited by the local government as not to interfere with other wireless systems. Hence during really bad channel condition (e.g. strong fading, shadowing, and interference, etc.) and transmission power has reached its maximum limit, the signal might get so corrupted such that correct decoding at the destination is impossible. It is known from the referenced papers that one advantage of cooperative transmission is to reduce the path loss effect from the shorter propagation distance,

mitigating noise and interference at the same time. Combined with MIMO-like performance feature, we show that the proposed system excels over existing transmission schemes in low SNR conditions.

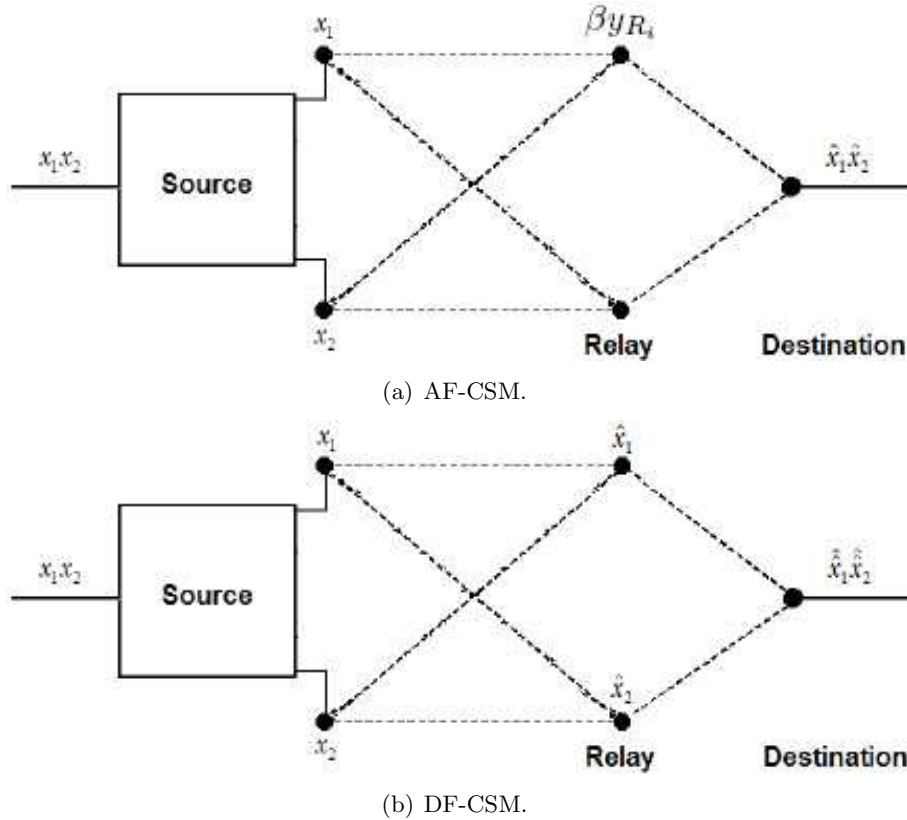


Figure 4.1 Downlink 2x2 AF and DF Cooperative Spatial Multiplexing systems.

We investigate the proposed system's performance under Rayleigh fading and AWGN noise with different transmission schemes, evaluating the bit-error rate by Monte-carlo simulations. The proposed system is then compared with current existing single-input-single-output (SISO), theoretical MIMO V-BLAST, and non-relayed Alamouti space-time transmit diversity systems.

4.1 Amplify-and-Forward System

Since AF-CSM and DF-CSM algorithms are already discussed in details in [28], [29], and [30], here we will review only the fundamental concepts. In the time slot t , the source, equipped

with M multiple antennas, transmits data $x_1x_2\dots x_M$ to $N(\geq M)$ relays R_1, R_2, \dots, R_N with a transmission power P_s at a rate of R_s/N bits/sec (bps). In baseband transmission model, the received signal plus noise, y_{R_i} , at relay R_i (equipped with single antenna) is given by

$$y_{R_i} = \sum_{j=1}^M h_{R_i, S_j} x_j + n_{R_i}, \quad i = 1, \dots, N \quad (4.1)$$

where h_{R_i, S_j} is the channel gain between the source antenna j and relay R_i , $x_j \in \{+\sqrt{E_s}, -\sqrt{E_s}\}$ is the transmitted symbol from the source, and n_{R_i} is the complex Gaussian noise with mean zero and variance $N_0/2$ per-dimension. We assume that h_{R_i, S_j} is rich-scattering complex Gaussian-distributed with mean zero and variance $E[|h_{R_i, S_j}|^2] = Ad_{R_i, S_j}^{-m}$, where d_{R_i, S_j} is the distance between the source and relay R_i , and m is the path loss exponent, typically $2 \leq m \leq 4$ [26]. The constant A captures the effects of antenna gain and carrier frequency and is given by $\left(\frac{4\pi d_0}{\lambda}\right)^{-m}$, with λ being the wavelength of the propagating signal, and d_0 is the reference distance (a point in the far field of the antenna) [26].

During the next time period $t + T$ (T being the source's one symbol period), N relays are selected for the data symbol amplification and forwarding. The user's receiver, equipped with single antenna, detects data $x_1x_2\dots x_N$ coherently using the V-BLAST successive interference cancelation (SIC) algorithm: nulling, cancellation, and ordering. The algorithm is described in detail in Appendix B. Furthermore, in order to keep the same spectral efficiency as in non-cooperative MIMO system, the data rate needs to be increased to R_s bps in the relay-destination transmission, .

4.1.1 Classical Relay Case

In the classical case, the relays act as conventional non-regenerative relay, whose task is to amplify the received spatial-multiplexed signal from the base station, with amplification factor β_i given by:

$$\beta_i \leq \sqrt{\frac{P_r}{\left[\sum_{j=1}^M |h_{R_i, S_j}|^2 P_s + N_0\right]}}, \quad i = 1, \dots, N \quad (4.2)$$

with P_r defined as the maximum available transmit power in each relay i .

The received signal y_D at the destination for classical AF case from each relay i , based on time-division multiplexing (TDM) transmission, is given by

$$y_{D,R_iAF} = g_{D,R_i}\beta_i y_{R_i} + n_D \quad (4.3)$$

where g_{D,R_i} is the channel gain between each relay R_i and destination D , $\beta_i y_{R_i}$ is the β -amplified received signal plus noise at relay R_i of x_j , and n_D is the complex Gaussian noise with mean zero and variance $N_0/2$ per-dimension. We assume that g_{D,R_i} is complex Gaussian distributed with mean zero and variance $E[|g_{D,R_i}|^2] = Ad_{D,R_i}^{-m}$. Here, d_{D,R_i} is the distance between relay R_i and destination D . The overall end-to-end system can be expressed by

$$\mathbf{y}_D = \mathbf{G}\mathbf{x} + \mathbf{N}_D \quad (4.4)$$

where \mathbf{N}_D is the noise matrix, and matrix \mathbf{G} captures the effect of source-relay & relay-destination channels, and also the relay amplification factor. The receiver buffers the received signal from each relay until every relay transmits, and then forms received signal vector $\mathbf{y}_D = [y_{D,R_1}, y_{D,R_2}, \dots, y_{D,R_N}]^T$ to be fed to the SIC decoder to obtain the estimated symbol \hat{x}_j .

4.1.2 Space-Time Coding Relay

Taking advantage of the transmission structure between N relays and the user terminal, we can implement an $N \times 1$ multiple-input-single-output (MISO) system here. One popular way to implement transmit-diversity is with the well-known Alamouti's space-time coding. In this section we will take a specific example where the data communication happens between a two-antenna base station source and a single user, through the help of two single-antenna relays, comprising a $2 \times 2 \times 1$ system.

At different time slots, the relays transmit space-time coded symbols based on Alamouti scheme, as shown in Table 4.1. Here s_1 and s_2 represent the received signal y_{R_1} and y_{R_2} at the relays respectively, K is the symbol period of one space-time symbol, while $*$ denotes complex conjugation operation.

Holding the assumption that the Rayleigh fading is constant over two symbol periods the

Time	Relay 1	Relay 2
$t + T$	s_1	s_2
$t + T + K$	$-s_2^*$	s_1^*

Table 4.1 Space-time coding transmission sequence

received signals at destination D are:

$$y_{D_T} = g_{D,R_1}\beta_1 s_1 + g_{D,R_2}\beta_2 s_2 + n_{D_T} \quad (4.5)$$

and

$$y_{D_K} = -g_{D,R_1}\beta_2 s_2^* + g_{D,R_2}\beta_1 s_1^* + n_{D_K} \quad (4.6)$$

at time $t + T$ and $t + T + K$ successively.

At the destination, the decoding scheme involves two steps. Before the original spatial-multiplexed symbols can be fed to the SIC decoder, the received space-time signal has to be decoded to obtain \tilde{s}_1 and \tilde{s}_2 which are the estimates of s_1 and s_2 . The combining scheme, after all space-time signals have been received, is given by:

$$\tilde{s}_1 = g_{D,R_1}^* y_{D_T} + g_{D,R_2} y_{D_K}^* \quad (4.7)$$

$$\tilde{s}_2 = g_{D,R_2}^* y_{D_T} - g_{D,R_1} y_{D_K}^* \quad (4.8)$$

which will further give:

$$\begin{aligned} \tilde{s}_1 &= (|g_{D,R_1}|^2 + |g_{D,R_2}|^2)\beta_1 s_1 + g_{D,R_1}^* n_{D_T} \\ &\quad + g_{D,R_2} n_{D_K}^* \end{aligned} \quad (4.9)$$

and

$$\begin{aligned} \tilde{s}_2 &= (|g_{D,R_1}|^2 + |g_{D,R_2}|^2)\beta_2 s_2 + g_{D,R_2}^* n_{D_T} \\ &\quad - g_{D,R_1} n_{D_K}^* \end{aligned} \quad (4.10)$$

of which can be simplified to:

$$\tilde{s}_1 = (|g_{D,R_1}|^2 + |g_{D,R_2}|^2)\beta_1 s_1 + N_{s_1} \quad (4.11)$$

$$\tilde{s}_2 = (|g_{D,R_1}|^2 + |g_{D,R_2}|^2)\beta_2 s_2 + N_{s_2} \quad (4.12)$$

with N_{s_1} and N_{s_2} being the cumulative AWGN in (4.9) and (4.10).

The final decoding process at the destination terminal involves feeding \tilde{s}_1 and \tilde{s}_2 to the SIC decoder in order to obtain \tilde{x}_1 and \tilde{x}_2 , which are the estimations of the transmitted symbols from the source.

4.1.3 Practical Issues

The algorithm for space-time coded relaying involves sending complex conjugates of the other relay's signal and amplification factor, namely $\beta_2 s_2^*$ from relay 1 and $\beta_1 s_1^*$ from relay 2 to the destination at time $t + T + K$, of which the relays are assumed to know perfectly. In practice, in order to be able to accomplish the space-time algorithm, every corresponding relay has to transmit s_1 and s_2 to each other through the wireless channel between them, exposing the signal to fading, interference, and noise. From then, received signal at each relay is given by:

$$y_{R_{12}} = g_{R_{12}} \beta_2 s_2 + n_{R_1} \quad (4.13)$$

at relay 1 from relay 2, and:

$$y_{R_{21}} = g_{R_{12}} \beta_1 s_1 + n_{R_2} \quad (4.14)$$

at relay 2 from relay 1, of which, assuming perfect knowledge of CSI, are estimated as

$$\hat{s}_2 = \beta_2 s_2 + N_{R_{12}} \quad (4.15)$$

$$\hat{s}_1 = \beta_1 s_1 + N_{R_{21}} \quad (4.16)$$

in relay 1 and relay 2, respectively. Here $g_{R_{12}}$ is complex Gaussian distributed with mean zero and variance $E[|g_{R_{12}}|^2] = A d_{R_1, R_2}^{-m}$, d_{R_1, R_2} is the distance between the relays, and $N_{R_{12}}$ & $N_{R_{21}}$ are the collective AWGN noise as the result of the estimation. Consequently, the space-time coded relayed signaling now follows Table 4.2. The signals received at time $t + T + 3K$ at the destination will then be:

$$y_{D_{3K}} = -g_{D, R_1} \hat{s}_2^* + g_{D, R_2} \hat{s}_1^* + n_{D_{3K}} \quad (4.17)$$

Time	Relay 1	Relay 2
$t + T$	s_1	IDLE
$t + T + K$	IDLE	s_2
$t + T + 2K$	s_1	s_2
$t + T + 3K$	$-\hat{s}_2^*$	\hat{s}_1^*

Table 4.2 Practical space-time coding transmission sequence

The decoding algorithm is done by feeding the post-combining space-time signals into the successive interference cancellation (SIC) decoder, and is described further in Appendix A. The ripple effect of (4.15) and (4.16) is that the noise component increases with the addition of $N_{R_{12}}$ and $N_{R_{21}}$. These noises propagate and will certainly affect the final decoding process. Another disadvantage would be the additional time slot needed for the relays to communicate with each other, which will reduce the spectral efficiency (i.e. capacity) of the system further. One possible way to overcome this problem is to increase the transmission bit-rate, while reducing the energy-per-bit accordingly. This way the total transmit energy of the system is still kept less or equal to that of SISO system.

4.2 Decode-and-Forward System

In decode-and-forward cooperative scheme, the relays act as regenerative relays, i.e. they make estimations of the source transmitted signals, before forwarding the estimations to the destination side. In baseband transmission scheme, the signal received at relay R_i is similar to (4.1). In the next sections, just like in AF case, we present several relaying schemes in order to get the data across from the relays to the destination.

4.2.1 Classical Relay Case

In the ideal case, the relays are assumed to know perfectly the received source-transmitted signal of one another such that they would be able to do successive interference cancellation collectively and estimate the original transmitted signal. Each relay R_i will then alternately forward \hat{x}_i with transmission power P_r , the estimates of x_i , to the destination with time-division

multiplexing scheme such that the destination receives:

$$y_{D,R_iDF} = g_{D,R_i}\hat{x}_i + n_{D_iK} \quad i = 1, \dots, N \quad (4.18)$$

at time $t + T + (i - 1)K$, where g_{D,R_i} is complex Gaussian distributed with mean zero and variance $E[|g_{D,R_i}|^2] = Ad_{D,R_i}^{-m}$, and n_{D_iK} is the receiver noise. Assuming perfect channel state information knowledge at the destination receiver, we can get \hat{x}_i , the estimates of the original transmitted x_i , easily from y_{D,R_iDF} .

4.2.2 Space-time Coding Relay

Should the classical relaying scheme is implemented, additional time slots as many as the number of relays will be needed to complete the transmission. This causes disadvantage in terms of system capacity being reduced proportional to the number of time slots needed. In order to counter the issue and considering the relay-destination transmission structure, we investigate the implementation of space-time coding in the relays. Specifically, we present the case for a $2 \times 2 \times 1$ system, in which a source equipped with two antennas is used in conjunction with two single-antenna relays and a single-antenna destination receivers.

After the relays estimate source-transmitted x_i as \hat{x}_i , space time code with $s_1 = \hat{x}_1$ and $s_2 = \hat{x}_2$ are formed and forwarded to the destination with transmission sequence following Table 4.1 using relay transmit power P_r . The received signal at the destination receiver at time slots $t + T$ and $t + T + K$ are given as:

$$y_{D_T} = g_{D,R_1}s_1 + g_{D,R_2}s_2 + n_{D_T} \quad (4.19)$$

$$y_{D_K} = -g_{D,R_1}s_2^* + g_{D,R_2}s_1^* + n_{D_K} \quad (4.20)$$

respectively.

The same combining scheme used in (4.7) and (4.8) is also employed here to produce:

$$\begin{aligned} \tilde{s}_1 = & (|g_{D,R_1}|^2 + |g_{D,R_2}|^2)s_1 + g_{D,R_1}^*n_{D_T} \\ & + g_{D,R_2}n_{D_K}^* \end{aligned} \quad (4.21)$$

and

$$\begin{aligned}\tilde{s}_2 &= (|g_{D,R_1}|^2 + |g_{D,R_2}|^2)s_2 + g_{D,R_2}^* n_{D_T} \\ &\quad - g_{D,R_1} n_{D_K}^*\end{aligned}\tag{4.22}$$

For final decoding, the combined signals \tilde{s}_1 and \tilde{s}_2 will be fed to the maximum likelihood detector in which, for PSK signals, s_i will be chosen iff

$$d^2(\tilde{s}_1, s_i) \leq d^2(\tilde{s}_1, s_k), \quad \forall i \neq k\tag{4.23}$$

from which \hat{x}_i , the final estimate of the source-transmitted x_i can be obtained.

4.2.3 Practical Issue

In decode-and-forward case, implementation-wise, before each relay can decode (estimate) the source-transmitted signal x_i into \hat{x}_i signal it has to know the other relay's y_{R_i} signals. This can be achieved by exchanging information between the relays:

$$y_{R_{12}} = g_{R_{12}}\beta_2 y_{R_2} + n_{R_1}\tag{4.24}$$

at relay 1 from relay 2, and:

$$y_{R_{21}} = g_{R_{12}}\beta_1 y_{R_1} + n_{R_2}\tag{4.25}$$

conversely, with $g_{R_{12}}$ being the Rayleigh fading channel between the relays, and β_i being the amplification factor in each relay. Assuming perfect CSI at the relays, the above signals can be estimated as

$$\hat{y}_{R_2} = \beta_2 y_{R_2} + N_{R_{12}}\tag{4.26}$$

$$\hat{y}_{R_1} = \beta_1 y_{R_1} + N_{R_{21}}\tag{4.27}$$

By using $\{y_{R_1}, \hat{y}_{R_2}\}$ in relay 1 and $\{\hat{y}_{R_1}, y_{R_2}\}$ in relay 2 and feeding those signals into each relay's SIC decoder, individual \hat{x}_i estimates can be obtained in each relay.

From here the relay can opt to forward \hat{x}_i to the final destination by employing classical or space-time coding relay. The classical relay case follows the method as described in section 3.1.

In the case where space-time coding relay is employed, each relay will individually construct space-time codes $s_{i_R_1}$ and $s_{i_R_2}$ from \hat{x}_i , such that the transmission scheme follows Table 4.3. Based on the space-time coding transmission, received signals at the destination at time slots

Time	Relay 1	Relay 2
$t + T$	y_{R_1}	IDLE
$t + T + K$	IDLE	y_{R_2}
$t + T + 2K$	$s_{1_R_1}$	$s_{2_R_2}$
$t + T + 3K$	$-s_{2_R_1}^*$	$s_{1_R_2}^*$

Table 4.3 Transmission sequence in practical space-time DF system

$t + T + 2K$ and $t + T + 3K$ are, respectively, given by

$$y_{D_{2K}} = g_{D,R_1} s_{1_R_1} + g_{D,R_2} s_{2_R_2} + n_{D_{2K}} \quad (4.28)$$

$$y_{D_{3K}} = -g_{D,R_1} s_{2_R_1}^* + g_{D,R_2} s_{1_R_2}^* + n_{D_{3K}} \quad (4.29)$$

If and only if the relays decode correctly the source-transmitted symbols, we can simplify further the space-time code and drop the relay indexing to $s_{1_R_1} = s_{1_R_2} = s_1$ and $s_{2_R_1} = s_{2_R_2} = s_2$. Then, for decoding purpose, the combining schemes for the space-time signals will give

$$\begin{aligned} \tilde{s}_1 &= g_{D,R_1}^* y_{D_{2K}} + g_{D,R_2} y_{D_{3K}}^* \\ &= (|g_{D,R_1}|^2 + |g_{D,R_2}|^2) s_1 + g_{D,R_1}^* n_{D_{2K}} \\ &\quad + g_{D,R_2} n_{D_{3K}}^* \end{aligned} \quad (4.30)$$

and

$$\begin{aligned} \tilde{s}_2 &= g_{D,R_2}^* y_{D_{2K}} - g_{D,R_1} y_{D_{3K}}^* \\ &= (|g_{D,R_1}|^2 + |g_{D,R_2}|^2) s_2 + g_{D,R_2}^* n_{D_{2K}} \\ &\quad - g_{D,R_1} n_{D_{3K}}^* \end{aligned} \quad (4.31)$$

In order to obtain the final estimation \hat{x}_i of the original source-transmitted symbols, \tilde{s}_1 and \tilde{s}_2 are fed to the maximum-likelihood detector with decision rule described in (4.23).

4.3 Numerical Results and Discussions

We apply our results to 2x2x1 (i.e. a base-station source equipped with two antennas, two single-antenna relays, and a single-antenna destination receiver) AF-CSM and DF-CSM downlink systems. Modulation of choice is BPSK ($m = 3$) where the normalized source-relay distance is 0.5 (i.e. relays are halfway between source and destination) under Rayleigh fading condition which is constant for at least two symbol periods, distance between relays of 0.1, and without loss of generality, we assume that antenna and receiver gain A is 1. The amount of total transmit power in the system accounts for the number of time slot needed to complete the end-to-end transmission, and is normalized and constrained such that the total system transmit power $P = 1$ is the same as in SISO system. Furthermore, we assume perfect knowledge of CSI at the relay and destination terminals. The total power P is divided uniformly among the transmitted antennas such that each antenna transmits at power $P/(M + N)$. Furthermore, we assume perfect knowledge of CSI at the relay and destination terminals. In all of the simulation figures, E_b/N_0 is defined as the transmit energy per-bit per-noise spectral density given by $(E_s + E_r)/N_0$, where E_s and E_r are the transmit energy per-bit at the source and relay antennas, respectively.

For a fair comparison in our simulations, we opted to choose "fair" in terms of spectral efficiency (a.k.a capacity, or throughput). All the systems compared, including our proposed system, were setup such that in one normalized $t_{V-BLAST}$ time slot, M bits of data are sent from the source to the destination, and i.e. the spectral efficiency is M bits/ $t_{V-BLAST}$ /Hz. This also means data rate of the SISO has to be boosted by M -factor for a fair comparison. Moreover, data rate of the proposed system at the source and relays were also adjusted accordingly to the corresponding relay schemes in order to achieve the same M bits/ $t_{V-BLAST}$ /Hz of spectral efficiency. This rate-adjustment setup cancels the throughput-limiting effect of additional time slots in CSM system. Thus, no disadvantage to the overall throughput is expected. In our simulations, M is two.

Fig. 4.2 shows the effect of different relay locations for the CSM system for $E_b/N_0 = 10$ dB. It can be observed that performance of the proposed schemes vary according to the source-relay

distance. According to our simulation results, the CSM schemes provide superior performance to SISO and V-BLAST when the normalized source-relay distance is between 0.35 and 0.9 and reached the maximum at 0.65. Beyond this range, the relays will be "too far" from either the destination or the source, such that the combined path loss effect of the wireless links downgrades the overall system performance. At 0.65 the links gives an optimal balance of received SNR at both relay and destination terminals, such that the relays are most reliable and optimal system performance is achieved.

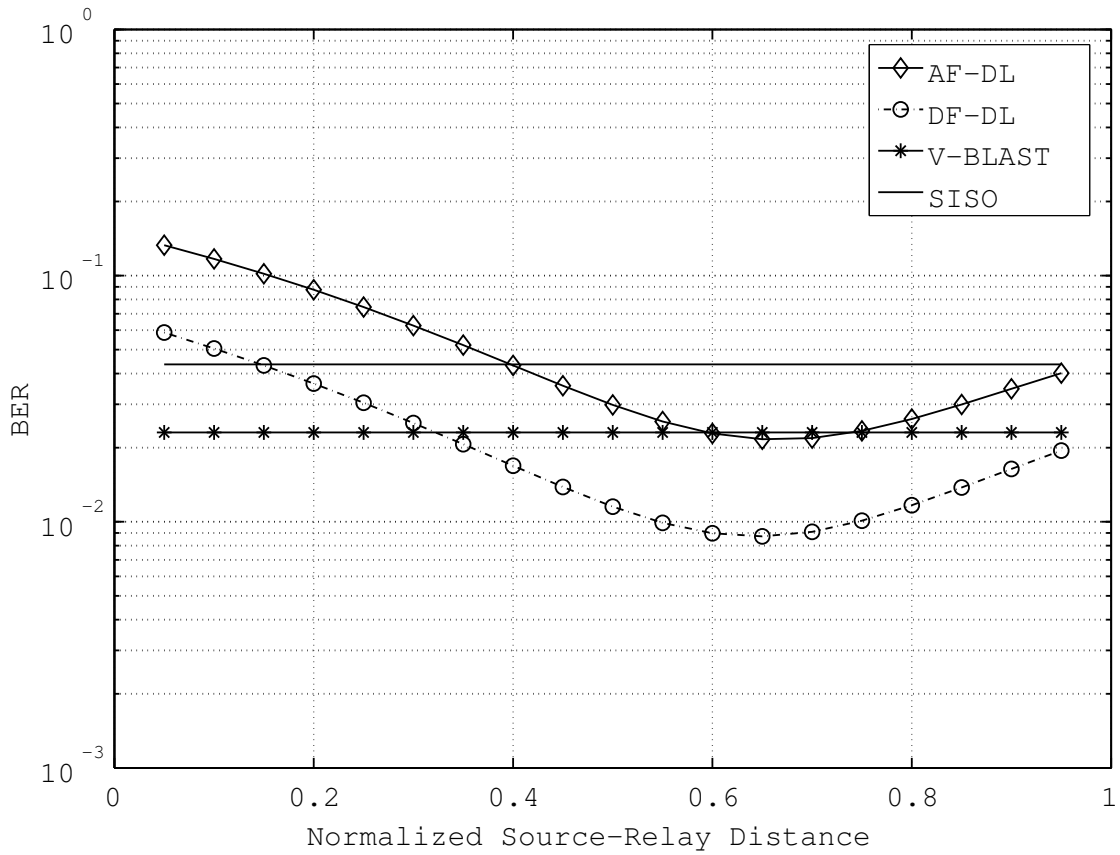


Figure 4.2 BER performance of downlink AF & DF CSM systems for different relay locations, $E_b/N_0 = 10$ dB.

Next, Fig. 4.3 depicts the utilization of four relay terminals (2x4x1 and 4x4x1 configurations) in downlink non-STC AF-CSM. It can be observed that the diversity gain is one for two relays utilization, while in four relays case, it is approximately three. From the slope

of the BER curves, the V-BLAST SIC decoding gives the CSM system a diversity order of $N - M + 1$, in concurrence with the V-BLAST diversity analysis given in [33]. The MIMO V-BLAST diversity gain seems to be preserved despite the extra wireless link in the MIMO CSM configuration. In order to preserve the total power P in the system, transmit power per-antenna has to be decreased with the increasing number of relays. Despite the smaller transmit power and non-STC transmission, the system is able to gain performance from the higher redundancy introduced by the extra relay terminals. These additional relays introduce extra time slots for the TDM transmission, thus the transmission rate at the relay terminals need to be adjusted properly to preserve the spectral efficiency.

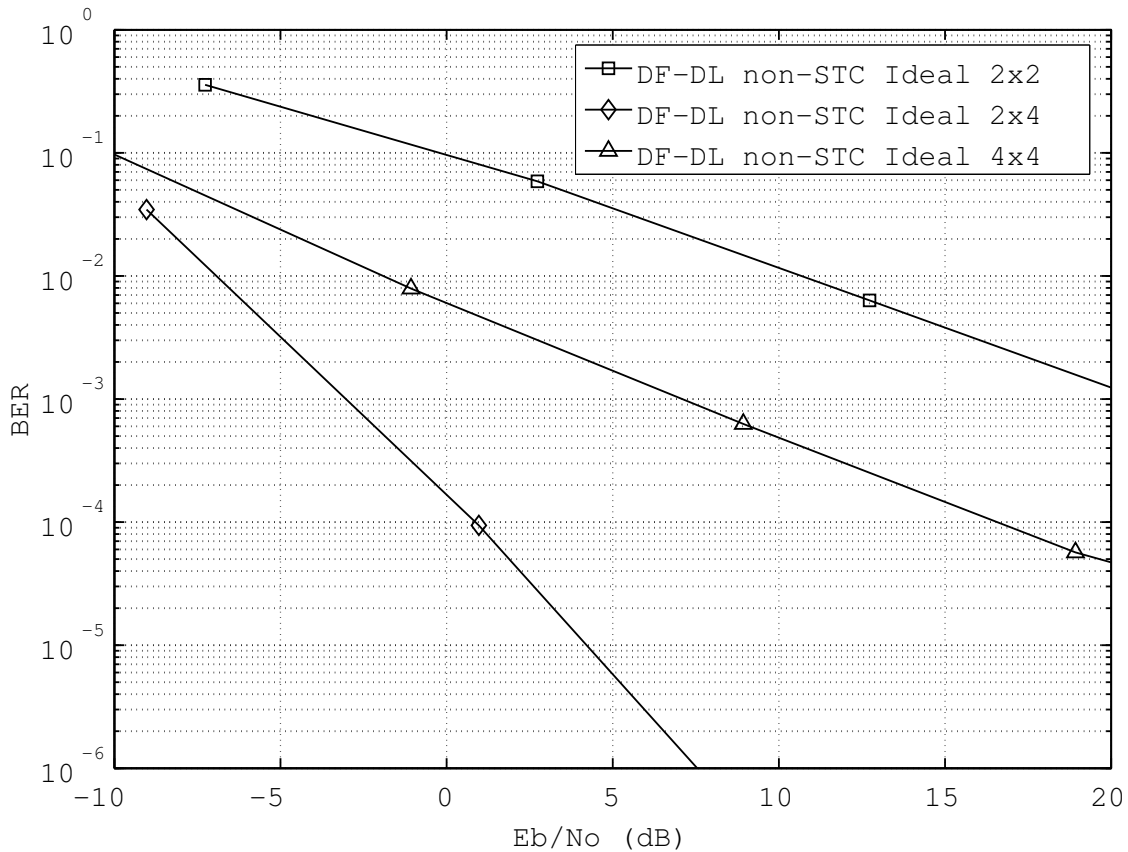


Figure 4.3 BER performance of downlink AF-CSM with two and four relays.

Fig. 4.4 compares the bit-error rate performance between downlink AF-CSM schemes (no

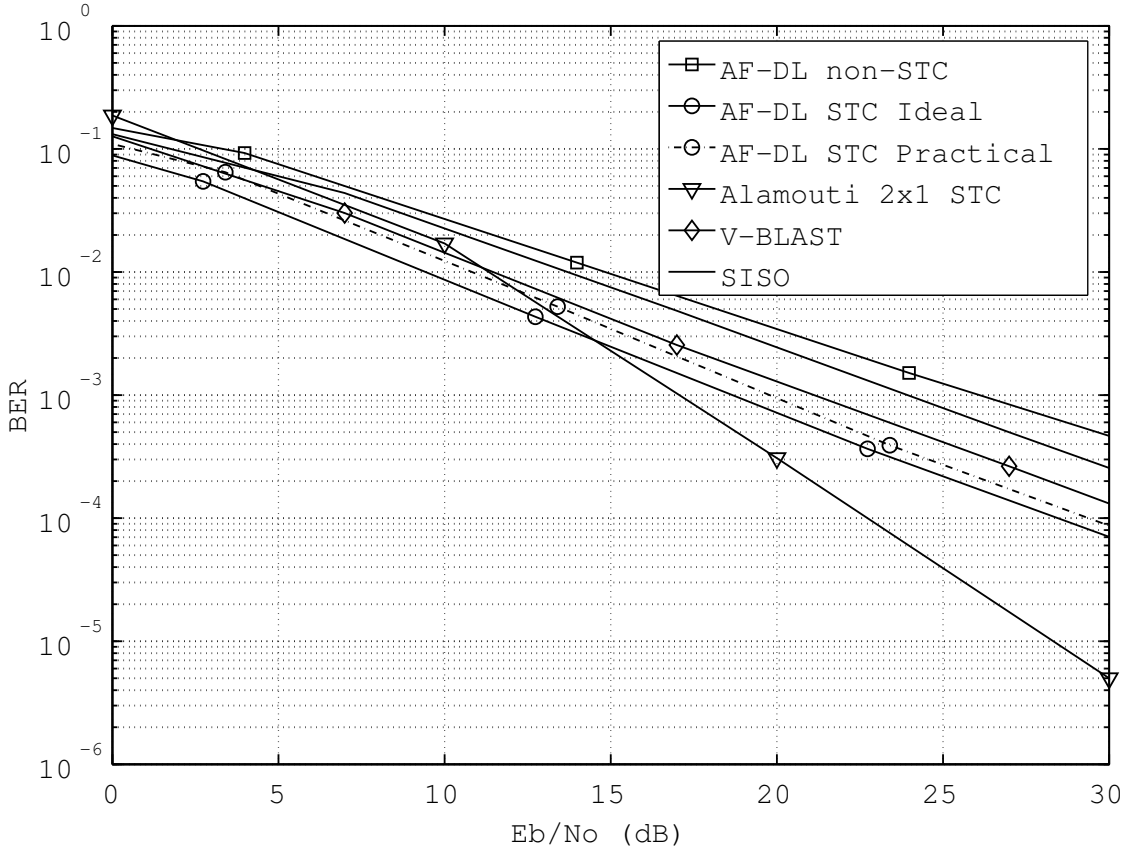


Figure 4.4 BER performance of downlink AF-CSM systems.

STC and STC relaying) with theoretical V-BLAST and SISO systems. Here it is shown that the space-time coding relaying system achieves better performance than of non-space-time coding (~ 3.7 dB at 10^{-3} BER). Logically, it is expected that the ideal AF-CSM STC system gives better performance over practical system, and this advantage gets bigger as the distance between the relays increases. Although in the low-SNR region the AF-CSM performs better than the direct source-destination Alamouti STC transmission scheme, as the channel condition gets better (higher SNR), the advantage of direct STC transmission is obvious. This is due to the pure STC decoding in direct STC gives a higher diversity order [21], as opposed to the STC-SIC decoding of AF-CSM which gives no diversity advantage at all. The superiority of AF-CSM system over conventional SISO and theoretical V-BLAST system is clearly depicted as well, with STC AF-CSM being the winner.

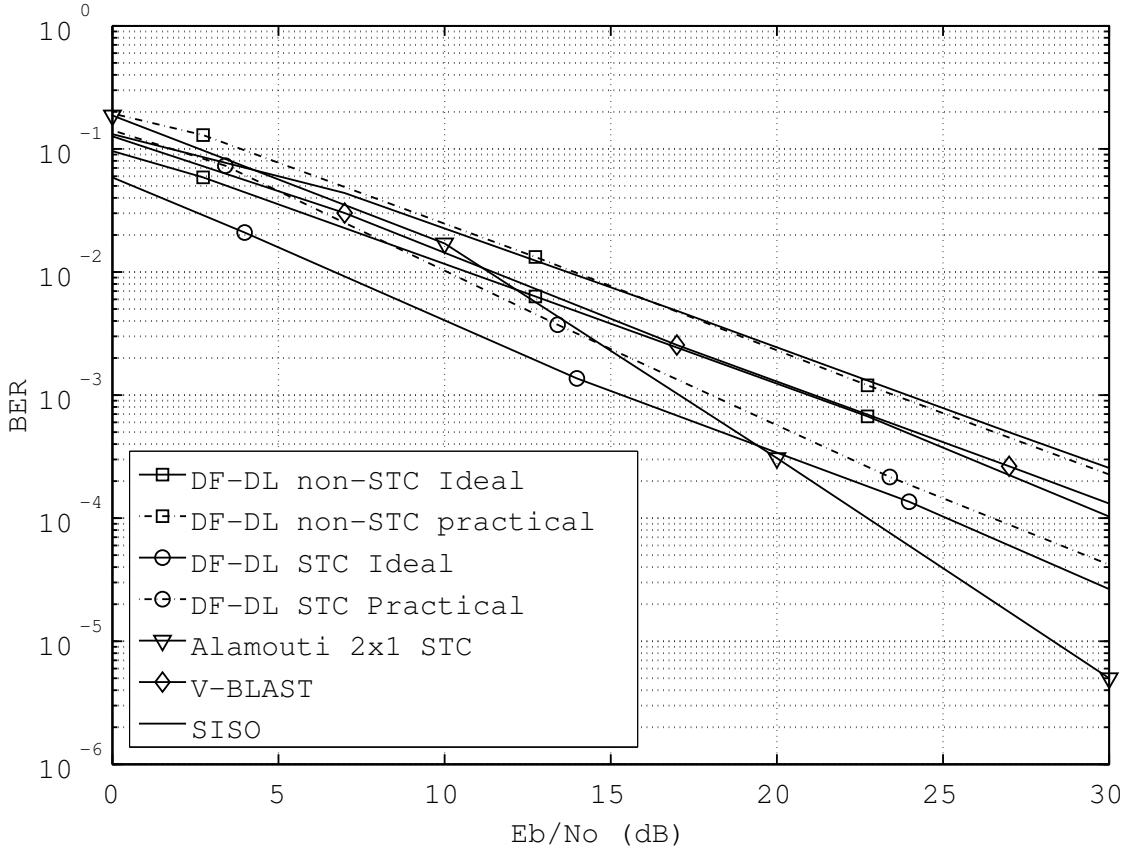


Figure 4.5 BER performance of downlink DF-CSM systems.

In Fig. 4.5, the performance of the downlink DF-CSM schemes generally behave similarly to its AF-CSM counterpart. Here the "DF-CSM non-STC practical" curve depicts the necessity of information of each relay's received source-transmitted to be sent between one another for the symbol decoding at each regenerative relay, before forwarding the estimation to the destination. Note that "AF-CSM non-STC" is the same for ideal and practical systems. The advantage of STC over non-STC system in DF-CSM is about 8dB at 10^{-3} BER, which is much bigger than in AF-CSM. With the same diversity advantage as before, in high-SNR region the direct STC transmission still gives the edge over the proposed system. One thing worth to be noted here is that in practical system, the STC DF-CSM does not really give much performance advantage over direct STC even in low-SNR region, where it is supposed to excel.

Head-to-head comparisons between the downlink AF and DF CSM systems are shown in

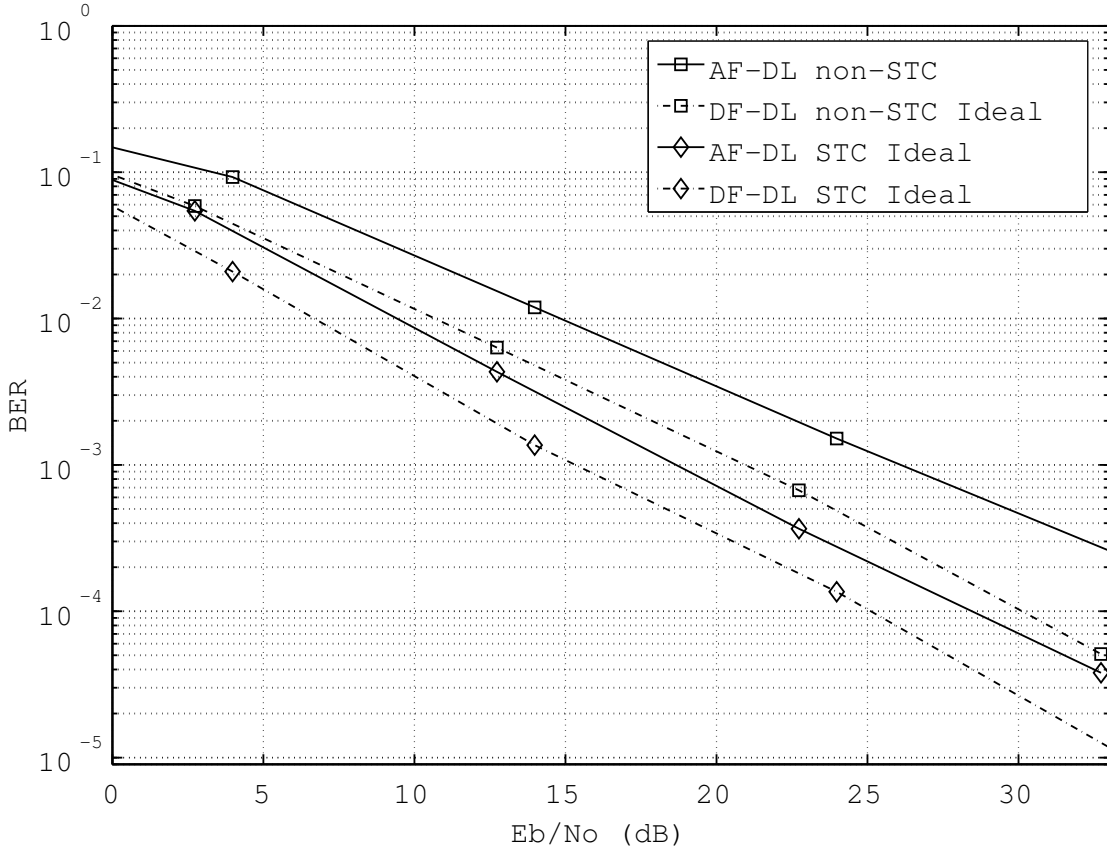


Figure 4.6 BER performance of ideal downlink AF-CSM and DF-CSM systems.

Fig. 4.6 and Fig. 4.7. Performance comparison of theoretical ideal system of the downlink (STC and non-STC) AF and DF CSM is depicted in Fig. 4.6. It follows the trend in previous works (e.g. [15]) that in general, regenerative (DF) systems give better BER performance over non-regenerative (AF) systems. In amplify-and-forward (AF) case, we do not expect that the STC to give additional diversity advantage since the final decoding at the destination receiver is conducted based on the successive interference cancelation (SIC) process (not STC decoding) which is also the method in V-BLAST. Thus, we expect the diversity gain of the AF-CSM system should be much similar to that of V-BLAST, which is $N - M + 1$. On the other hand, in decode-and-forward (DF) with STC relays, the final decoding at the destination receiver employs the maximum likelihood estimator (which is the decoding method used in STC as

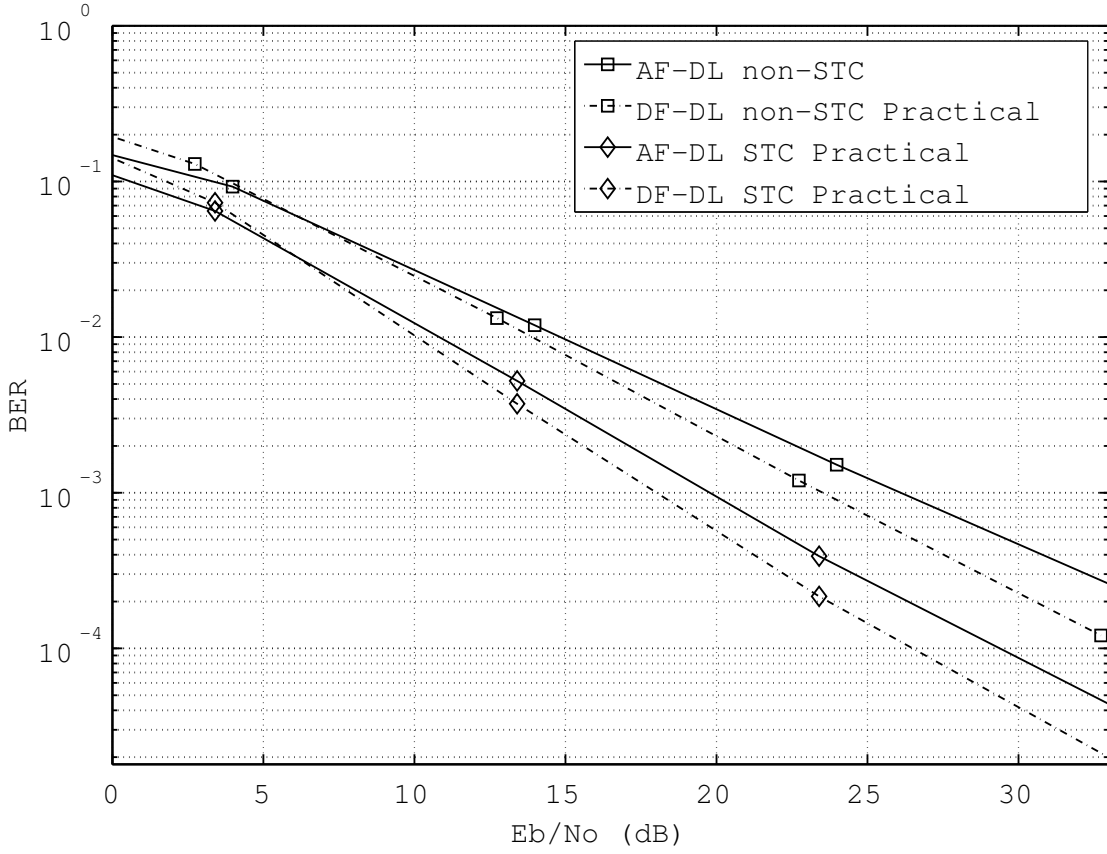


Figure 4.7 BER performance of practical downlink AF-CSM and DF-CSM systems.

proposed by Alamouti). We expect that the reliability effect of the symbols transmitted from the relay terminals (which are already estimations of the original source-transmitted symbols) cancels the diversity gain that could be obtained by STC decoding, such that the overall diversity gain is just $N - M + 1$ (similar to non-STC case). Nevertheless, the addition of STC at the relay proves to mitigate path loss very well.

Finally, due to the fact that in low-SNR region AF-CSM is superior to DF-CSM, and also in high-SNR, DF-CSM does not offer significant advantage, we propose that space-time coded AF-CSM is the scheme of choice given the source-relay-destination structure described in this paper. It may be useful to note that even if the STC scheme does not seem to offer any noticeable diversity gain over non-STC systems, it definitely improves the BER performance

from the repetitive transmission which increases the received SNR at the destination end.

4.4 Conclusions

We investigate and propose the utilization of regenerative and non-regenerative relaying terminals in downlink cooperative MIMO communications, such as in base-station/router to user transmission under different schemes. Between the source and relays, the symbols are transmitted using MIMO spatial-multiplexing technique. Depending on the type of relaying scheme, the relays either fully decode or amplify the received signal before retransmitting it to the destination using simple TDM transmission or Alamouti's space-time coding.

Based on the Monte-carlo simulation results, in both ideal and practical AF-CSM and DF-CSM, space-time coding relays gives superior BER performance over non-space-time coding scheme. In practical non-STC scheme, AF-CSM should be the scheme of choice due to the big performance advantage over DF-CSM. While in STC-scheme, if the 2dB advantage over AF-CSM is considered worth the resource expense, then DF-CSM should be the transmission scheme of choice. Otherwise, it is much preferred to choose AF-CSM due to less complexity at the relay terminals. In general, although the high-complexity and resource-exhaustive natures of the proposed system may hinder its practical implementation in real-world system, it is worthwhile to consider "CSM Mode" only during low-SNR condition and revert back to non-relaying direct STC technique when channel condition improves.

CHAPTER 5. THEORETICAL PERFORMANCE ANALYSIS OF UPLINK AND DOWNLINK COOPERATIVE SPATIAL MULTIPLEXING SYSTEMS

In this chapter, we derive the theoretical analysis on the performance of the uplink/downlink classical amplify-and-forward (AF) and decode-and-forward (DF) CSM systems described in the previous chapters. Since the derivations could get quite mathematically complicated, we limit our analysis to 1x2x2 AF and 2x2x1 DF systems.

With the help of Gram-Schmidt orthogonalization process [33], we derive the approximate closed-form solutions to average bit-error rate (BER) and outage probability performance of both uplink and downlink AF-CSM and DF-CSM systems, which so far to our knowledge, has never been published before. The results will then be compared to Monte-Carlo simulation results, followed by discussions on the issue. This work should be applicable to give an estimate on the performance of the AF and DF CSM systems without having to run time-consuming Monte-Carlo simulations. Before we begin with the main analysis, it will be convenient to recall some definitions which will be the fundamental keys to the analysis.

Definition 1 (Harmonic Mean): The harmonic mean of two numbers X_1 and X_2 , $\mu_H(X_1, X_2)$, is defined as the reciprocal of the arithmetic mean of the reciprocals of X_1 and X_2 [31]:

$$\begin{aligned}\mu_H(X_1, X_2) &= \frac{2}{\frac{1}{X_1} + \frac{1}{X_2}} \\ &= \frac{2X_1X_2}{X_1 + X_2}\end{aligned}\tag{5.1}$$

Definition 2 (Exponential RV): X is defined to be exponentially distributed with parameter $\beta > 0$ is the PDF of X is given by [32]

$$p_X(x) = \beta e^{-\beta x} U(x)\tag{5.2}$$

where $U(\cdot)$ is the unit step function.

Definition 3 (Limiting Form of Modified Bessel Function): For fixed v and $z \rightarrow 0$, the modified Bessel function can be approximated by [37, eq.9.6.9]

$$K_v(z) \sim \frac{1}{2}\Gamma(v) \left(\frac{1}{2}z\right)^{-v} \quad (5.3)$$

where $\Gamma(\cdot)$ is the Gamma function.

For the reader's convenience purpose, we quote several key results from [34] which will be used in our analysis as well.

Lemma 1 (PDF of $1/X$): Given a RV $X \sim \mathcal{E}(\beta)$, the PDF of $Y = 1/X$ is calculated as

$$p_Y(y) = \frac{\beta}{y^2} e^{-\beta/y} U(y) \quad (5.4)$$

Lemma 2 (MGF of $1/X$): Given a RV $X \sim \mathcal{E}(\beta)$, the MGF of $Y = 1/X$ is given by

$$\mathcal{M}_Y(s) = 2\sqrt{\beta s} K_1(2\sqrt{\beta s}) \quad (5.5)$$

where $K_1(\cdot)$ is the first order modified Bessel function of the second kind defined in [37].

Theorem 1 (CDF of the Harmonic Mean of Two Exponential RVs): Let X_1 and X_2 be two independent exponential RVs with parameters β_1 and β_2 , respectively. The CDF of $X = \mu_H(X_1, X_2)$, $P_X(x)$ is given by

$$P_X(x) = 1 - x\sqrt{\beta_1\beta_2} e^{-x(\beta_1+\beta_2)/2} K_1\left(x\sqrt{\beta_1\beta_2}\right) \quad (5.6)$$

5.1 Outage Probability Analysis

The outage probability is defined as the probability that the received signal drops below a threshold value. Following the assumptions of the previous section, we present the derivation of outage probability for AF-CSM and DF-CSM in the case where two relays are employed and the destination is equipped with two antennas.

5.1.1 Uplink Amplify-and-Forward

In the AF case, recall that the received signals at the relays and destination are given by

$$y_{R_i} = h_{R_i,S}x_i + n_{R_i} \quad (5.7)$$

and

$$y_{D_j,AF} = \sum_{i=1}^M g_{D_j,R_i} \alpha_i y_{R_i} + n_{D_j} \quad j = 1, 2, \dots, N \quad (5.8)$$

where $h_{R_i,S}$ is the channel gain between the source and relay R_i , g_{D_j,R_i} is the channel gain between the relay R_i and destination D_j , $x_i \in \{+\sqrt{E_s}, -\sqrt{E_s}\}$ is the transmitted symbol from the source, noise components n is complex Gaussian with mean zero and variance $N_0/2$ per-dimension, and α is the amplifying factor.

We can represent the end-to-end system model by (4.4), similar to a $M \times N$ MIMO V-BLAST, with \mathbf{G} capturing the end-to-end channel effect and amplification in the transmission process. The channel matrix is presented column-wise, i.e. $\mathbf{G} = [\mathbf{g}_1, \dots, \mathbf{g}_N]$ where \mathbf{g}_i is a column vector. Based on the definition of \mathbf{G} , the overall SNR of $1 \times 2 \times N$ AF-CSM system at the destination, which corresponds to a particular transmitted symbol x_i , can be written as

$$\gamma_{x_i} = \sum_{j=1}^N \frac{[h_{R_i,S} \alpha_i g_{D_j,R_i}]^2}{[\alpha_1 g_{D_j,R_1} + \alpha_2 g_{D_j,R_2} + 1] \frac{N_0}{2}} \quad (5.9)$$

The calculation of the outage probability can be mathematically involved if we use amplification factor in (3.15). For this reason, we opted for the much more mathematically tractable tight upper bound [35] given by selecting the amplification factor α in each relay i to be

$$\alpha_i = \sqrt{\frac{E_r}{[|h_{R_i,S}|^2 E_s]}} \quad (5.10)$$

. By substituting this expression for α_i into (5.9), the SNR expression can be rewritten as

$$\gamma_i = \frac{2}{M} \sum_{j=1}^N \frac{\gamma'_{R_i,S} \gamma'_{D_j,R_i}}{\gamma'_{R_i,S} + \gamma'_{D_j,R_i}} \quad (5.11)$$

where $\gamma_{R_i,S}$ and γ_{D_j,R_i} are the SNR of source-relay and relay-destination, respectively, while also making a special note that $\gamma'_{R_i,S} = E_s \gamma_{R_i,S}$ and $\gamma'_{D_j,R_i} = M E_r \gamma_{D_j,R_i}$. Fig.5.1 compares the performance difference given by applying relay amplifying factor of (3.15) and (5.10). As we can see, (5.10) gives the upper bound in terms of system performance.

In the case of arbitrary N , since the transmit power in each terminal is distributed equally, (5.11) can be approximated by

$$\tilde{\gamma}_i = \frac{2N}{M} \left(\frac{\gamma'_{R_i,S} \gamma'_{D_j,R_i}}{\gamma'_{R_i,S} + \gamma'_{D_j,R_i}} \right) \quad (5.12)$$

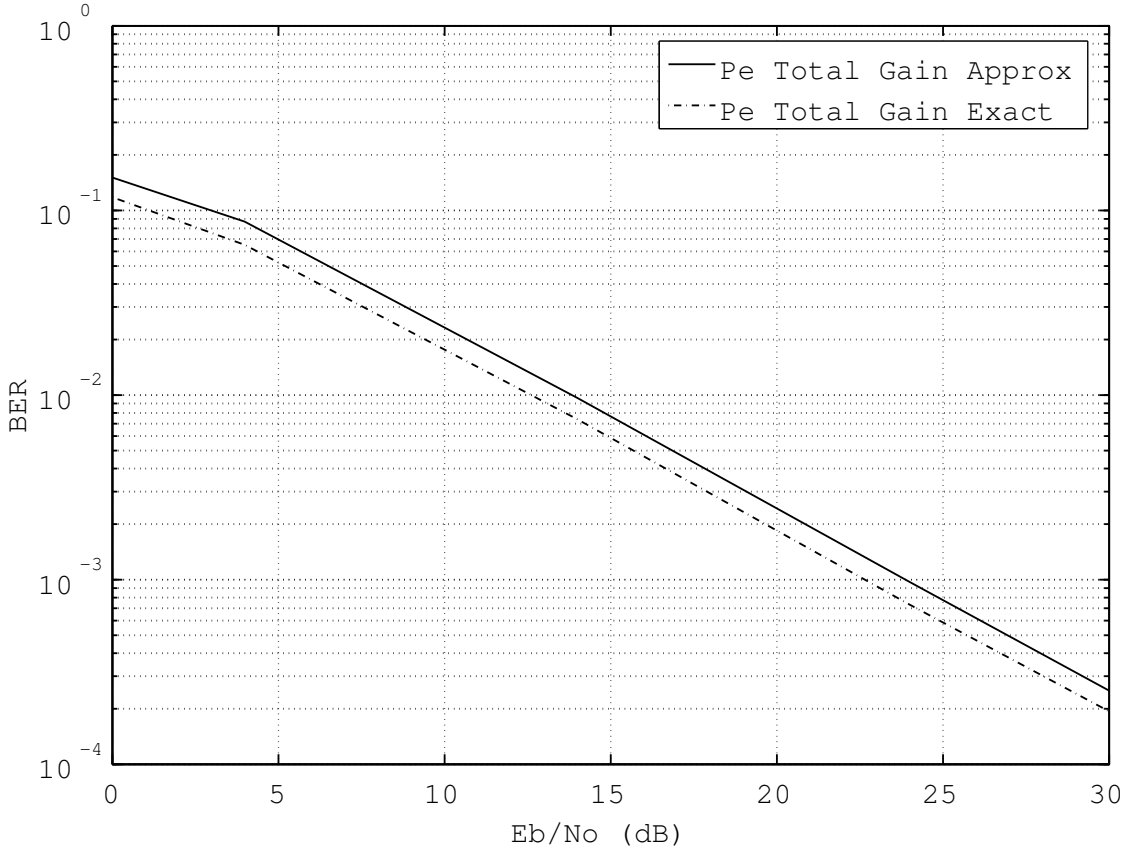


Figure 5.1 Comparison of exact (3.15) and approximate (5.10) relay amplifying factors.

In order to show how accurate the approximation is, SNR Monte-Carlo (5.11) and SNR Theory(5.12) are plotted in Fig.5.2 for several values of N . For $N = 2$, we could see almost no difference at all between the lines. When $N = 8$, due to accumulation of approximations, a small discrepancy between the values can be noticed, though it is still minimal.

Loyka and Gagnon presented in details a way to derive the outage probability of V-BLAST system in [33] using the Gram-Schmidt orthogonalization process, which will be the base of our methodology as well. In the derivation of outage probability, we are interested only in the vector signal received by the Rx antennas from the i th *virtual* Tx antenna:

$$\mathbf{y}_{D_i} = \mathbf{g}_i \quad (5.13)$$

Based on the Gram-Schmidt process, the received vector can be represented geometrically as

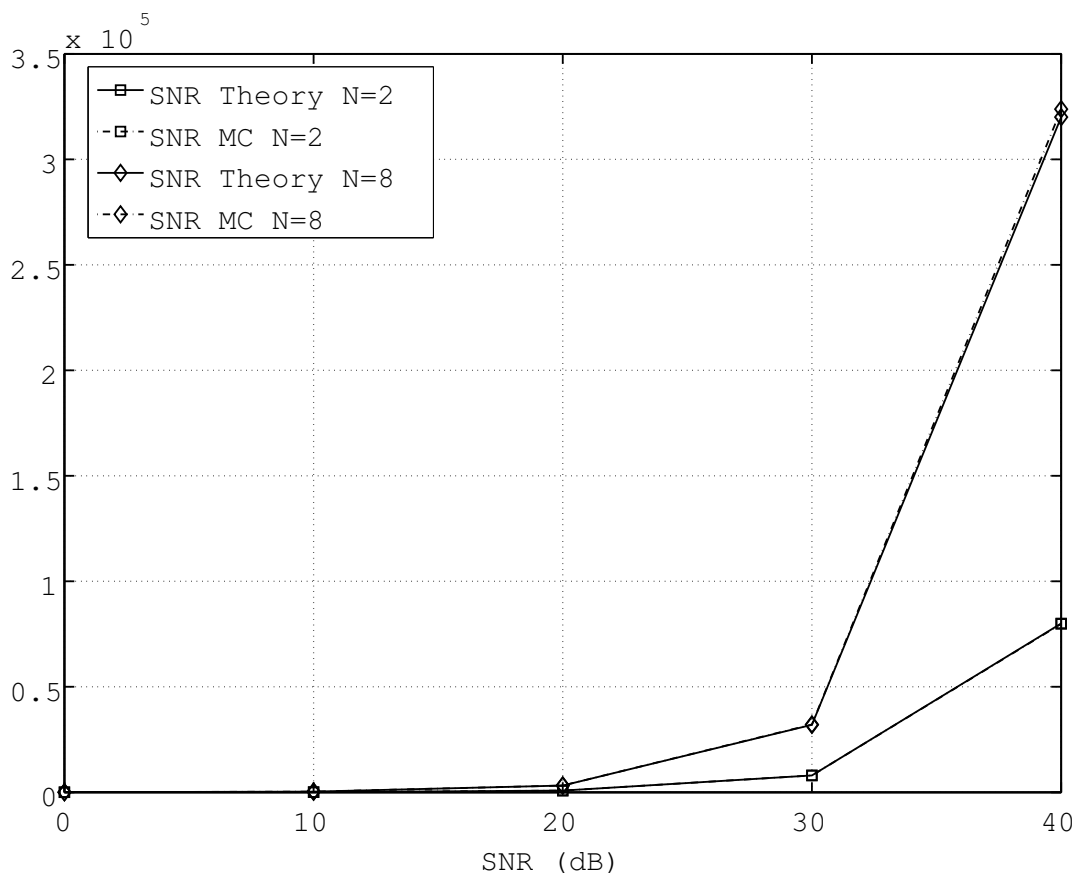


Figure 5.2 Comparison of exact (5.11) and approximate (5.12) SNR.

in Fig. 5.3. Then, \mathbf{g}_i can be decomposed into parallel $\mathbf{g}_{i\parallel}$ and orthogonal $\mathbf{g}_{i\perp}$ components with respect to the space spanned by the columns of \mathbf{G} , during the interference nulling out step. After the rotation by Ψ degree, the vector lengths and distributions are still preserved so that we can use the unprimed notations for ease of reading.

The outage probability of a $1 \times 2 \times N$ system is given by the CDF of $|\mathbf{g}_i|^2$ which is also the CDF of γ_i . Realizing the similarity between *Definition 1* and (5.12) in which

$$\tilde{\gamma}_i = a\mu_H(X_1, X_2) \quad (5.14)$$

we can conveniently use *Theorem 1* with transformation of random variables to get

$$\Pr[|\mathbf{g}_i|^2 < x] = 1 - \frac{x}{a} \sqrt{\beta_1 \beta_2} e^{-x(\beta_1 + \beta_2)/(2a)} K_1 \left(\frac{x}{a} \sqrt{\beta_1 \beta_2} \right) \quad (5.15)$$

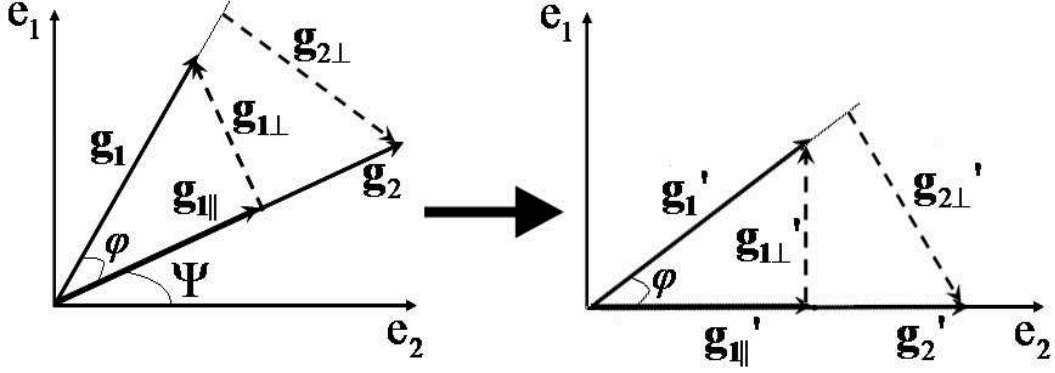


Figure 5.3 Geometrical representation of received vector signal & its rotation for $M = N = 2$ CSM.

where $a = N/M$ with M and N being the number of relays and receive antennas at the destination, respectively.

Thus, for a particular $1 \times 2 \times 2$ system, the outage probability will be given by

$$\begin{aligned}
 \Pr[|\mathbf{g}_1|^2 < x] &= \Pr[|\mathbf{g}_2|^2 < x] \\
 &= 1 - x\sqrt{\beta_1\beta_2}e^{-x(\beta_1+\beta_2)/(2)}K_1\left(x\sqrt{\beta_1\beta_2}\right) \\
 &= F_g(x)
 \end{aligned} \tag{5.16}$$

Since there are two symbols transmitted simultaneously, the detection will be conducted in two steps, one for each transmitted symbol. Hence, after the interference nulling, the next step is to decide which symbol should be detected first. This is done by applying the optimal SNR-based ordering discussed in [29] which is just a matter of selecting the received symbol with the larger SNR magnitude:

$$\begin{aligned}
 s_{r_1} &= \max[|\mathbf{g}_{1\perp}|^2, |\mathbf{g}_{2\perp}|^2] \\
 &= (\sin^2 \varphi)\max[|\mathbf{g}_1|^2, |\mathbf{g}_2|^2]
 \end{aligned} \tag{5.17}$$

This equation states that the signal power after optimal ordering (s_{r_1}) is obtained by comparing and taking the maximum of $|\mathbf{g}_{1\perp}|^2$ and $|\mathbf{g}_{2\perp}|^2$. A similar analogy is that the substream with largest pre-detection power will be detected first. Following the steps, the distribution F_{AF_1}

of s_{r_1} can be obtained by solving

$$\begin{aligned}
F_{AF_1}(x) &= \Pr[s_{r_1} < x] \\
&= \Pr\left[\max[|\mathbf{g}_1|^2, |\mathbf{g}_2|^2] < \frac{x}{\sin^2 \varphi}\right] \\
&= \int_0^{\pi/2} F_g^2\left(\frac{x}{\sin^2 \varphi}\right) f_\varphi(\varphi) d\varphi
\end{aligned} \tag{5.18}$$

Appendix A.2 shows the details on how to solve this integral where we have used the approximation of modified Bessel function for small arguments given in (5.3) to get the outage probability expression at the first detection step:

$$\begin{aligned}
F_{AF_1}(x) &= 1 - 2e^{-\frac{x(\beta_1 + \beta_2)}{2}} + e^{-x(\beta_1 + \beta_2)} \\
&\quad + x(\beta_1 + \beta_2) \left[\Gamma\left(0, \frac{x(\beta_1 + \beta_2)}{2}\right) - \Gamma(0, x(\beta_1 + \beta_2)) \right]
\end{aligned} \tag{5.19}$$

where $\Gamma(0, x)$ is the incomplete Gamma function defined in [37].

For the derivation of outage probability at the second detection step, we find the minimum length of the received vector without the need for further interference nulling:

$$s_{r_2} = \min[|\mathbf{g}_1|^2, |\mathbf{g}_2|^2] \tag{5.20}$$

which leads us to the outage probability $F_{AF_2}(x)$ of

$$\begin{aligned}
F_{AF_2}(x) &= \Pr[s_{r_2} < x] = 1 - [1 - F_g(x)]^2 \\
&= 1 - x^2 \beta_1 \beta_2 e^{-x(\beta_1 + \beta_2)} K_1^2\left(x \sqrt{\beta_1 \beta_2}\right)
\end{aligned} \tag{5.21}$$

The outage probability analysis above were carried out in terms of normalized signal powers. In order to get the outage probabilities in terms of instantaneous SNR, define γ_{th} as the threshold SNR, then substitute $x \rightarrow \gamma_{th}$ and $x \rightarrow 2\gamma_{th}$ for the first and second steps, respectively and finally, $\beta_1 \rightarrow 1/\bar{\gamma}_1$ and $\beta_2 \rightarrow 1/\bar{\gamma}_2$ with $\bar{\gamma}_1$ and $\bar{\gamma}_2$ being the average SNR at each link.

5.1.2 Uplink Decode-and-Forward

In DF-CSM, outage event is defined as the condition when outage occurs in either one of the source-relay or relay-destination links. The source-relay link is just an SISO with outage

probability given by

$$\begin{aligned} F_{R_i,S}(x) &= \Pr [|h_{R_i,S}|^2 < x] \\ &= 1 - e^{-\beta_1 x} \end{aligned} \quad (5.22)$$

As for the relay-destination link is a spatial multiplexing with V-BLAST successive interference cancelation decoding algorithm, we follow [33] to obtain the outage probability at the first and second decoding stage as

$$F_{RD_1}(x) = 1 - 2e^{-\beta_2 x} + \left(1 + \frac{\beta_2}{2}x\right) e^{-2\beta_2 x} \quad (5.23)$$

and

$$F_{RD_2}(x) = 1 - e^{-2\beta_2 x} (1 + \beta_2 x)^2 \quad (5.24)$$

Hence, the total end-to-end outage probability for decode-and-forward CSM system is given by

$$F_{DF_1} = F_{R_1,S} + [(1 - F_{R_1,S})F_{RD_1}] \quad (5.25)$$

$$F_{DF_2} = F_{R_2,S} + [(1 - F_{R_2,S})F_{RD_2}] \quad (5.26)$$

By definition of outage probability in DF-CSM system, the first right-hand side part of (5.25) and (5.26) states that outage occurs in the source-relay link (no outage in relay-destination link), while the second part tells that outage occurs only in the relay-destination link. Applying (5.22), (5.23), and (5.24) to (5.25) and (5.26), we obtain the end-to-end outage probabilities

$$F_{DF_1}(x) = 1 - 2e^{-(\beta_1+2\beta_2)x} + e^{-(\beta_1+4\beta_2)x} + \beta_2 x e^{-(\beta_1+4\beta_2)x} \quad (5.27)$$

at the first decoding stage, and

$$F_{DF_2}(x) = 1 - e^{-(\beta_1+4\beta_2)x} (1 + 2\beta_2 x)^2 \quad (5.28)$$

at the second decoding stage. Just as in AF case, the outage probability analysis above were carried out in terms of normalized signal powers. In order to get the outage probabilities in terms of instantaneous SNR, define γ_{th} as the threshold SNR, then substitute $x \rightarrow \gamma_{th}$, and finally $\beta_1 \rightarrow 1/\bar{\gamma}_1$ and $\beta_2 \rightarrow 1/\bar{\gamma}_2$ with $\bar{\gamma}_1$ and $\bar{\gamma}_2$ being the average SNR at each link.

5.1.3 Downlink Amplify-and-Forward

The downlink AF is different than the uplink scheme such that now the received signals are

$$y_{R_i} = \sum_{j=1}^M h_{R_i, S_j} x_j + n_{R_i}, \quad i = 1, \dots, N$$

at the relays, and

$$y_{D, R_i AF} = g_{D, R_i} \alpha_i y_{R_i} + n_D$$

at the destination, with the amplification factor given by

$$\alpha_i \leq \sqrt{\frac{E_r}{\left[\sum_{j=1}^M |h_{R_i, S_j}|^2 E_s + N_0 \right]}}, \quad i = 1, \dots, N$$

The end-to-end SNR of $2 \times N \times 1$ AF-CSM system at the destination, which corresponds to a particular transmitted symbol x_j , can be written as

$$\gamma_{x_j} = \sum_{i=1}^N \frac{[h_{R_i, S_j} \alpha_i g_{D, R_i}]^2}{[(\alpha_i g_{D, R_i}) + 1] \frac{N_0}{2}} \quad (5.29)$$

Just like in uplink case, a tight lower gain for the relay gain is much preferred for a feasible theoretical analysis:

$$\alpha_i \leq \sqrt{\frac{E_r}{\left[\sum_{j=1}^M |h_{R_i, S_j}|^2 E_s \right]}}, \quad i = 1, \dots, N \quad (5.30)$$

which leads us to another expression for the end-to-end SNR:

$$\gamma_i = \frac{2}{M} \sum_{j=1}^N \frac{\gamma'_{R_i, S_j} \gamma'_{D, R_i}}{\gamma'_{R_i, S_j} + \gamma'_{D, R_i}} \quad (5.31)$$

where $\gamma_{R_i, S}$ and γ_{D_j, R_i} are the SNR of source-relay and relay-destination, respectively, while also making a special note that $\gamma'_{R_i, S} = M E_s \gamma_{R_i, S}$ and $\gamma'_{D, R_i} = E_r \gamma_{D, R_i}$. In the case of small N , since the transmit power in each terminal is distributed equally, 5.31 can be approximated by

$$\tilde{\gamma}_i = \frac{2N}{M} \left(\frac{\gamma'_{R_i, S_j} \gamma'_{D, R_i}}{\gamma'_{R_i, S_j} + \gamma'_{D, R_i}} \right) \quad (5.32)$$

Having found the SNR of the AF-DL system and from the definition, the expression for the outage probability of $2 \times N \times 1$ system is given by

$$\Pr[|\mathbf{g}_i|^2 < x] = 1 - \frac{x}{a} \sqrt{\beta_1 \beta_2} e^{-x(\beta_1 + \beta_2)/(2a)} K_1 \left(\frac{x}{a} \sqrt{\beta_1 \beta_2} \right) \quad (5.33)$$

where $a = N/2$, N is the number of relaying terminals. Note that even if the outage probability expression is similar to AF-UL case, the parameter values are indeed different in each case. Accordingly, the expression for $2 \times 2 \times 1$ system will be written as

$$\begin{aligned} \Pr[|\mathbf{g}_1|^2 < x] &= \Pr[|\mathbf{g}_2|^2 < x] \\ &= 1 - x \sqrt{\beta_1 \beta_2} e^{-x(\beta_1 + \beta_2)/2} K_1 \left(x \sqrt{\beta_1 \beta_2} \right) \\ &= F_g(x) \end{aligned} \quad (5.34)$$

Now the task is to find which one to be detected first from the two transmitted symbols. In similar fashion, we use (5.17) and detect the symbol with higher SNR first to get the outage probability in the first detection step:

$$\begin{aligned} F_{AFDL_1}(x) &= 1 - 2e^{-\frac{x(\beta_1 + \beta_2)}{2}} + e^{-x(\beta_1 + \beta_2)} \\ &\quad + x(\beta_1 + \beta_2) \left[\Gamma \left(0, \frac{x(\beta_1 + \beta_2)}{2} \right) - \Gamma(0, x(\beta_1 + \beta_2)) \right] \end{aligned} \quad (5.35)$$

Next, by using (5.20) we find the outage probability in the second detection step is given by

$$\begin{aligned} F_{AFDL_2}(x) &= \Pr[s_{r_2} < x] = 1 - [1 - F_g(x)]^2 \\ &= 1 - x^2 \beta_1 \beta_2 e^{-x(\beta_1 + \beta_2)} K_1^2 \left(x \sqrt{\beta_1 \beta_2} \right) \end{aligned} \quad (5.36)$$

Note that the outage probability analysis were carried out in terms of normalized signal powers. In order to get the outage probabilities in terms of instantaneous SNR, substitute $x \rightarrow \gamma_{th}$ and $x \rightarrow 2\gamma_{th}$ for the first and second steps, respectively and finally, $\beta_1 \rightarrow 1/\bar{\gamma}_1$ and $\beta_2 \rightarrow 1/\bar{\gamma}_2$ with $\bar{\gamma}_1$ and $\bar{\gamma}_2$ being the average SNR at each link.

5.1.4 Downlink Decode-and-Forward

Similar to uplink DF-CSM, outage event is defined as the condition when outage occurs in either one of the source-relay or relay-destination links. In downlink case, the source-relay link

is just now the MIMO spatial multiplexing with outage probabilities for 2x2x1 system given by

$$F_{R,S_1}(x) = 1 - 2e^{-\beta_1 x} + \left(1 + \frac{\beta_1}{2}x\right) e^{-2\beta_1 x} \quad (5.37)$$

at the first detection stage and

$$F_{R,S_2}(x) = 1 - e^{-2\beta_1 x} (1 + \beta_1 x)^2 \quad (5.38)$$

at the second detection stage.

The relay-destination link is now SISO links with outage probability

$$\begin{aligned} F_{D,R_i}(x) &= \Pr [|h_{D,R_i}|^2 < x] \\ &= 1 - e^{-\beta_2 x} \end{aligned} \quad (5.39)$$

Hence, the total end-to-end outage probability for decode-and-forward CSM system is given by

$$F_{DFDL_1} = F_{R,S_1} + [(1 - F_{R,S_1})F_{D,R_1}] \quad (5.40)$$

$$F_{DFDL_2} = F_{R,S_2} + [(1 - F_{R,S_2})F_{D,R_2}] \quad (5.41)$$

By definition of outage probability in DF-CSM system, the first right-hand side part of (5.40) and (5.41) states that outage occurs in the source-relay link (no outage in relay-destination link), while the second part tells that outage occurs only in the relay-destination link. Applying (5.39), (5.37), and (5.38) to (5.40) and (5.41), we obtain the end-to-end outage probabilities for the downlink DF-CSM to be

$$F_{DFDL_1}(x) = 1 - 2e^{-(2\beta_1+\beta_2)x} + e^{-(4\beta_1+\beta_2)x} + \beta_1 x e^{-(4\beta_1+\beta_2)x} \quad (5.42)$$

at the first decoding stage, and

$$F_{DFDL_2}(x) = 1 - e^{-(4\beta_1+\beta_2)x} (1 + 2\beta_1 x)^2 \quad (5.43)$$

at the second decoding stage. The outage probability analysis above were carried out in terms of normalized signal powers. In order to get the outage probabilities in terms of instantaneous SNR, define γ_{th} as the threshold SNR, then substitute $x \rightarrow \gamma_{th}$, and finally $\beta_1 \rightarrow 1/\bar{\gamma}_1$ and $\beta_2 \rightarrow 1/\bar{\gamma}_2$ with $\bar{\gamma}_1$ and $\bar{\gamma}_2$ being the average SNR at each link.

5.2 Theoretical Bit-error Rate Analysis

In this section, we derive the average BER analytically using the results derived in previous section. Considering the fact that the instantaneous SNR distribution differs in all detection steps, the average BER also follows the same norm. The general expression for average BER at the i th detection step is given by

$$\overline{P_{e,i}} = \int_0^{\infty} \rho_i(\gamma) P_e(\gamma) d\gamma \quad (5.44)$$

where $\rho_i(\gamma)$ is the SNR pdf at the i th step, and $P_e(\gamma)$ is the instantaneous BER for a given instantaneous SNR realization of γ .

The probability of error is defined as the condition where there is at least one error during the detection steps, either at the first, second, or both steps. Hence, the total instantaneous BER will be

$$P_{e,tot} = P_{e,1} + P_{e,2}(1 - P_{e,1}) \quad (5.45)$$

where $P_{e,i}$ is the instantaneous BER at the i th step with instantaneous SNR of γ_i . Taking the expectation over channel fading, we get $\overline{P_{e,i}} = \langle P_{e,i} \rangle_{\gamma_{S_i}}$ from where we define the total average BER as

$$\overline{P_{e,tot}} = \langle P_{e,1} \rangle_{\gamma_{S_1}} + \langle P_{e,2} \rangle_{\gamma_{S_2}} - \langle P_{e,1} P_{e,2} \rangle_{\gamma_{S_1} \gamma_{S_2}} \quad (5.46)$$

$$\leq \overline{P_{e,1}} + \overline{P_{e,2}} \quad (5.47)$$

Mathematically, it is much more feasible to state the total BER as (5.47) than (5.46) because $\langle P_{e,1} P_{e,2} \rangle_{\gamma_{S_1} \gamma_{S_2}}$ is not independent of each other, thus the calculation gets quite involved. Moreover, the effect of $\langle P_{e,1} P_{e,2} \rangle_{\gamma_{S_1} \gamma_{S_2}}$ is *negligible* such that (5.47) gives a tight upper bound to the total average BER.

To better illustrate our results, we present the case where coherent BPSK is the modulation of choice. The instantaneous BER for BPSK is given by [38]:

$$P_e(\gamma) = Q(\sqrt{2\gamma}), \quad Q(x) = \frac{1}{\sqrt{2\pi}} \int_x^{\infty} e^{-\frac{t^2}{2}} dt \quad (5.48)$$

5.2.1 Uplink Amplify-and-Forward

In order to avoid having to do integration of Q-function in (5.44), for BPSK-modulated signal we use a simplified form of average BER calculation [33] given by

$$\begin{aligned}\overline{P_{e,i}} &= \int_0^\infty \rho_i(\gamma) P_e(\gamma) d\gamma \\ &= - \int_0^\infty F'_{AF_i}(\gamma) \frac{dP_e(\gamma)}{d\gamma} d\gamma\end{aligned}\quad (5.49)$$

with some transformations of variable

$$F'_{AF_1}(\gamma) = F_{AF_1}(\gamma) \quad F'_{AF_2}(\gamma) = F_{AF_2}(2\gamma) \quad (5.50)$$

Using (5.48), (5.49), and adjusting the previously calculated outage probability expressions into (5.50), we obtain the closed-form solution for the total average BER of 1x2x2 AF-CSM system at the first and second detection steps as

$$\begin{aligned}\overline{P_{e,1AF}} &= \frac{1}{2} - \frac{2}{\sqrt{\mathcal{O}_{\bar{\gamma}} + 2}} + \frac{1}{2} \sqrt{\frac{1}{\mathcal{O}_{\bar{\gamma}} + 1}} \\ &+ \frac{\Gamma(\frac{3}{2})\mathcal{O}_{\bar{\gamma}}}{3\sqrt{\pi}} \left[\frac{{}_2F_1\left(1, \frac{3}{2}; \frac{5}{2}; \frac{2}{\mathcal{O}_{\bar{\gamma}} + 2}\right)}{(\frac{\mathcal{O}_{\bar{\gamma}}}{2} + 1)\sqrt{\frac{\mathcal{O}_{\bar{\gamma}}}{2} + 1}} - \frac{{}_2F_1\left(1, \frac{3}{2}; \frac{5}{2}; \frac{1}{\mathcal{O}_{\bar{\gamma}} + 1}\right)}{(\mathcal{O}_{\bar{\gamma}} + 1)\sqrt{\mathcal{O}_{\bar{\gamma}} + 1}} \right]\end{aligned}\quad (5.51)$$

$$\overline{P_{e,2AF}} = \frac{1}{2} - \frac{1}{2} \sqrt{\frac{1}{2\mathcal{O}_{\bar{\gamma}} + 1}} \quad (5.52)$$

with

$$\mathcal{O}_{\bar{\gamma}} = \left(\frac{\bar{\gamma}'_{R_i,S} + \bar{\gamma}'_{D_j,R_i}}{\bar{\gamma}'_{R_i,S} \bar{\gamma}'_{D_j,R_i}} \right) \quad (5.53)$$

where $\bar{\gamma}_{R_i,S}$ and $\bar{\gamma}_{D_j,R_i}$ being the average SNR of source-relay and relay-destination links, respectively, while $\bar{\gamma}'_{R_i,S} = E_s \bar{\gamma}_{R_i,S}$ and $\bar{\gamma}'_{D_j,R_i} = M E_r \bar{\gamma}_{D_j,R_i}$. ${}_2F_1(\cdot)$ is the Gauss hypergeometric function defined in [37, Ch.15]. For the complete derivation details, the reader is referred to the Appendix.

In the general case of 1x2xN AF-CSM system, $\mathcal{O}_{\bar{\gamma}}$ is defined as

$$\mathcal{O}_{\bar{\gamma}} = \frac{2}{N} \left(\frac{\bar{\gamma}'_{R_i,S} + \bar{\gamma}'_{D_j,R_i}}{\bar{\gamma}'_{R_i,S} \bar{\gamma}'_{D_j,R_i}} \right) \quad (5.54)$$

5.2.2 Uplink Decode-and-Forward

For uplink DF-CSM, the average BER can be obtained by applying (5.27) and (5.28) into

$$\begin{aligned}\overline{P_{e,i}} &= \int_0^\infty \rho_i(\gamma) P_e(\gamma) d\gamma \\ &= - \int_0^\infty F'_{AF_i}(\gamma) \frac{dP_e(\gamma)}{d\gamma} d\gamma\end{aligned}$$

as in AF-CSM. We will use the fact that the source-relay and relay-destination links are independent, but not mutually exclusive of each other.

The average BER of DF-CSM in the first detection step is then given by solving

$$\begin{aligned}\overline{P_{e,1_{DF}}} &= \int_0^\infty F_{DF_1}(x) \left(\frac{1}{2\sqrt{\pi x}} e^{-x} \right) dx \\ &= \int_0^\infty \left(1 - 2e^{-(\beta_1+2\beta_2)x} + e^{-(\beta_1+4\beta_2)x} + \beta_2 x e^{-(\beta_1+4\beta_2)x} \right) \left(\frac{1}{2\sqrt{\pi x}} e^{-x} \right) dx\end{aligned}\quad (5.55)$$

in which we use [39, eq.3.381.4]

$$\int_0^\infty x^{\nu-1} e^{-\mu x} dx = \mu^{-\nu} \Gamma(\nu) \quad [\operatorname{Re}\mu > 0, \operatorname{Re}\nu > 0] \quad (5.56)$$

and get

$$\overline{P_{e,1_{DF}}} = \frac{1}{2} - \frac{1}{\sqrt{\beta_1 + 2\beta_2 + 1}} + \frac{1}{2\sqrt{\beta_1 + 4\beta_2 + 1}} + \frac{\Gamma(\frac{3}{2})\beta_2}{2\sqrt{\pi(\beta_1 + 4\beta_2 + 1)^3}} \quad (5.57)$$

Similarly, the average BER in the second detection step can be found by solving

$$\begin{aligned}\overline{P_{e,2_{DF}}} &= \int_0^\infty F_{DF_2}(x) \left(\frac{1}{2\sqrt{\pi x}} e^{-x} \right) dx \\ &= \int_0^\infty \left(1 - e^{-(\beta_1+4\beta_2)x} (1 + 2\beta_2 x)^2 \right) \left(\frac{1}{2\sqrt{\pi x}} e^{-x} \right) dx\end{aligned}\quad (5.58)$$

for which, after several straight away integrations, gives the expression

$$\overline{P_{e,2_{DF}}} = \frac{1}{2} - \frac{1}{2\sqrt{\beta_1 + 4\beta_2 + 1}} - \frac{2\Gamma(\frac{3}{2})\beta_2}{\sqrt{\pi(\beta_1 + 4\beta_2 + 1)^3}} + \frac{2\Gamma(\frac{5}{2})\beta_2^2}{\sqrt{\pi(\beta_1 + 4\beta_2 + 1)^5}} \quad (5.59)$$

where $\beta_1 \rightarrow 1/\bar{\gamma}_{R_i,S}$ and $\beta_2 \rightarrow 1/\bar{\gamma}_{D_j,R_i}$ with $\bar{\gamma}_{R_i,S}$ and $\bar{\gamma}_{D_j,R_i}$ being the average SNR at each link.

The total end-to-end average BER of DF-CSM is obtained by calculating

$$\overline{P_{e,totDF}} = \overline{P_{e,1DF}} + \overline{P_{e,2DF}} - \overline{P_{e,1DF}P_{e,2DF}} \quad (5.60)$$

$$\leq \overline{P_{e,1DF}} + \overline{P_{e,2DF}} \quad (5.61)$$

of which can be conveniently plotted without having to run lengthy Monte-Carlo simulations.

5.2.3 Downlink Amplify-and-Forward

The analysis for probability of error in downlink AF is very similar to the uplink case where we start with the definition:

$$\begin{aligned} \overline{P_{e,i}} &= \int_0^\infty \rho_i(\gamma) P_e(\gamma) d\gamma \\ &= - \int_0^\infty F'_{AFDL_i}(\gamma) \frac{dP_e(\gamma)}{d\gamma} d\gamma \end{aligned} \quad (5.62)$$

with some transformation of variables

$$F'_{AFDL_1}(\gamma) = F_{AFDL_1}(\gamma) \quad F'_{AFDL_2}(\gamma) = F_{AFDL_2}(2\gamma) \quad (5.63)$$

Using (5.48), (5.62), and adjusting the appropriate outage probability expressions into (5.63), we obtain the closed-form solution for the total average BER of 2x2x1 AF-CSM system at the first and second detection steps as

$$\begin{aligned} \overline{P_{e,1AFDL}} &= \frac{1}{2} - \frac{2}{\sqrt{\mathcal{O}_{\bar{\gamma}} + 2}} + \frac{1}{2} \sqrt{\frac{1}{\mathcal{O}_{\bar{\gamma}} + 1}} \\ &+ \frac{\Gamma(\frac{3}{2})\mathcal{O}_{\bar{\gamma}}}{3\sqrt{\pi}} \left[\frac{{}_2\mathcal{F}_1\left(1, \frac{3}{2}; \frac{5}{2}; \frac{2}{\mathcal{O}_{\bar{\gamma}} + 2}\right)}{(\frac{\mathcal{O}_{\bar{\gamma}}}{2} + 1)\sqrt{\frac{\mathcal{O}_{\bar{\gamma}}}{2} + 1}} - \frac{{}_2\mathcal{F}_1\left(1, \frac{3}{2}; \frac{5}{2}; \frac{1}{\mathcal{O}_{\bar{\gamma}} + 1}\right)}{(\mathcal{O}_{\bar{\gamma}} + 1)\sqrt{\mathcal{O}_{\bar{\gamma}} + 1}} \right] \end{aligned} \quad (5.64)$$

$$\overline{P_{e,2AFDL}} = \frac{1}{2} - \frac{1}{2} \sqrt{\frac{1}{2\mathcal{O}_{\bar{\gamma}} + 1}} \quad (5.65)$$

with

$$\mathcal{O}_{\bar{\gamma}} = \left(\frac{\bar{\gamma}'_{R_i, S_j} + \bar{\gamma}'_{D, R_i}}{\bar{\gamma}'_{R_i, S_j} \bar{\gamma}'_{D, R_i}} \right) \quad (5.66)$$

where $\bar{\gamma}_{R_i, S_j}$ and $\bar{\gamma}_{D, R_i}$ being the average SNR of source-relay and relay-destination links, respectively, while $\bar{\gamma}'_{R_i, S_j} = ME_s \bar{\gamma}_{R_i, S_j}$ and $\bar{\gamma}'_{D, R_i} = E_r \bar{\gamma}_{D, R_i}$. ${}_2F_1(\cdot)$ is the Gauss hypergeometric function defined in [37, Ch.15]. For the complete derivation details, the reader is referred to the Appendix. For the complete derivation details, the reader is referred to the Appendix.

In the general case of $2 \times N \times 1$ AF-CSM system, $\mathcal{O}_{\bar{\gamma}}$ is defined as

$$\mathcal{O}_{\bar{\gamma}} = \frac{2}{N} \left(\frac{\bar{\gamma}'_{R_i, S_j} + \bar{\gamma}'_{D, R_i}}{\bar{\gamma}'_{R_i, S_j} \bar{\gamma}'_{D, R_i}} \right) \quad (5.67)$$

5.2.4 Downlink Decode-and-Forward

For downlink DF-CSM, the average BER can be obtained in similar manner as in uplink DF-CSM, which is by applying (5.42) and (5.43) into

$$\begin{aligned} \overline{P_{e,i}} &= \int_0^\infty \rho_i(\gamma) P_e(\gamma) d\gamma \\ &= - \int_0^\infty F'_{AF_i}(\gamma) \frac{dP_e(\gamma)}{d\gamma} d\gamma \end{aligned}$$

The average BER of DF-CSM in the first detection step is then given by solving

$$\begin{aligned} \overline{P_{e,1_{DF}}} &= \int_0^\infty F_{DFDL_1}(x) \left(\frac{1}{2\sqrt{\pi x}} e^{-x} \right) dx \\ &= \int_0^\infty \left(1 - 2e^{-(2\beta_1 + \beta_2)x} + e^{-(4\beta_1 + \beta_2)x} + \beta_1 x e^{-(4\beta_1 + \beta_2)x} \right) \left(\frac{1}{2\sqrt{\pi x}} e^{-x} \right) dx \end{aligned} \quad (5.68)$$

in which we use [39, eq.3.381.4]

$$\int_0^\infty x^{\nu-1} e^{-\mu x} dx = \mu^{-\nu} \Gamma(\nu) \quad [\operatorname{Re} \mu > 0, \operatorname{Re} \nu > 0] \quad (5.69)$$

and get

$$\overline{P_{e,1_{DFDL}}} = \frac{1}{2} - \frac{1}{\sqrt{2\beta_1 + \beta_2 + 1}} + \frac{1}{2\sqrt{4\beta_1 + \beta_2 + 1}} + \frac{\Gamma(\frac{3}{2})\beta_1}{2\sqrt{\pi}(4\beta_1 + \beta_2 + 1)^3} \quad (5.70)$$

Similarly, the average BER in the second detection step can be found by solving

$$\begin{aligned} \overline{P_{e,2_{DFDL}}} &= \int_0^\infty F_{DFDL_2}(x) \left(\frac{1}{2\sqrt{\pi x}} e^{-x} \right) dx \\ &= \int_0^\infty \left(1 - e^{-(4\beta_1 + \beta_2)x} (1 + 2\beta_1 x)^2 \right) \left(\frac{1}{2\sqrt{\pi x}} e^{-x} \right) dx \end{aligned} \quad (5.71)$$

for which, after several straight away integrations, gives the expression

$$\overline{P_{e,2DFDL}} = \frac{1}{2} - \frac{1}{2\sqrt{4\beta_1 + \beta_2 + 1}} - \frac{2\Gamma(\frac{3}{2})\beta_1}{\sqrt{\pi(4\beta_1 + \beta_2 + 1)^3}} + \frac{2\Gamma(\frac{5}{2})\beta_1^2}{\sqrt{\pi(4\beta_1 + \beta_2 + 1)^5}} \quad (5.72)$$

where $\beta_1 \rightarrow 1/\bar{\gamma}_{R_i,S_j}$ and $\beta_2 \rightarrow 1/\bar{\gamma}_{D,R_i}$ with $\bar{\gamma}_{R_i,S_j}$ and $\bar{\gamma}_{D,R_i}$ being the average SNR at source-relay and relay-destination links, respectively.

The total end-to-end average BER of DF-CSM is obtained by calculating

$$\overline{P_{e,totDFDL}} = \overline{P_{e,1DFDL}} + \overline{P_{e,2DFDL}} - \overline{P_{e,1DFDL}P_{e,2DFDL}} \quad (5.73)$$

$$\leq \overline{P_{e,1DFDL}} + \overline{P_{e,2DFDL}} \quad (5.74)$$

of which can be conveniently plotted without having to run lengthy Monte-Carlo simulations.

5.3 Numerical Results and Discussions

We apply our results to 1x2x2 (i.e. a source, two relays, and a two-antenna receiver) AF-CSM and DF-CSM systems with BPSK modulation ($m = 3$) where the normalized source-relay distance is 0.5 (i.e. relays are halfway between source and destination) under Rayleigh fading condition and without loss of generality, set the antenna gains to 1. The amount of total transmit power in the system is constrained by $P = P_s + NP_r$, and we take the case where $P_s = P_r$.

Fig. 5.4 shows the pre-processing (F_g) and post-ordering (F_1 and F_2) outage probabilities of uplink AF-CSM and DF-CSM systems. Based on the definition of outage conditions, DF system has more tendency to go into outage and it is reflected by its higher pre-processing outage probability curve (F_{pre} DF-UL), when compared to AF (F_{pre} AF-UL). On the other hand, in AF scheme post-ordering state, due to the noisy end-to-end double gaussian channel, the symbol with minimum SNR tends to show higher outage behavior (F_2 AF-UL). From the slope of the outage probability curves, we can see that the diversity order of uplink CSM system at the i th processing stage is 1.

The theoretical average BER performance for uplink AF-CSM is shown in Fig. 5.5. Since we assume that the first transmitted symbol is detected first based on SNR ordering, the symbol

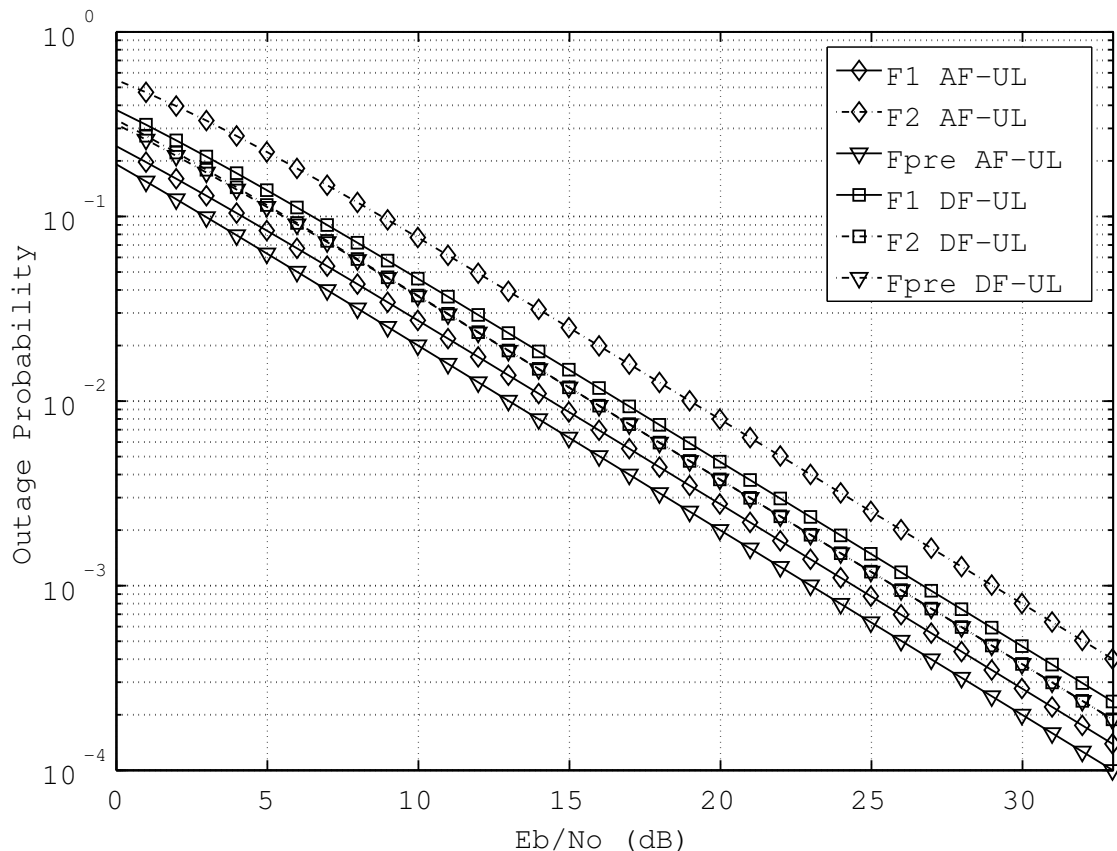


Figure 5.4 Theoretical Outage Probability of Uplink AF and DF-CSM.

with larger SNR magnitude will mostly be decoded correctly, thus the lower BER curve. This also shows that accuracies in both detection steps are equally important, such that they equally contribute to the overall system performance. It is also shown that our analysis model (PeTot AF-UL) is accurate enough compared to the Monte-Carlo result (AF-UL MC) despite the approximations and simplifying assumptions made in the derivation steps.

Fig. 5.6 shows the theoretical average BER performance of uplink DF-CSM, in which we can see that our analysis model is extremely accurate.

Fig. 5.7 and Fig. 5.8 show different performance criteria of downlink AF-CSM and DF-CSM systems. As we can see, downlink systems behave more or less similar than uplink scheme, except that in downlink CSM, DF scheme's pre-processing outage probability is lower than AF's. This is due to the employment of spatial multiplexing early in the source-relay link,

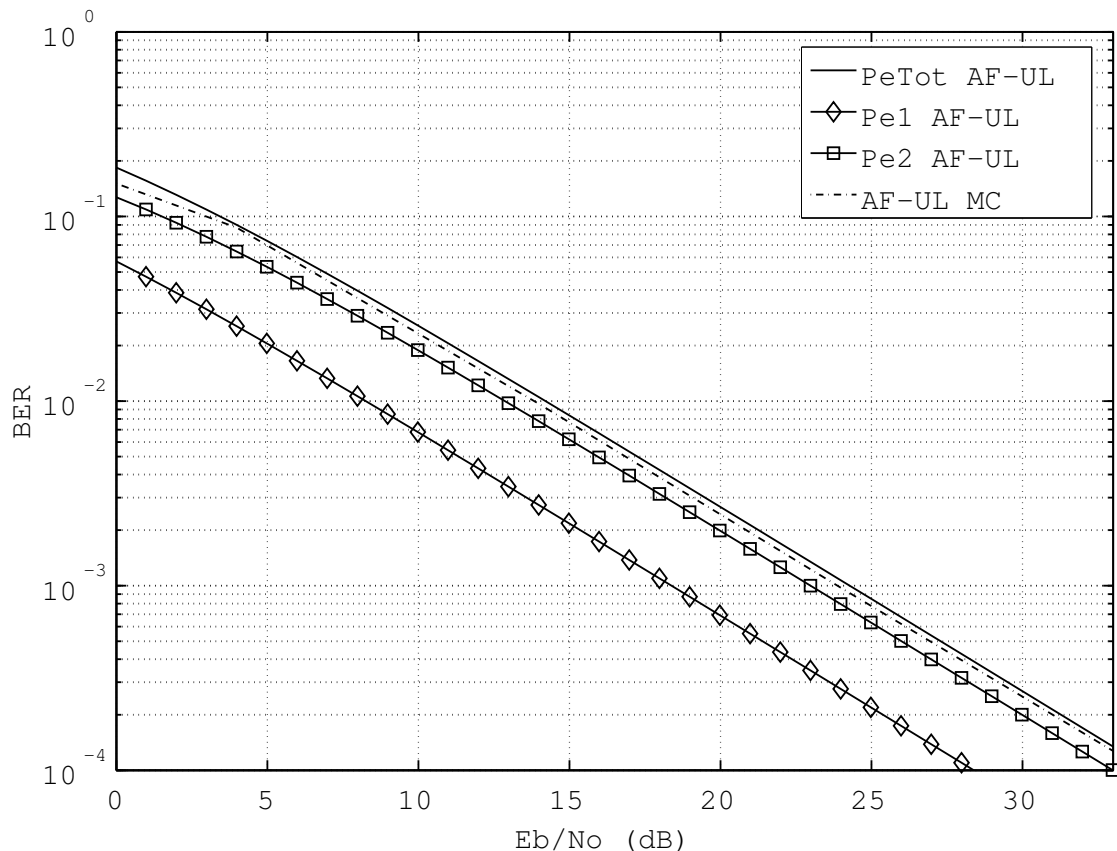


Figure 5.5 Theoretical BER of Uplink AF-CSM.

such that the transmitted signal is less likely to go into outage condition.

The performance of the CSM systems can definitely be optimized further by allocating the source and relay transmit power accordingly, depending on the relay locations [28], [29], and [30]. Having derived the theoretical expressions for the outage probability and BER, we can conveniently plot the behavior of the systems at different relay locations. As an example, Fig.5.9 depicts the dynamic behavior of the CSM systems at a low SNR condition of 10dB. With this figure, the system may select relays at locations which will maximize the performance depending on the transmission needs. For instance, if user download performance is the priority, the system selects relays which are relatively closer to the destination side. Likewise, if a user is uploading data, selecting relays which are close to the user side would be best. For voice data calls, the system should have a balance error-rate performance for both uplink and downlink

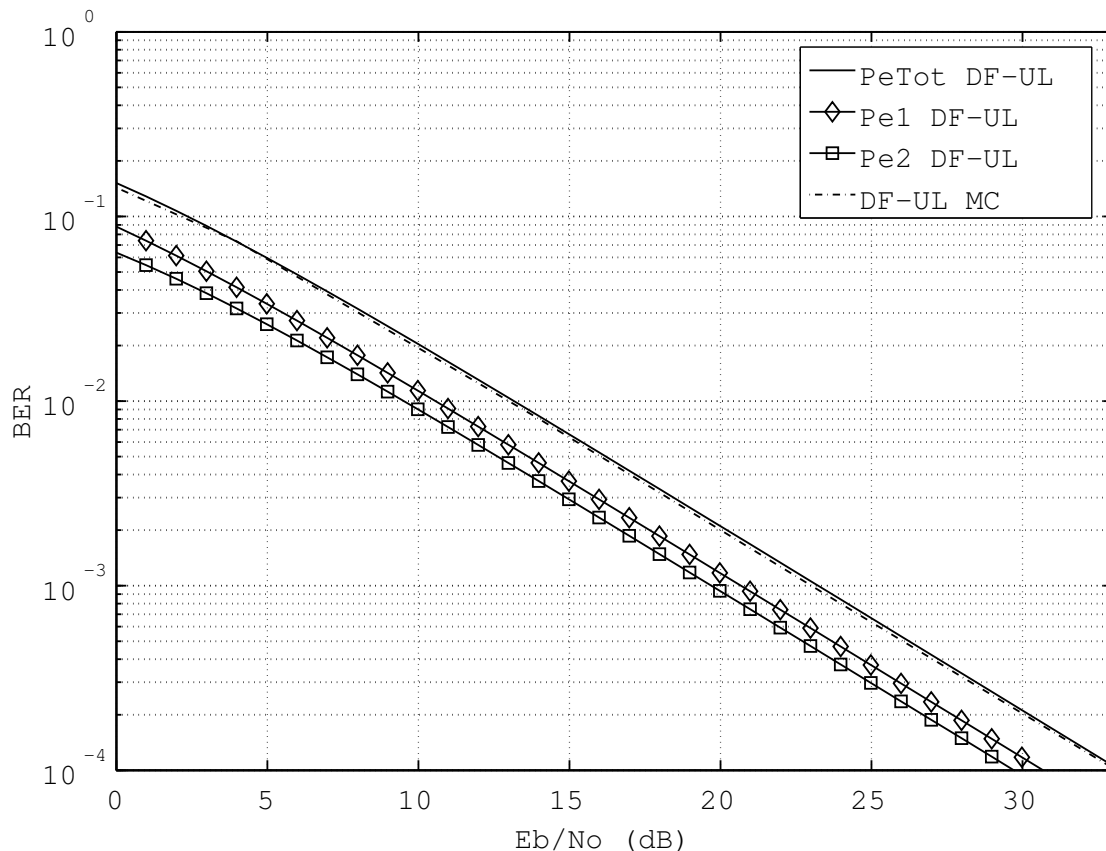


Figure 5.6 Theoretical BER of Uplink DF-CSM.

transmissions such that relays located about half-way between the user and base-station are preferred. Moreover, when the relays are located at particular distances from the source, performance-wise, CSM systems will even surpass theoretical MIMO V-BLAST.

Fig.5.10 shows the BER performance of the uplink and downlink CSM systems for various SNR and normalized source-relay distances in 3-D surface plots. It can be seen that the performance trend of the systems are similar: it improves with increasing SNR, and reaches global maximum at a particular source-relay distance.

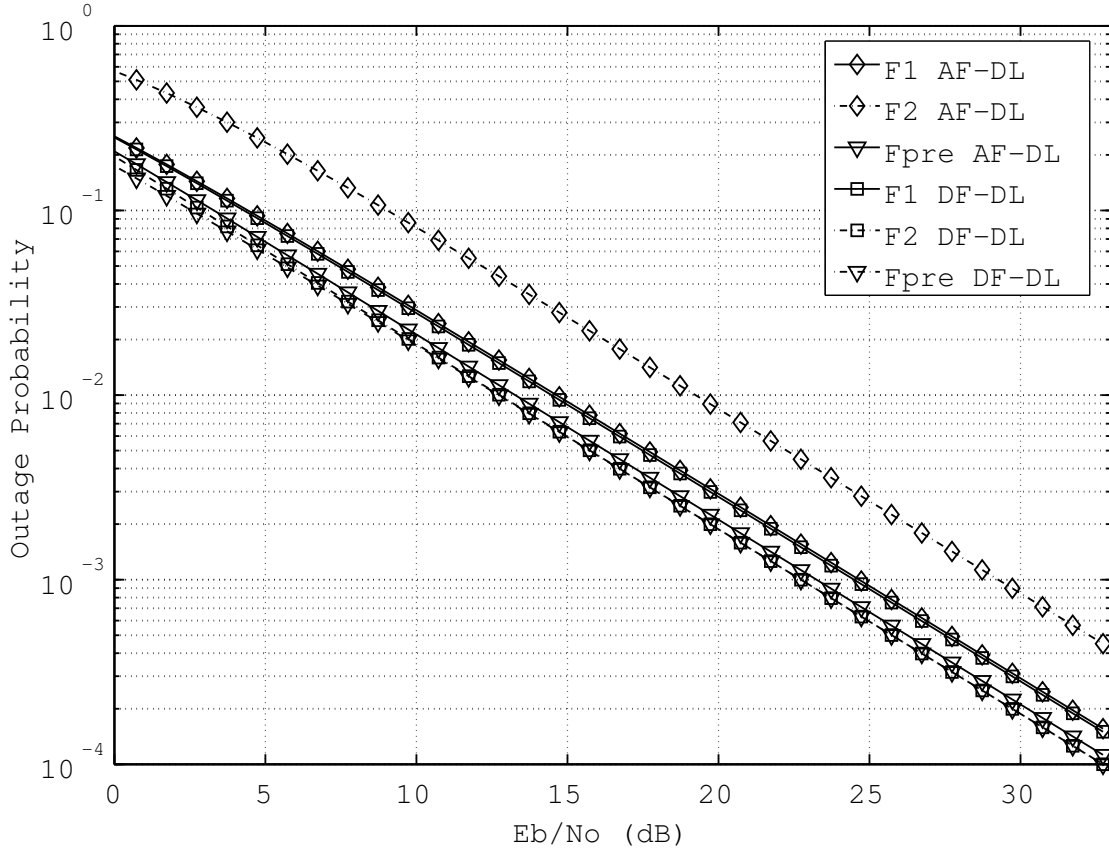


Figure 5.7 Theoretical Outage Probability of Downlink AF and DF-CSM.

5.4 Conclusions

We derived closed-form solutions for the theoretical outage probability and average bit error rate performance of both uplink and downlink amplify-and-forward and decode-and-forward cooperative spatial multiplexing system using the Gram-Schmidt orthogonalization process. In uplink DF-CSM case, it is very crucial to maintain a good source-relay link, such that the relays make reliable estimation of the transmitted signal in order to avoid propagation error during the final decoding process. Following similar derivation methods, average BER analysis for other modulation schemes (e.g. FSK, QPSK, QAM, etc) can also be derived easily by changing (5.48) to the respective appropriate expressions. It is shown that our analytical results give a good estimation on the performance of the uplink-downlink AF and DF CSM

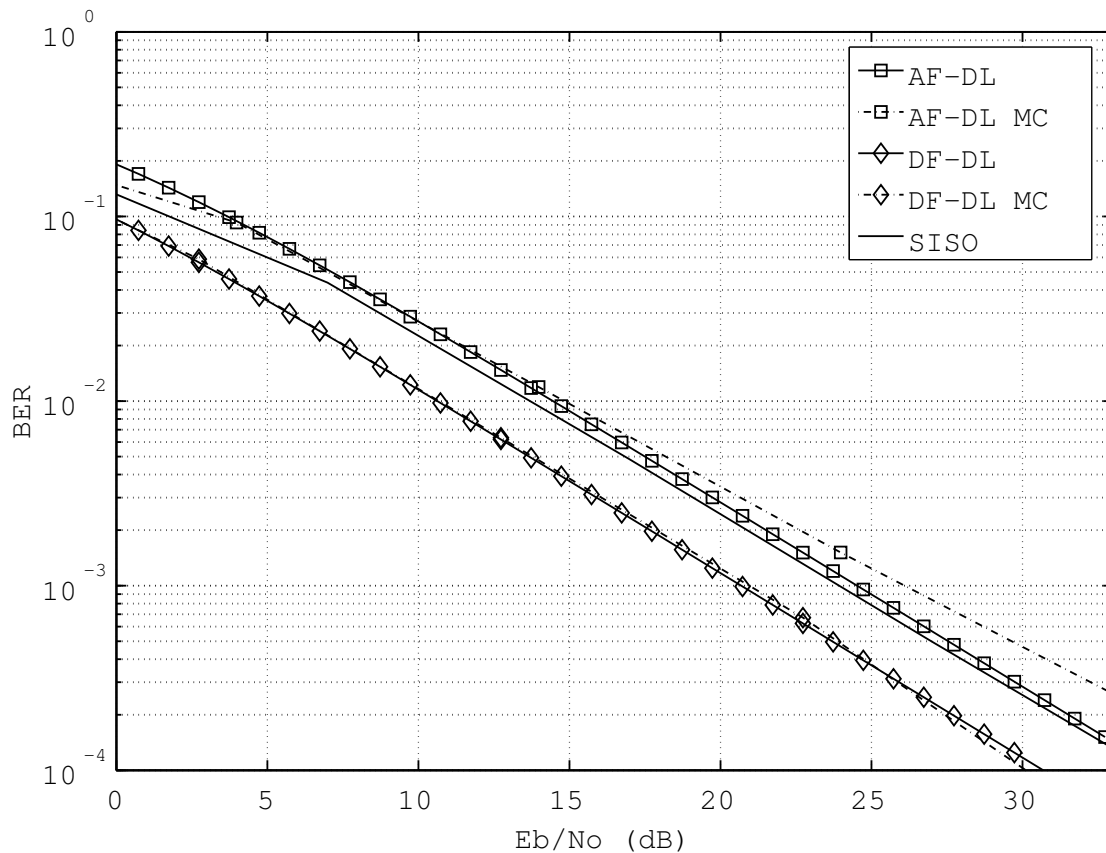
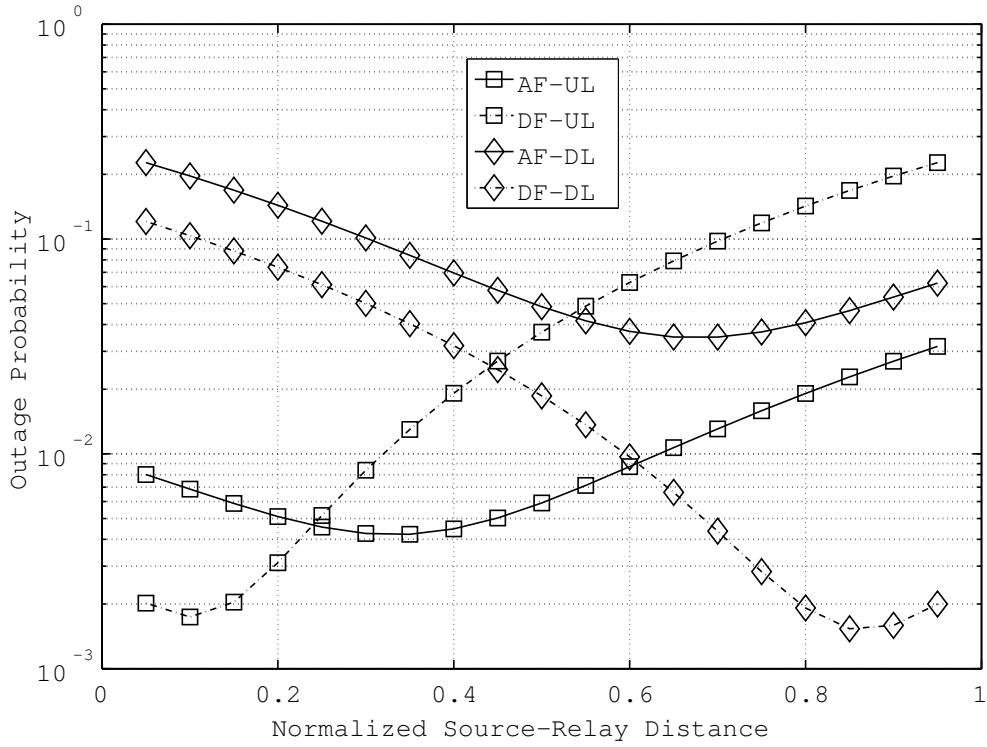


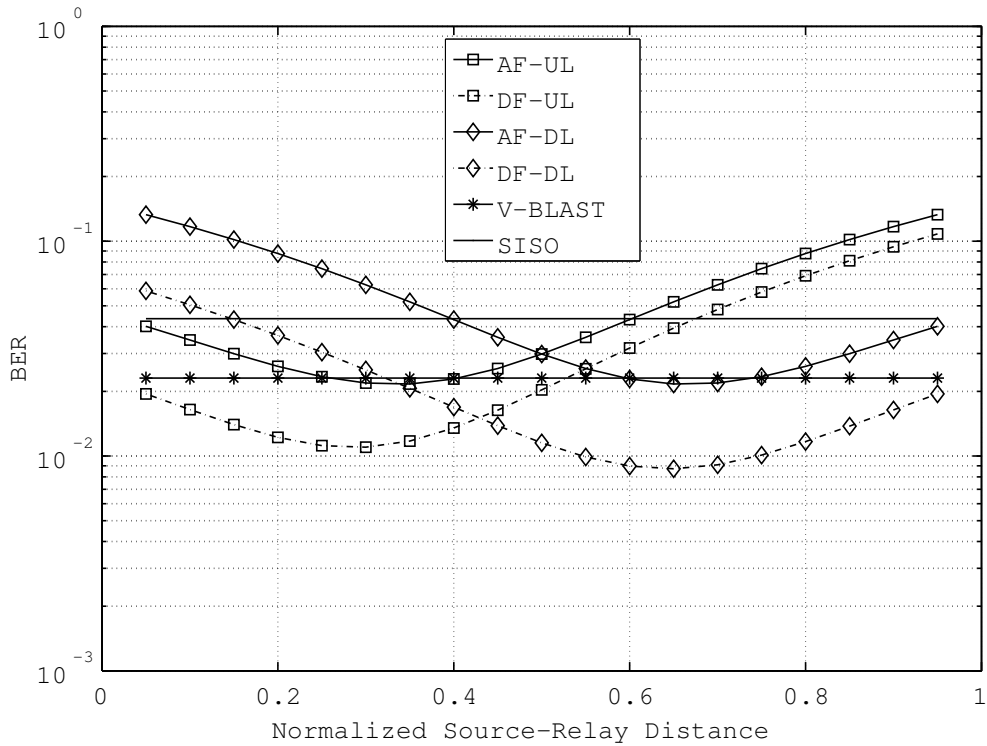
Figure 5.8 Theoretical BER of Downlink AF and DF-CSM.

systems, and hence time-consuming Monte-Carlo simulations can be avoided.

Although a rigorous algorithm is beyond the scope of this work, our derivations can also be used as a great tool to approach the relay selection problem. By plotting relay locations vs. BER or outage probability, given a particular link condition, one can observe the dynamic system behavior conveniently when relays of certain locations are selected. This way, the system is able to choose the relays (out of many candidates) which will maximize the end-to-end system performance based on the transmission goal.



(a) Outage probability



(b) Probability of bit-error

Figure 5.9 Relay location vs. BER performance, SNR = 10dB.

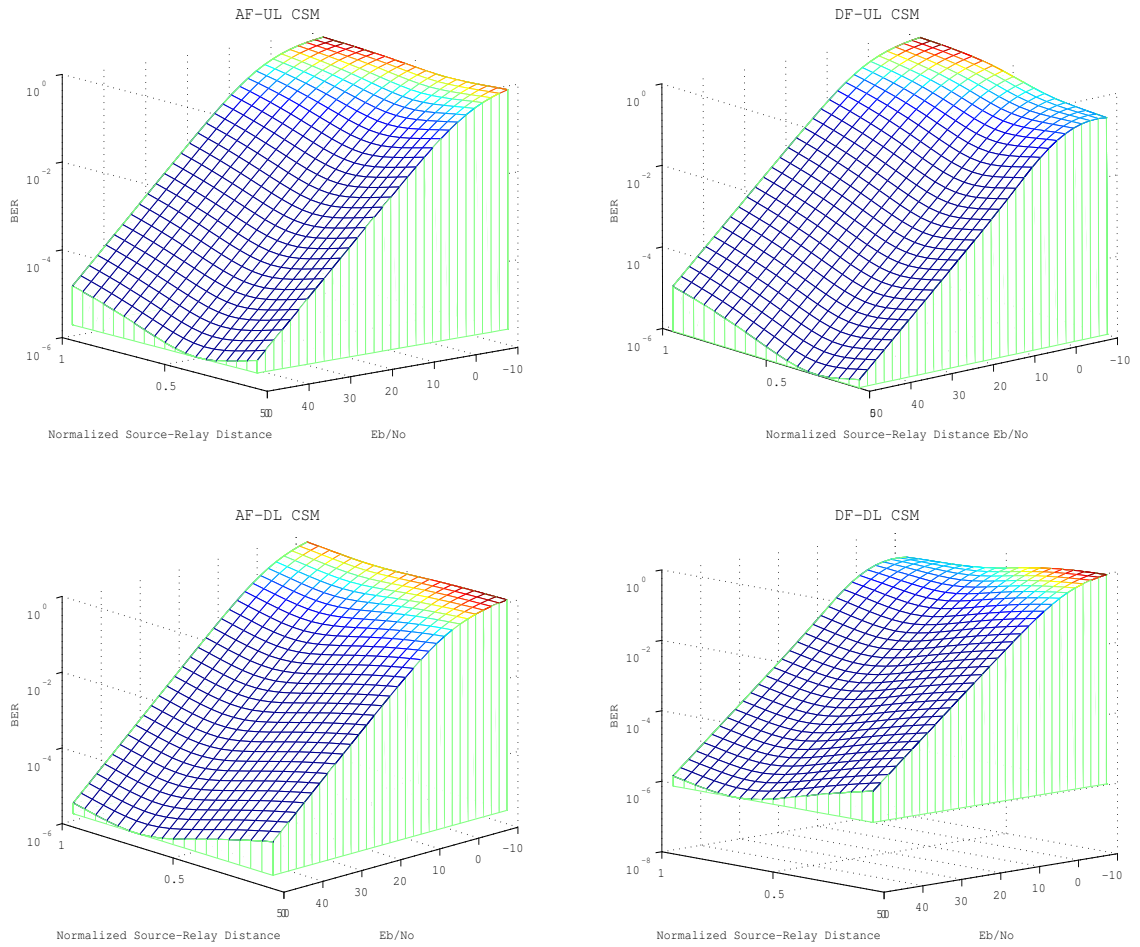


Figure 5.10 Theoretical BER of Downlink AF and DF-CSM, various SNR & source-relay distances.

CHAPTER 6. THEORETICAL CAPACITY OF COOPERATIVE SPATIAL MULTIPLEXING SYSTEM

The concept of channel capacity is an important one to be analyzed in any communications systems. Looking back into 1948, the breakthrough paper “A Mathematical Theory of Communication” by Claude E. Shannon [1] was the first one to describe of achieving error-free communication rate given input distribution, transmission power, noise power, and bandwidth. This maximum achievable error-free rate is what people now refer as channel capacity. And ever since, research on transceivers operating to the capacity limit has been the goal for communications engineers and information theorists.

Shannon described that a bandlimited signal, which is limited to duration T and bandwidth W , is given by

$$C = WT \log_2 \left(1 + \frac{S}{N} \right) \quad (6.1)$$

Since our analysis deals for normalized channel capacity for simplicity, the capacity expression can then be simplified to

$$C = \log_2 \left(1 + \frac{S}{N} \right) \quad (6.2)$$

with unit bits/s/Hz and S/N being the signal-to-noise ratio at the receiving antenna.

Instead of analyzing the instantaneous capacity under ergodic channel which tells us the maximum capacity of a system given a particular realization of the channel, our particular interest is when the channel is non-ergodic. Under non-ergodicity assumption, channel realizations are randomly fixed at the beginning of the transmission and kept constant over the duration of the codeword transmission. As a result, capacity will then be a random variable itself, and there will be non-zero probability that the channel cannot support the transmis-

sion rate. The probability of the channel capacity falls below a pre-determined threshold c_{th} is defined as the outage capacity probability. Outage capacity can be analyzed in a straight forward sense by applying simple transformations of RV and (6.2) to our previous results for outage probability expressions. Furthermore, we also assume that the CSI are known only to the receiving terminals, and the modulation of choice is BPSK.

6.1 Uplink Amplify-and-Forward

In uplink AF-CSM, the capacity is calculated for end-to-end system given by

$$C = 0.5 \times \log_2(1 + \bar{\gamma}_{eq}) \quad (6.3)$$

where $\bar{\gamma}_{eq}$ is the equivalent SNR given in (5.12), and the factor 0.5 denotes the bandwidth compared to no relay case. For a $1 \times M \times N$ system where there are M decoding steps which give different post-processing SNR, the channel capacity will be determined by the lowest symbol rate such that

$$C_{AF-UL} = 0.5 \times M \times \min \{ \log_2(1 + \bar{\gamma}_i) \} \quad i = 1, 2 \dots M \quad (6.4)$$

where $\bar{\gamma}_i$ is the post-processing SNR at the i^{th} detection steps whose cumulative distribution functions (CDF) are described by (5.19) and (5.21).

Using simple transformation of RV, we show that the channel outage capacity of $1 \times 2 \times 2$ uplink AF-CSM system in the first and second detection steps are respectively given by

$$C_{AF_1}(c_{th}) = 1 - 2e^{-\frac{C(\beta_1 + \beta_2)}{2}} + e^{-C(\beta_1 + \beta_2)} + C(\beta_1 + \beta_2) \left[\Gamma \left(0, \frac{C(\beta_1 + \beta_2)}{2} \right) - \Gamma(0, C(\beta_1 + \beta_2)) \right] \quad (6.5)$$

and

$$C_{AF_2}(c_{th}) = 1 - C^2 \beta_1 \beta_2 e^{-C(\beta_1 + \beta_2)} K_1^2 \left(C \sqrt{\beta_1 \beta_2} \right) \quad (6.6)$$

where

$$C = 2^{c_{th}/(0.5M)} - 1 \quad (6.7)$$

From (6.5) and (6.6), the total outage capacity probability is then given by

$$C_{AF-UL} = C_{AF_1} + C_{AF_2} - C_{AF_1} \times C_{AF_2} \quad (6.8)$$

6.2 Uplink Decode-and-Forward

The uplink DF-CSM utilizes regenerative relay such that the source message is fully decoded by the relays. DF transmission also requires that both the relays and destination decode the entire codeword without error. Hence, the channel capacity of $1 \times M \times N$ uplink DF-CSM is given by

$$C_{DF-UL} = 0.5 \times \min\{C_{sr}, C_{rd}\} \quad (6.9)$$

where C_{sr} and C_{rd} are capacities of the source-relay and relay-destination links, respectively.

Broadcast link from the source to relay can be viewed as M number of SISO transmissions originating from the same source terminal. Hence the maximum source-relay channel capacity C_{sr} is determined by M times the minimum of source to i^{th} relay transmission rates

$$C_{sr} = 0.5 \times M \times \min\{C_{sr_i}\} \quad i = 1, 2 \dots M \quad (6.10)$$

On the other hand, relay to destination link takes the form of a MIMO with V-BLAST configuration such that the capacity equals M times the smallest capacity of the M decoding steps, with similar methodology as uplink AF-CSM case

$$C_{rd} = 0.5 \times M \times \min\{\log_2(1 + \bar{\gamma}_{r_i d})\} \quad i = 1, 2 \dots M \quad (6.11)$$

where $\bar{\gamma}_{r_i d}$ is the post-processing SNR in i^{th} decoding stage.

For a $1 \times 2 \times 2$ uplink DF-CSM system, outage capacity C_{sr} is given by

$$C_{sr} = 1 - e^{-2\beta_1 C} \quad (6.12)$$

and relay-destination outage capacities at the first and second detection stage are

$$C_{r_1 d} = 1 - 2e^{-\beta_2 C} + \left(1 + \frac{\beta_2}{2} C\right) e^{-2\beta_2 C} \quad (6.13)$$

$$C_{r_2 d} = 1 - (1 + \beta_2 C)^2 e^{-2\beta_2 C} \quad (6.14)$$

where $\mathcal{C} = 2^{c_{th}/(0.5M)} - 1$. From (6.9), the outage capacity probability of uplink DF-CSM system is

$$C_{DF-UL} = C_{sr} + C_{rd} - C_{sr} \times C_{rd} \quad (6.15)$$

6.3 Downlink Amplify-and-Forward

The channel capacity for $M \times N \times 1$ downlink AF-CSM can be calculated in the similar manner as uplink case, where the end-to-end system is equivalent to $M \times N$ MIMO transmission. Since the transmitter does not know the highest rate for each antenna, the capacity will be given by

$$C_{AF-DL} = 0.5 \times M \times \min \{ \log_2 (1 + \bar{\gamma}_i) \} \quad i = 1, 2 \dots M \quad (6.16)$$

where $\bar{\gamma}_i$ is the post-processing SNR at the i^{th} detection steps whose cumulative distribution functions (CDF) are described by (5.35) and (5.36).

In lieu of our previous analysis, the probability of channel outage of $2 \times 2 \times 1$ downlink AF-CSM system in the first and second detection steps are respectively given by

$$C_{AF_1}(c_{th}) = 1 - 2e^{-\frac{\mathcal{C}(\beta_1 + \beta_2)}{2}} + e^{-\mathcal{C}(\beta_1 + \beta_2)} + \mathcal{C}(\beta_1 + \beta_2) \left[\Gamma \left(0, \frac{\mathcal{C}(\beta_1 + \beta_2)}{2} \right) - \Gamma(0, \mathcal{C}(\beta_1 + \beta_2)) \right] \quad (6.17)$$

and

$$C_{AF_2}(c_{th}) = 1 - \mathcal{C}^2 \beta_1 \beta_2 e^{-\mathcal{C}(\beta_1 + \beta_2)} K_1^2 \left(\mathcal{C} \sqrt{\beta_1 \beta_2} \right) \quad (6.18)$$

where $\mathcal{C} = 2^{c_{th}/(0.5M)} - 1$. From (6.17) and (6.18), the total outage capacity probability is then given by

$$C_{AF-DL} = C_{AF_1} + C_{AF_2} - C_{AF_1} \times C_{AF_2} \quad (6.19)$$

6.4 Downlink Decode-and-Forward

Similar to uplink case, downlink DF-CSM also constitutes that both the relays and destination decode the entire codeword without error. Then, the channel capacity of $M \times N \times 1$

downlink DF-CSM is given by

$$C_{DF-DL} = \min\{C_{sr}, C_{rd}\} \quad (6.20)$$

where C_{sr} and C_{rd} are capacities of the source-relay and relay-destination links, respectively.

The source-relay link is described as $M \times N$ MIMO V-BLAST transmission with outage capacity C_{sr} equals to

$$C_{sr} = 0.5 \times M \times \min\{\log_2(1 + \bar{\gamma}_{s_j r})\} \quad j = 1, 2 \dots M \quad (6.21)$$

The relay-destination link consists of $N \times 1$ MISO transmission in which either time division multiplex (TDM) or space-time coding transmission is utilized. When TDM transmission (sometimes also referred as spatial cycling [36]) is chosen, i^{th} relay transmits in turn until all relays are done transmitting, thus N total time slots are needed to complete TDM relay-destination transmission. The outage capacity C_{rd} for TDM transmission will be given by

$$C_{rd-TDM} = 1 - e^{-\beta_2 \mathcal{C}_1} \quad (6.22)$$

where $\mathcal{C}_1 = 2^{2c_{th}} - 1$.

As we have mentioned before in Chapter 4, by exploring the relay-destination structure in downlink DF-CSM, we can opt to utilize Alamouti's $N \times 1$ space-time coding scheme, instead of TDM. In this configuration, the outage capacity C_{rd} for 2×1 system is stated as

$$C_{rd-STC} = 1 - e^{-\beta_2 \mathcal{C}_1} (1 + \beta_2 \mathcal{C}_1) \quad (6.23)$$

while also noting that each SISO link operates at half the original information rate [36].

For $2 \times 2 \times 1$ system, the outage capacity in first and second detection steps of source-relay link transmission are given as

$$C_{s_1 r} = 1 - 2e^{-\beta_1 \mathcal{C}} + \left(1 + \frac{\beta_1}{2} \mathcal{C}\right) e^{-2\beta_1 \mathcal{C}} \quad (6.24)$$

$$C_{s_2 r} = 1 - (1 + \beta_1 \mathcal{C})^2 e^{-2\beta_1 \mathcal{C}} \quad (6.25)$$

with $\mathcal{C} = 2^{c_{th}/(0.5M)} - 1$. (6.21) can then be restated as

$$C_{sr} = C_{s_1 r} + C_{s_2 r} - C_{s_1 r} C_{s_2 r} \quad (6.26)$$

Putting everything together, the outage capacity probability for 2x2x1 downlink DF-CSM is given by rewriting (6.20) into

$$C_{DF-DL-TDM} = C_{sr} + C_{rd-TDM} - C_{sr}C_{rd-TDM} \quad (6.27)$$

for TDD-relaying scheme, and

$$C_{DF-DL-STC} = C_{sr} + C_{rd-STC} - C_{sr}C_{rd-STC} \quad (6.28)$$

for space-time coding relays.

6.5 Numerical Results and Discussions

We apply our outage capacity analysis to various system configurations and scenarios. For the uplink system, 1x2x2 configuration is the system of choice, while for downlink system, we choose a 2x2x1 configuration. The transmission channels are assumed to be Rayleigh-faded and the modulation of choice is BPSK. The system will go into outage when the transmission rate drops below the threshold c_{th} bits/s/Hz. Transmit power budget for the end-to-end system is constrained by P , which is the amount of power needed to achieve spectral efficiency of 2 bps in single-input-single-output (SISO) system. We choose source-relay distances of 0.2 and 0.3 for uplink AF and DF CSM systems, respectively. Similarly, in downlink CSM, source-relay distances of 0.75 and 0.65 for AF and DF systems are selected. Based on Fig.5.9, these relay locations approximately give the best BER performance for each system. The term E_b/N_0 on the horizontal axis of some figures refers to the amount of energy needed to transmit one bit of data from the source to the destination sink per-noise power, which is sometimes loosely called signal-to-noise-ratio (SNR) as well.

Fig.6.1 depicts the outage capacity performance of uplink CSM system plotted against various E_b/N_0 values, where threshold capacity $c_{th} = 2$ bits/s/Hz. Here we see that the lowest probability that the transmission rate cannot support rate lower than 2 bits/s/Hz is given by AF-UL, where it even surpasses the non-practical MIMO V-BLAST. As predicted before, SISO is the system which will highly likely go into capacity outage in the low SNR region.

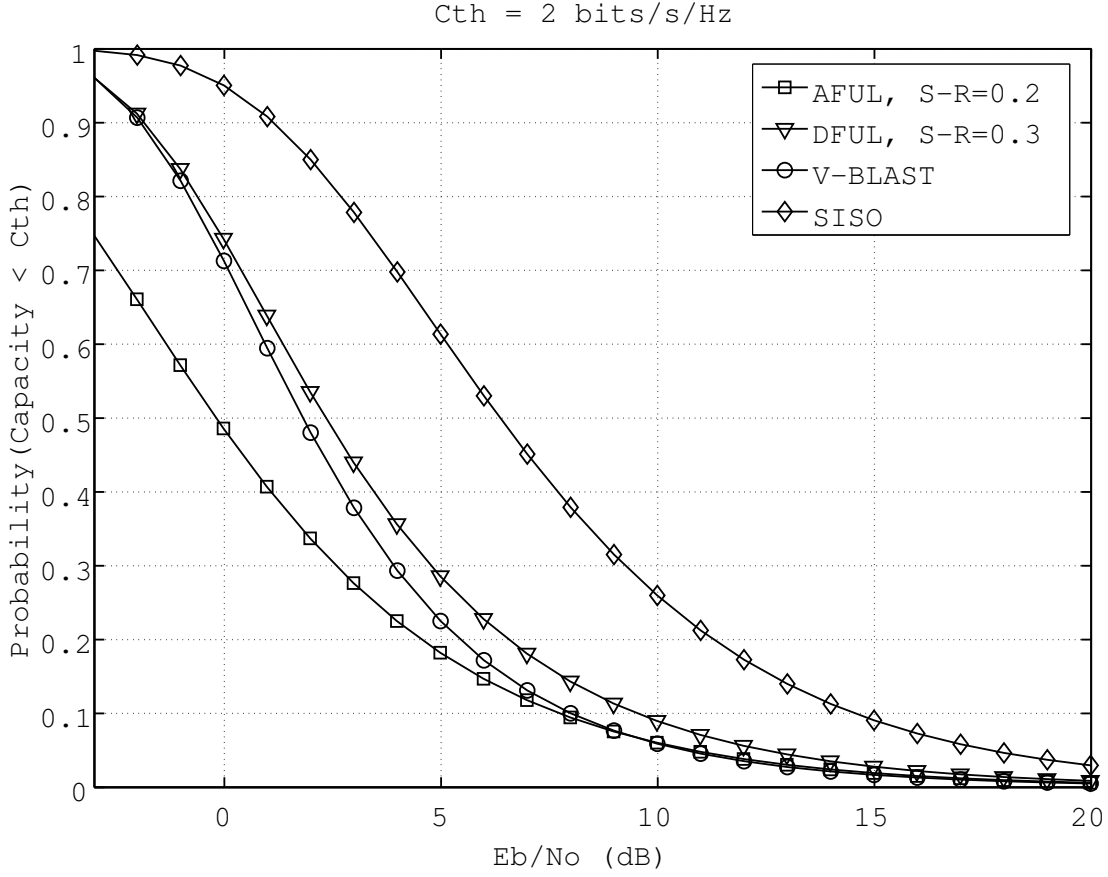


Figure 6.1 Outage capacity of uplink CSM systems, $c_{th} = 2$ bits/s/Hz.

Fig.6.2 shows the complementary distribution function (CCDF) of uplink CSM system, which tells us the probability that a system supports rate greater than the threshold c_{th} at $E_b/N_0 = 10$ dB. For example, for 90% of the time, AF-UL system can support a capacity of about 2.3 bits/s/Hz. The relaying scheme of AF gives an advantage over DF, since the non-regenerative relays does not limit the transmission rate of the end-to-end system.

For downlink CSM systems (Fig.6.3), at extremely low SNR condition ($E_b/N_0 < 1$ dB), we can see that AF-DL provides the lowest capacity outage probability. In general, unless space-time coding is applied, CSM system cannot surpass the outage capacity performance of the V-BLAST system. Nevertheless, the CSM system offers superior outage capacity compared to SISO in all SNR region.

At $E_b/N_0 = 10$ dB, from the CCDF curves in Fig.6.4, it can be seen that outage capacity

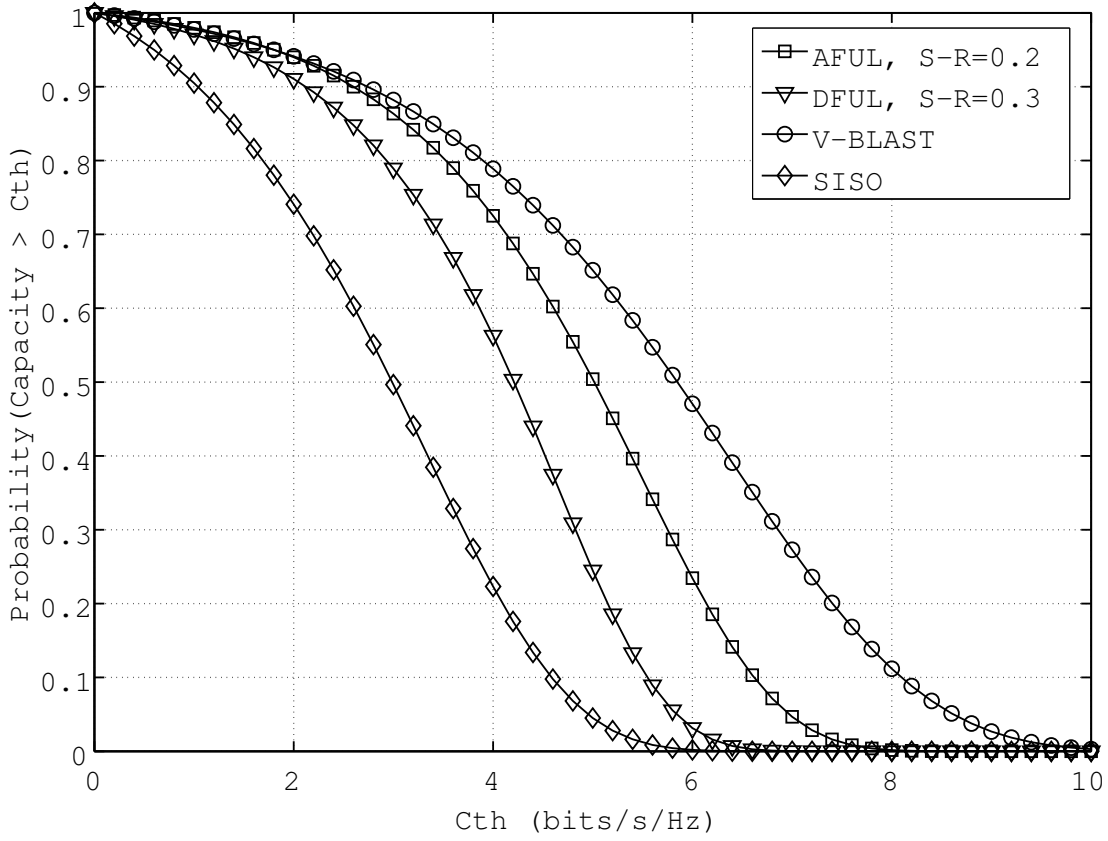


Figure 6.2 Outage capacity of uplink CSM systems, $E_b/N_0 = 10$ dB.

performance DF systems deteriorates faster than comparing systems. STC clearly helps boosting DF performance when $c_{th} < 3.8$ bits/s/Hz. But when higher outage capacity performance is demanded, the attractiveness of DF-STC disappears. At some c_{th} values, unless STC is applied, DF even becomes inferior to SISO. Again, we can definitely observe the rate-limiting effect of DF configuration.

6.6 Conclusions

In this chapter, we conducted an analysis on the outage capacity which tells us the probability of the system cannot support transmission below some threshold rate c_{th} . By plotting the complementary CDF (CCDF) instead, we can observe the probability that the system

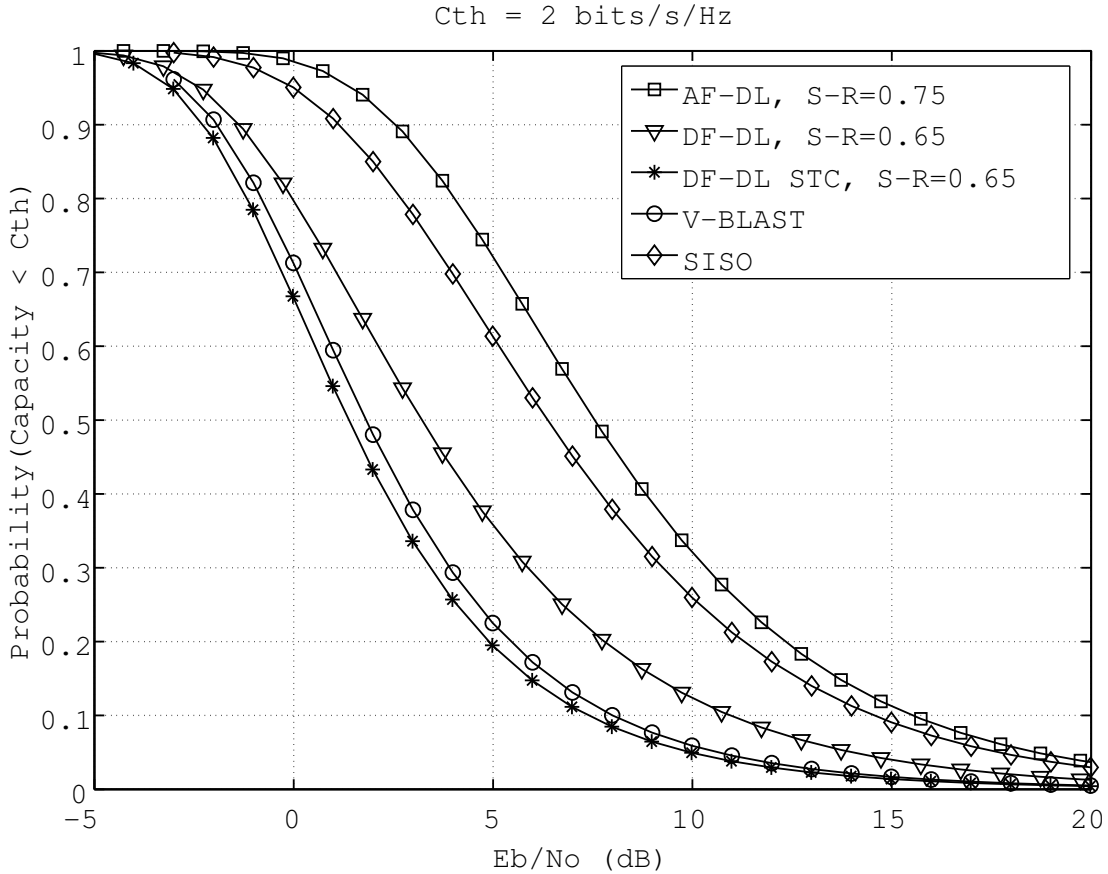


Figure 6.3 Outage capacity of downlink CSM systems, $c_{th} = 2 \text{ bits/s/Hz}$.

will support transmission rate at c_{th} or higher. In general, CSM system outage capacity performance is much superior to SISO, and it even surpasses that of non-practical V-BLAST at certain transmission conditions. We also observed that the DF configuration has a rate-limiting effect on the capacity of the end-to-end system since the relays are required to make correct estimations before they retransmit the source message to the destination. Applying simple space-time coding on the relay-destination transmission of DF-DL-CSM certainly helps improving the capacity performance with extra marginal complexity over the TDM scheme.

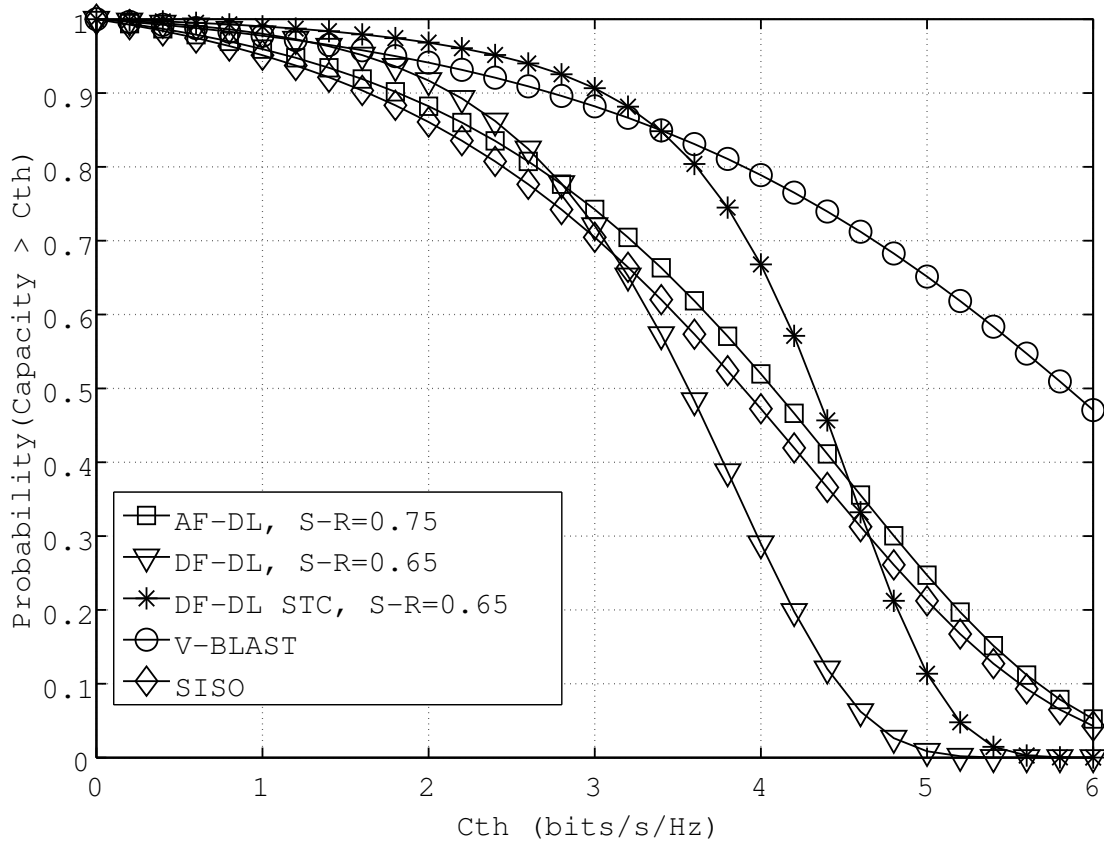


Figure 6.4 Outage capacity of downlink CSM systems, $E_b/N_0 = 10$ dB.

CHAPTER 7. OPTIMAL POWER ALLOCATION SCHEME FOR COOPERATIVE SPATIAL MULTIPLEXING SYSTEMS

Based on the systems proposed in chapter 3 and 4, it can be seen that the performance of the cooperative spatial multiplexing (CSM) systems depends on the relay locations. Given that the physical characteristics of the terminals being identical, the physical distance of the source-relay and relay-destination dictates the amount of propagation loss induced in the individual links.

In previous chapters, the transmit power is distributed equally among the number of terminals such the available transmit power in each terminal is $P/(M + N)$, where M and N are the number of source and relaying terminals, respectively. In this chapter, given a total power budget P equal to that of a SISO system and perfect channel state information (CSI) knowledge at the transceivers, we derive and propose an optimal power allocation scheme which maximizes the performance of the CSM system in terms of outage probability (P_{out}) and bit-error rate performance. Our derivation assumes that the channel is Rayleigh-distributed such that the power follows exponential distribution. The average SNR of the links $\bar{\gamma}_n$ is then also exponentially distributed and can be written as $\bar{\gamma}_n = G_n p_n$ with G_n is a parameter which captures parameters such as antenna gains, path loss, shadowing, noise power, etc. p_n is defined as the transmit power of the user and relay terminals. The parameters captured in G_n usually vary depending on the propagation model chosen for the transmission.

Recall in chapter 5 that an outage occurs is the signal power falls below a preset threshold γ_{th} . Based on this definition, maximizing the system performance in terms of outage probability equals to minimizing the outage probability itself. Moreover, since the BER performance follows the same norm as outage probability, if the outage probability is minimized, consequently

the probability of bit-error will be minimized as well. Hence, in order to solve the problem, one only need to choose between minimization of the outage probability or BER. Based on the results obtained, since the expressions for outage probability are much simpler that of the BER, we opt to solve the problem based on outage performance.

For $1 \times M \times N$ *uplink* CSM systems, the problem can be formulated as

$$\begin{aligned} & \min && P_{out} && (7.1) \\ \text{subject to} & & \left\{ \begin{array}{l} p_s + Mp_r = P \\ p_n \leq P_n, \quad n \in \{s, r\} \end{array} \right. && (7.2) \end{aligned}$$

while for $M \times N \times 1$ *downlink* CSM systems, the above problem needs to be rewritten for different constraints:

$$\begin{aligned} & \min && P_{out} && (7.3) \\ \text{subject to} & & \left\{ \begin{array}{l} Mp_s + Np_r = P \\ p_n \leq P_n, \quad n \in \{s, r\} \end{array} \right. && (7.4) \end{aligned}$$

where P_n is the maximum transmit power available at the source or relay terminals and $\{s, r\} = \{\text{source}, \text{relay}\}$.

Since the CSM system is a multi-rate system, the main objective here is to find a combination of transmit *energy* (instead of power) at the source (E_s) and relays (E_r) that minimizes the outage probability and BER of the system, for the given link conditions. In other words, the problem is just a maximum likelihood estimation (MLE) problem.

7.1 Uplink Amplify-and-Forward

In AF-CSM systems, outage decisions are determined at the destination nodes based on

$$P_{out} = Pr[\gamma_i < \gamma_{th}] \quad (7.5)$$

where γ_i is the end-to-end SNR of the system. Recall the expression for the outage probability of $1 \times 2 \times N$ uplink AF system from (5.17)

$$F_g(x) = 1 - \frac{x}{aN} \sqrt{\beta_s \beta_r} e^{-x(\beta_s + \beta_r)/(2aN)} K_1 \left(\frac{x}{aN} \sqrt{\beta_s \beta_r} \right)$$

where $a = E_r/E_s$ and N is the number of receive antennas at the destination.

Rewriting the problem and the constraints based on transmit energy-per-bit instead of power, we get

$$\begin{aligned} \min \quad & P_{out} = 1 - \frac{\gamma_{th}}{aN} \sqrt{\beta_s \beta_r} e^{-\gamma_{th}(\beta_s + \beta_r)/(2aN)} K_1 \left(\frac{\gamma_{th}}{aN} \sqrt{\beta_s \beta_r} \right) \\ \text{subject to} \quad & E_s + E_r = \frac{P}{2MR_s} \end{aligned} \quad (7.6)$$

where $2R_s$ is the bit-rate of an SISO system achieving the same spectral efficiency as the CSM systems, E_s and E_r are the transmit energy-per-bit of the source and relays, respectively. Minimizing P_{out} in (7.6) is just the same as maximizing the logarithm of its second term such that the problem can be restated as

$$\max \quad \frac{-\gamma_{th}}{2aN} \left(\frac{1}{G_r E_r} + \frac{1}{G_s E_s} \right) + \frac{1}{2} \log \left(\frac{\gamma_{th}}{aN G_r G_s E_r E_s} \right) + \log \left(K_1 \left(\frac{\gamma_{th}}{aN \sqrt{G_r G_s E_r E_s}} \right) \right) \quad (7.7)$$

with the same constraint as the original statement. Note that we have expressed β_n explicitly as $\beta_n = 1/\bar{\gamma}_n$ and $\bar{\gamma}_n = G_n E_n$, $n \in \{s, r\}$.

To solve the maximization problem, we opt for the Lagrange multiplier method and write the objective function as

$$\begin{aligned} J = \quad & \frac{-\gamma_{th}}{2aN} \left(\frac{1}{G_r E_r} + \frac{1}{G_s E_s} \right) + \frac{1}{2} \log \left(\frac{\gamma_{th}}{aN G_r G_s E_r E_s} \right) \\ & + \log \left(K_1 \left(\frac{\gamma_{th}}{aN \sqrt{G_r G_s E_r E_s}} \right) \right) - \eta \left(E_s + E_r - \frac{P}{2MR_s} \right) \end{aligned} \quad (7.8)$$

One can use numerical method of choice and solve for E_s and E_r in (7.8). These solutions are the optimal transmit energy allocated which minimize the outage probability and probability of bit error, thus maximizing the end-to-end system performance.

Since numerical methods may sometimes cost a lot of computing resource, we propose a semi-optimal power allocation scheme. Using the approximation of modified Bessel function given in (5.3) and realizing that the first term in ((7.8)) is the dominant quantity, we rewrite the Lagrange optimization problem as

$$J = \frac{-\gamma_{th}}{2aN} \left(\frac{1}{G_r E_r} + \frac{1}{G_s E_s} \right) - \eta \left(E_s + E_r - \frac{P}{2MR_s} \right) \quad (7.9)$$

which can be solved feasibly by hand calculation to give out the simple solutions

$$E_s = \frac{P}{2MR_s \left(\frac{G_r}{G_s} - 1\right)} \left(\frac{G_r}{G_s} - \sqrt{\frac{G_r}{G_s}}\right) \quad (7.10)$$

$$E_r = \frac{P}{2MR_s \left(\frac{G_s}{G_r} - 1\right)} \left(\frac{G_s}{G_r} - \sqrt{\frac{G_s}{G_r}}\right) \quad (7.11)$$

One can notice a very interesting fact that the solutions are independent of the number of receive antennas N at the destination sink. Consequently, for a $1 \times 2 \times N$ uplink AF-CSM system, the semi-optimal energy allocations between the source and two relays, given a total end-to-end transmit power of P are

$$E_s = \frac{P}{4R_s \left(\frac{G_r}{G_s} - 1\right)} \left(\frac{G_r}{G_s} - \sqrt{\frac{G_r}{G_s}}\right) \quad (7.12)$$

$$E_r = \frac{P}{4R_s \left(\frac{G_s}{G_r} - 1\right)} \left(\frac{G_s}{G_r} - \sqrt{\frac{G_s}{G_r}}\right) \quad (7.13)$$

7.2 Uplink Decode-and-Forward

In DF-CSM systems, an outage occurs if either one of the links carrying a particular symbol x_j is in outage condition. In other words, it is the complement of all links operating above the threshold γ_{th} . For a $1 \times 2 \times 2$ DF-CSM system, the source-relay link is exponentially distributed, while the relay-destination link has a chi-square with $2N$ degrees of freedom (χ_{2N}^2) distribution, the outage probability is given by

$$\begin{aligned} P_{out} &= 1 - \left(\int_{\gamma_{th}}^{\infty} \beta_s e^{-x\beta_s} dx\right) \left(\int_{\gamma_{th}}^{\infty} \frac{x\beta_r^2}{\Gamma(2)} e^{-x\beta_r} dx\right) \\ &= 1 - e^{-\gamma_{th}(\beta_s + \beta_r)} (1 + \gamma_{th}\beta_r) \end{aligned} \quad (7.14)$$

The outage probability minimization problem can then be formulated as

$$\begin{aligned} \min \quad & P_{out} = 1 - e^{-\gamma_{th}(\beta_s + \beta_r)} (1 + \gamma_{th}\beta_r) \\ \text{subject to} \quad & E_s + E_r = \frac{P}{4R_s} \end{aligned} \quad (7.15)$$

Or similar to AF case, minimizing (7.15) is equivalent to maximizing the logarithm of the second term in the objective function. By explicitly stating $\beta_n = 1/\bar{\gamma}_n$ and $\bar{\gamma}_n = G_n E_n$,

$n \subset \{s, r\}$, and the problem is rewritten as

$$\max \quad -\gamma_{th} \left(\frac{1}{G_s E_s} + \frac{1}{G_r E_r} \right) + \log \left(1 + \frac{\gamma_{th}}{G_r E_r} \right) \quad (7.16)$$

subject to the same constraint as before. Using Lagrange multiplier to solve the optimization problem, we write the objective function as

$$J = -\gamma_{th} \left(\frac{1}{G_s E_s} + \frac{1}{G_r E_r} \right) + \log \left(1 + \frac{\gamma_{th}}{G_r E_r} \right) - \eta \left(E_s + E_r - \frac{P}{4R_s} \right) \quad (7.17)$$

from which a solution is found as

$$E_s^2 = \frac{G_r^2}{\gamma_{th} G_s} \left(\frac{P}{4R_s} - E_s \right)^3 + \frac{G_r}{G_s} \left(\frac{P}{4R_s} - E_s \right)^2 \quad (7.18)$$

Unfortunately in order to find an exact solution, (7.18) needs to be solved numerically which can be time consuming before convergence is reached.

By analyzing (7.16) closer, we can see that compared to the $\log(\cdot)$ term, the first term is a much more dominant quantity. Hence, by maximizing only the first term, (7.16) will be maximized. The simplified objective function now becomes

$$J = -\gamma_{th} \left(\frac{1}{G_s E_s} + \frac{1}{G_r E_r} \right) - \eta \left(E_s + E_r - \frac{P}{4R_s} \right) \quad (7.19)$$

from whose solution, a semi-optimal power allocation can be achieved. Working out on the math further, solutions for the Lagrange are found to be given by

$$E_s = \frac{P}{4R_s \left(\frac{G_r}{G_s} - 1 \right)} \left(\frac{G_r}{G_s} - \sqrt{\frac{G_r}{G_s}} \right) \quad (7.20)$$

$$E_r = \frac{P}{4R_s \left(\frac{G_s}{G_r} - 1 \right)} \left(\frac{G_s}{G_r} - \sqrt{\frac{G_s}{G_r}} \right) \quad (7.21)$$

which, surprisingly, are just the same semi-optimal power allocations as in AF case.

7.3 Downlink Amplify-and-Forward

The derivation for optimal power allocation in downlink AF is similar to the uplink case, of which, the definition of outage is given by (7.5). Now let's recall the outage probability expression for downlink AF-CSM:

$$F_g(x) = 1 - \frac{2x}{aN} \sqrt{\beta_1 \beta_2} e^{-x(\beta_1 + \beta_2)/(aN)} K_1 \left(\frac{2x}{aN} \sqrt{\beta_1 \beta_2} \right)$$

where $a = E_r/E_s$, N is the number of relaying terminals. The outage probability minimization problem and constraint for downlink AF will be

$$\min P_{out} = 1 - \frac{2\gamma_{th}}{aN} \sqrt{\beta_1\beta_2} e^{-\gamma_{th}(\beta_1+\beta_2)/(aN)} K_1 \left(\frac{2\gamma_{th}}{aN} \sqrt{\beta_1\beta_2} \right) \quad (7.22)$$

$$\text{subject to} \quad ME_s + N^2E_r = \frac{P}{2R_s} \quad (7.23)$$

Minimizing P_{out} above is equivalent to maximizing the logarithm of the second term in the right hand side so that the problem becomes

$$\max \frac{-\gamma_{th}}{aN} \left(\frac{1}{G_rE_r} + \frac{1}{G_sE_s} \right) + \log \left(\frac{\gamma_{th}}{aN G_r G_s E_r E_s} \right) + \log \left(K_1 \left(\frac{2\gamma_{th}}{aN \sqrt{G_r G_s E_r E_s}} \right) \right) \quad (7.24)$$

Formulating the problem into Lagrange multiplier optimization, we get

$$\begin{aligned} J &= \frac{-\gamma_{th}}{aN} \left(\frac{1}{G_rE_r} + \frac{1}{G_sE_s} \right) + \log \left(\frac{\gamma_{th}}{aN G_r G_s E_r E_s} \right) \\ &\quad + \log \left(K_1 \left(\frac{2\gamma_{th}}{aN \sqrt{G_r G_s E_r E_s}} \right) \right) - \eta(ME_s + N^2E_r) \end{aligned} \quad (7.25)$$

By simple algebra proof, it can be shown that the first term is much more dominant than the logarithm terms. This allows the Lagrange multiplier problem to be simplified into a semi-optimal power allocation problem:

$$J = \frac{-\gamma_{th}}{aN} \left(\frac{1}{G_rE_r} + \frac{1}{G_sE_s} \right) - \eta(ME_s + N^2E_r) \quad (7.26)$$

which is mathematically, much more feasible to be solved. With a straight forward calculation, we obtain the semi-optimal power allocations for the transmit energy-per-bit at the source and relay to be

$$E_s = \frac{P}{2MR_s \left(\frac{MG_r}{N^2G_s} - 1 \right)} \left(\frac{MG_r}{N^2G_s} - \sqrt{\frac{MG_r}{N^2G_s}} \right) \quad (7.27)$$

$$E_r = \frac{P}{2N^2R_s \left(\frac{N^2G_s}{MG_r} - 1 \right)} \left(\frac{N^2G_s}{MG_r} - \sqrt{\frac{N^2G_s}{MG_r}} \right) \quad (7.28)$$

And finally, for a particular 2x2x1 downlink DF-CSM system, the semi-optimal power allocation is given by

$$E_s = \frac{P}{4R_s \left(\frac{G_r}{2G_s} - 1 \right)} \left(\frac{G_r}{2G_s} - \sqrt{\frac{G_r}{2G_s}} \right) \quad (7.29)$$

$$E_r = \frac{P}{8R_s \left(\frac{2G_s}{G_r} - 1 \right)} \left(\frac{2G_s}{G_r} - \sqrt{\frac{2G_s}{G_r}} \right) \quad (7.30)$$

7.4 Downlink Decode-and-Forward

Definition of outage in downlink DF-CSM system is the condition where either one of the links carrying a particular symbol x_j is in outage condition. In other words, it is the complement of all links operating above the threshold γ_{th} . For a $M \times N \times 1$ DF-CSM system, the source-relay link is chi-square with $2N$ degrees of freedom (χ_{2N}^2) distributed, while the relay-destination link follows an exponential distribution. Our particular of interest is the $2 \times 2 \times 1$ system, of which the outage probability of the system is defined as

$$\begin{aligned} P_{out} &= 1 - \left(\int_{\gamma_{th}}^{\infty} \frac{x\beta_s^2}{\Gamma(2)} e^{-x\beta_s} dx \right) \left(\int_{\gamma_{th}}^{\infty} \beta_r e^{-x\beta_r} dx \right) \\ &= 1 - e^{-\gamma_{th}(\beta_s + \beta_r)} (1 + \gamma_{th}\beta_s) \end{aligned} \quad (7.31)$$

The outage probability minimization problem is then formulated as

$$\begin{aligned} \min \quad & P_{out} = 1 - e^{-\gamma_{th}(\beta_s + \beta_r)} (1 + \gamma_{th}\beta_s) \\ \text{subject to} \quad & ME_s + N^2 E_r = \frac{P}{2R_s} \end{aligned} \quad (7.32)$$

As we have seen several times before, minimizing (7.32) is equivalent to maximizing the logarithm of the second term in the objective function. By explicitly stating $\beta_n = 1/\bar{\gamma}_n$ and $\bar{\gamma}_n = G_n E_n$, $n \in \{s, r\}$, and the problem can be rewritten as

$$\begin{aligned} \max \quad & -\gamma_{th} \left(\frac{1}{G_s E_s} + \frac{1}{G_r E_r} \right) + \log \left(1 + \frac{\gamma_{th}}{G_s E_s} \right) \\ \text{subject to} \quad & E_s + 2E_r = \frac{P}{4R_s} \end{aligned} \quad (7.33)$$

By utilizing Lagrange multiplier method to solve the optimization problem, we write the objective function as

$$J = -\gamma_{th} \left(\frac{1}{G_s E_s} + \frac{1}{G_r E_r} \right) + \log \left(1 + \frac{\gamma_{th}}{G_s E_s} \right) - \eta \left(E_s + 2E_r - \frac{P}{4R_s} \right) \quad (7.34)$$

from which a solution is found to be

$$E_r^2 = \frac{G_s^2}{2\gamma_{th}G_r} \left(\frac{P}{4R_s} - 2E_r \right)^3 + \frac{G_s}{2G_r} \left(\frac{P}{4R_s} - 2E_r \right)^2 \quad (7.35)$$

Unfortunately in order to find an exact solution for both E_s and E_r , the recursive expression in (7.35) needs to be solved numerically which can be time consuming and resource-exhaustive.

By analyzing (7.33) closer, we can see that compared to the $\log(\cdot)$ term, the first term is a much more dominant quantity. Hence, by maximizing only the first term, (7.33) will be maximized. The simplified objective function now becomes

$$J = -\gamma_{th} \left(\frac{1}{G_s E_s} + \frac{1}{G_r E_r} \right) - \eta \left(E_s + 2E_r - \frac{P}{4R_s} \right) \quad (7.36)$$

With simple calculations, solutions to the Lagrange multiplier problem, which will give the semi-optimal power allocations in downlink DF system, are found to be

$$E_s = \frac{P}{4R_s \left(\frac{G_r}{2G_s} - 1 \right)} \left(\frac{G_r}{2G_s} - \sqrt{\frac{G_r}{2G_s}} \right) \quad (7.37)$$

$$E_r = \frac{P}{4R_s \left(\frac{2G_s}{G_r} - 1 \right)} \left(\frac{2G_s}{G_r} - \sqrt{\frac{2G_s}{G_r}} \right) \quad (7.38)$$

7.5 Numerical Results and Discussions

We apply our semi-optimal power optimal allocation scheme to the analysis derived in Chapter 5, which results are also verified by MATLAB Monte-Carlo simulations. For the uplink system, 1x2x2 configuration is the system of choice, while for downlink system, we choose a 2x2x1 configuration. The transmission channels are assumed to be Rayleigh-faded and the modulation of choice is BPSK. The system will go into outage when the received signal drops below the threshold $\gamma_{th} = 0\text{dB}$. Transmit power budget for the end-to-end system is constrained by P , which is the same amount of power used to transmit two bits of data at R_s bps in single-input-single-output (SISO) system. The term E_b/N_0 on the horizontal axis of some figures refers to the amount of energy needed to send one bit of data from the source to the destination sink per-noise power, which is sometimes loosely called signal-to-noise-ratio as well.

Fig.7.1 shows the result when the optimal power allocation scheme is applied to uplink AF system. The base performance for comparison is the BER of the system obtained by Monte-Carlo simulation with uniform power distribution, i.e. transmit power P are distributed equally among all terminals. With the proposed power allocation scheme applied to the system, we

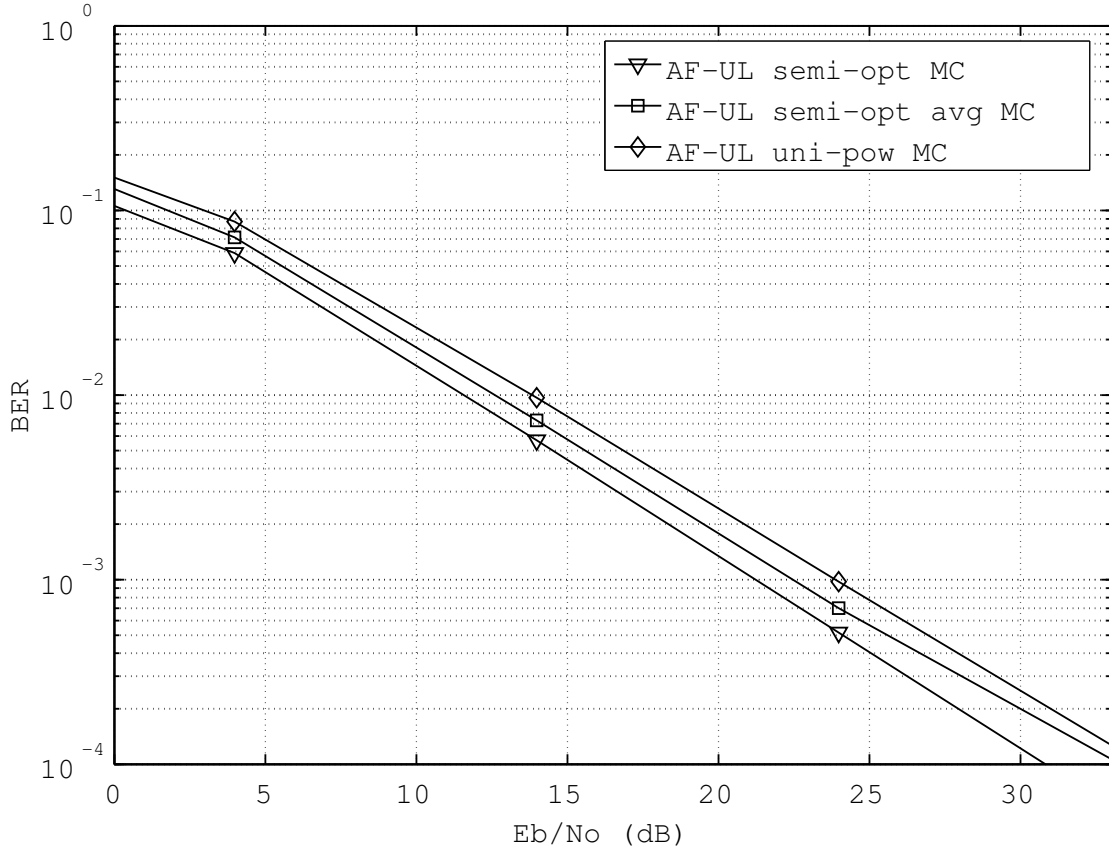


Figure 7.1 BER performance of AF uplink systems with uniform and optimal power allocation schemes.

see that the performance improves up to 2.5dB for 10^{-2} BER. Even if the power is fixed based on the average channel realization for the whole transmission duration (AF-UL semi-opt avg MC), instead of varying based on instantaneous channel realizations (AF-UL semi-opt MC), the system still performs superiorly compared to uniform power scheme. By fixing the power allocation for the whole transmission duration, the complexity of the system decreases considerably and it is proven by the much shorter time needed to complete the Monte-Carlo simulations. To further verify the validity of our power allocation scheme, we apply it to the theoretical analysis results obtained in Chapter 5, and we can see that the proposed power allocation scheme fits our analysis model as well.

When applied to uplink DF systems, the semi-optimal power scheme helps to improve the

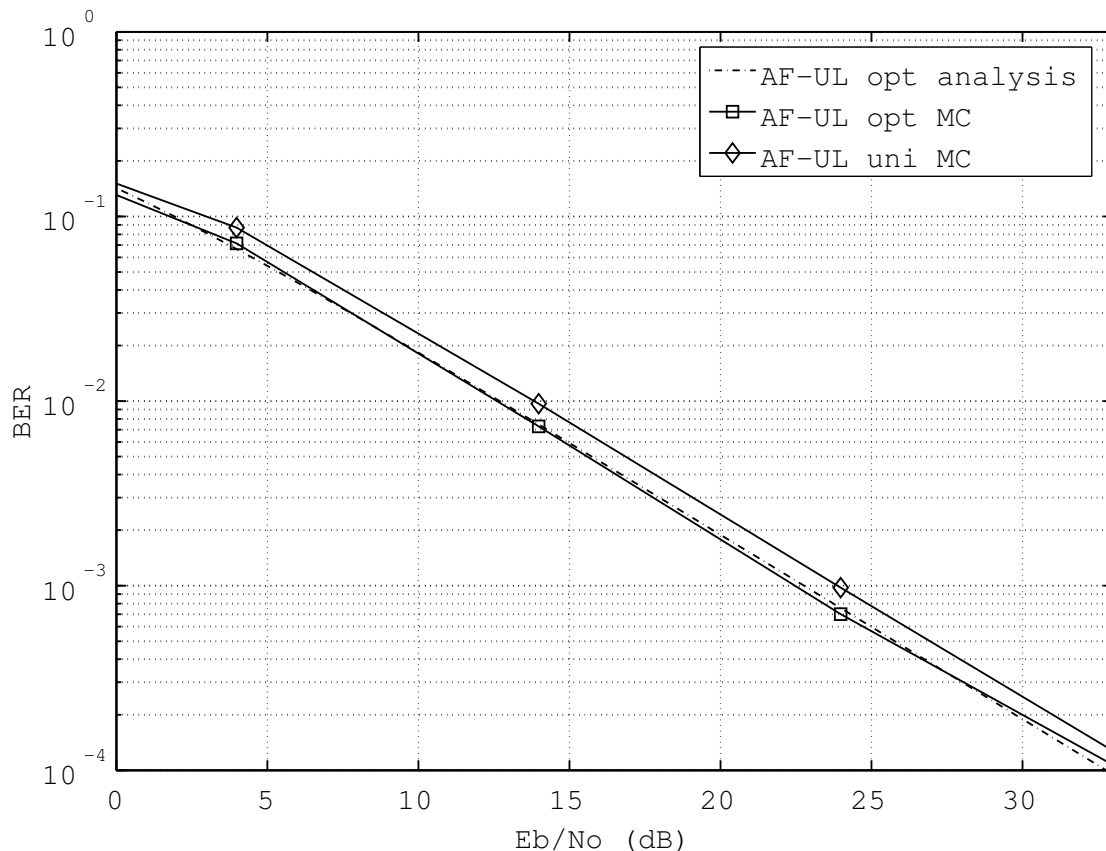


Figure 7.2 BER performance of AF uplink systems with uniform and optimal power allocation schemes.

performance as well as seen in Fig.7.3. As we have seen before, allowing the power allocation to change based on the instantaneous channel condition, we trade complexity for better performance (DF-UL opt MC).

Fig.7.4 shows both downlink AF and DF with the semi-optimal power allocation applied. Based on the figure, it turns out that the AF benefits more from the optimal power scheme compared to the DF system.

Given a end-to-end transmit power budget of P and a particular source-relay distance, Fig.7.5 shows how power are optimally allocated among the terminals in uplink and downlink systems, respectively. Based on these figures, we confirm the result we had in chapters 3 and 4, that the power needs to be adjusted accordingly according to the relay locations in

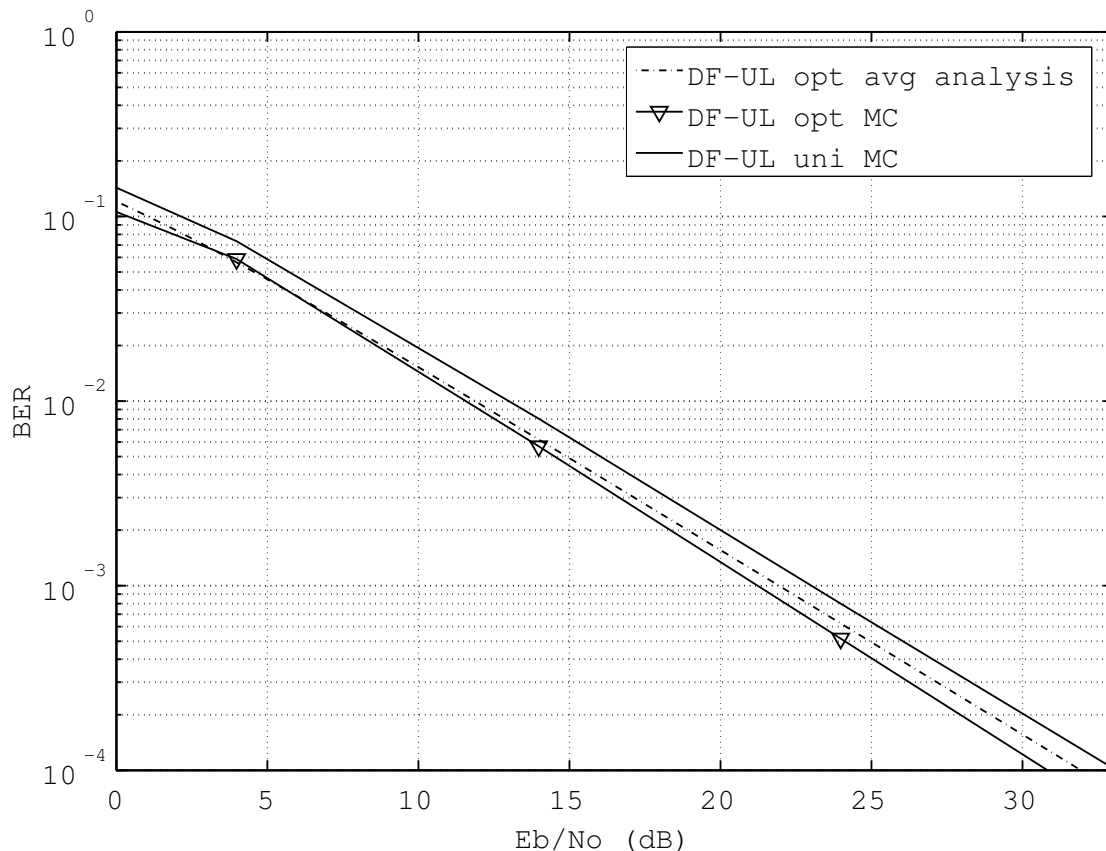


Figure 7.3 BER performance of DF uplink systems with uniform and optimal power allocation schemes.

order to maximize the system performance.

To give a better idea on the relationship between relay locations and BER performance, Fig.7.6 to Fig.7.8 were plotted for several SNR conditions. Several important observations can be made here. First, uplink and downlink systems behave differently in terms of preference in relay location. Uplink systems prefer the relay to be located close to the source, while downlink systems prefer the other way around. Second, for some systems, selecting relays too close to the source or destination may actually reduce the performance. Third, most importantly, these figures allow us to see which type of relaying techniques (AF or DF) should be used for uplink and downlink transmissions in order to maximize the performance. Should the system be given the full freedom to choose the relays from many neighboring terminals,

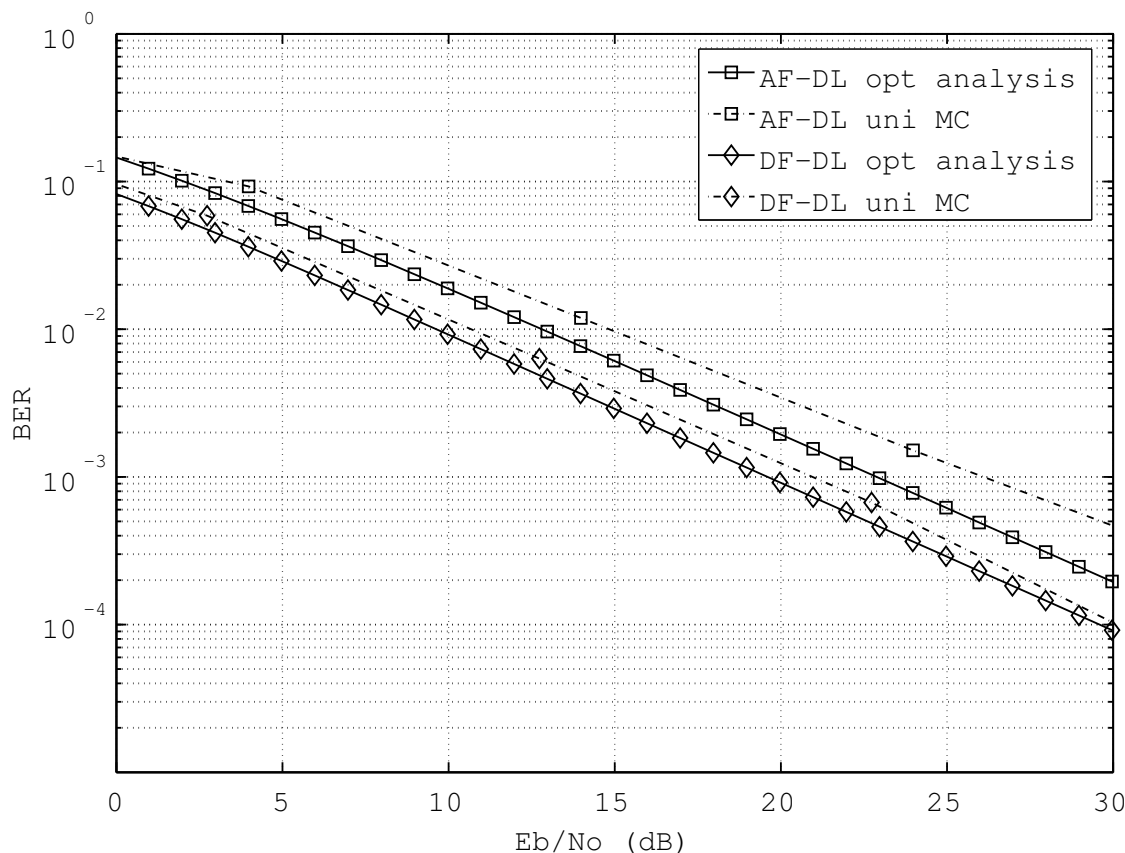


Figure 7.4 BER performance of AF & DF downlink systems with uniform and optimal power allocation schemes.

depending on data contents it may opt to choose to maximize performance on the uplink only, downlink only, or balance communications. For example, if it is a voice call, we may prefer a system which gives balance performance on both uplink and downlink transmissions. While for on-demand movie or music streaming, we may opt for a system which gives the maximum downlink performance. For higher SNR systems, the graphs do not change a lot (Fig.7.8) and the BER is low enough for a reliable transmission at any relay location. On the other hand, one needs to pay extra attention under low-SNR conditions where the systems behave quite differently.

In particular, Fig.7.6 and Fig.7.7 show a better picture what the optimal power allocation scheme actually does to the BER performance of the systems. Although in general the optimal

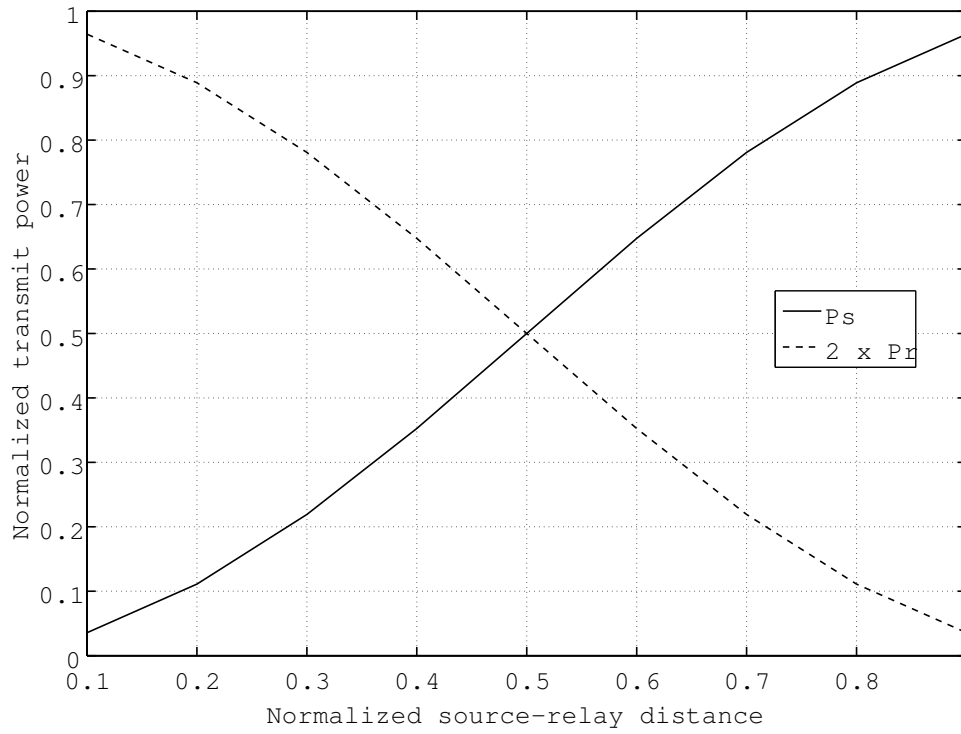
power scheme lowers the BER, at some particular relay distances it has a counter-effect of increasing the BER instead. The optimal power scheme seems to try to *level* the BER curves such that at any relay distance, given the particular link conditions, the systems will perform uniformly. We can also see that applying the power scheme, it is almost guaranteed that CSM will perform better than SISO system at all distances.

From Fig.7.9 and Fig.7.10, we observe that applying optimal power allocation scheme to the uplink CSM system actually has a slight reduction effect on the outage capacity performance. This is a trade-off one has to pay in order to get a better performance in bit error-rate and outage probability performance. For the overall performance gain in other categories, this capacity trade-off price sounds very reasonable. As we can also see from the plots, the power allocation scheme seems to have a bigger impact on AF systems, compared to DF.

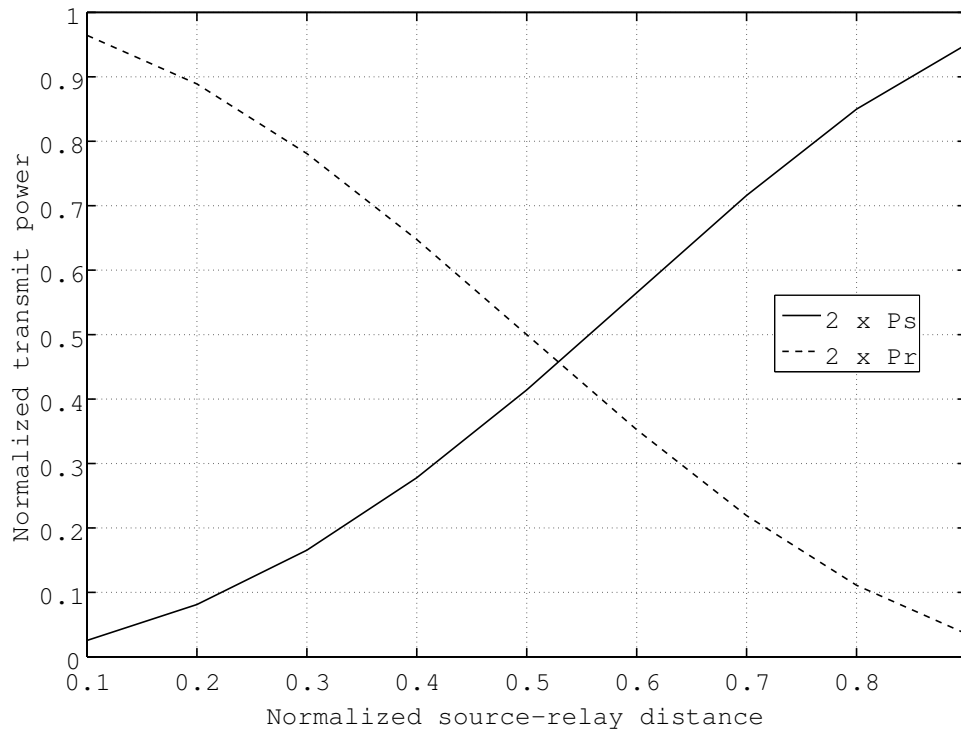
7.6 Conclusions

In this chapter, we propose an optimal and a semi-optimal power allocation schemes for the uplink and downlink cooperative spatial multiplexing systems employing amplify-and-forward (non-regenerative) and decode-and-forward (regenerative) relaying techniques. The power allocation scheme is derived by minimizing the outage probability, which is a function of the link SNRs of a particular system, then solving for the individual link SNR values. By allocating the power budget between the source and relay terminals based on the SNR solutions, both outage probability and BER performance are maximized. Hence, these SNR values are the optimal power allocation.

The outage probability minimization problem is handled by Lagrange multiplier problem, and in some cases, finding exact solutions to the optimization problem can only be done numerically, thus requiring extra complexity. To overcome this inconvenience, we propose a semi-optimal power allocation scheme obtained by simplifying the Lagrange objective function, which can be solved by simple algebra. It is shown that this option, despite being inferior to the optimal solution, still offers improvement in terms of performance compared to the uniform power allocation scheme.

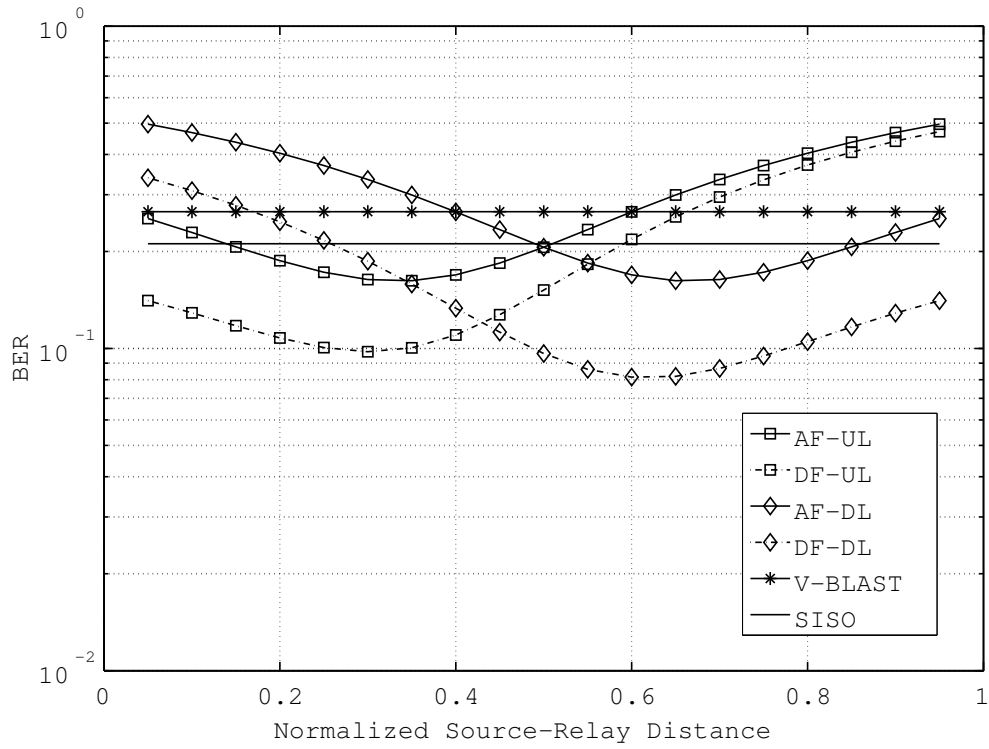


(a) Uplink CSM

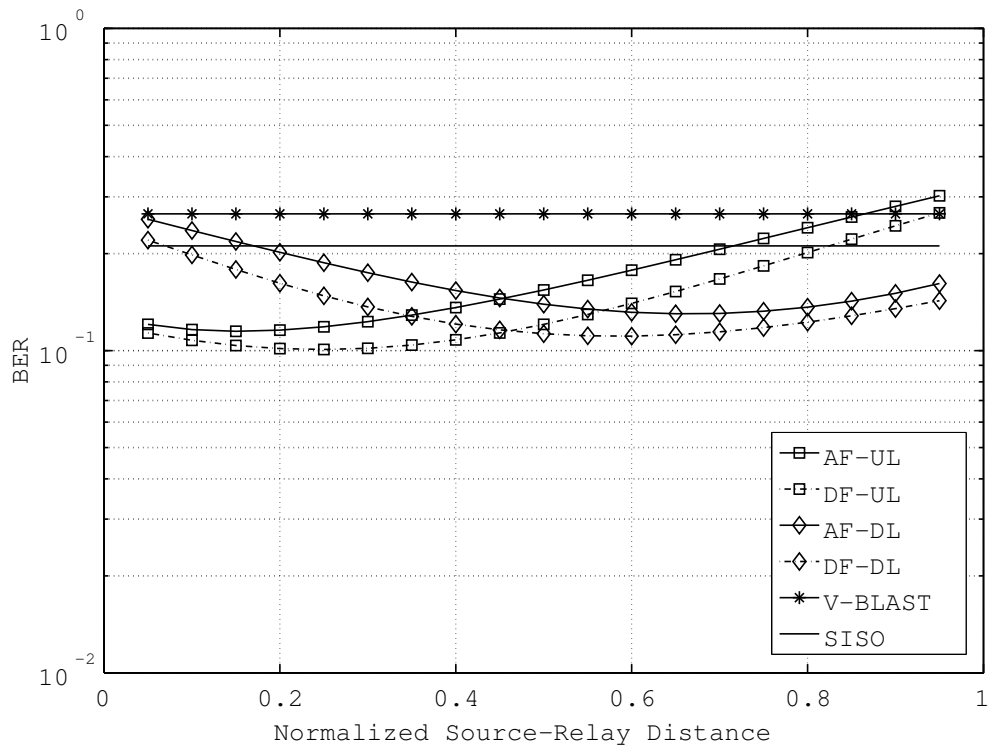


(b) Downlink CSM

Figure 7.5 Optimal power allocation scheme for CSM systems.

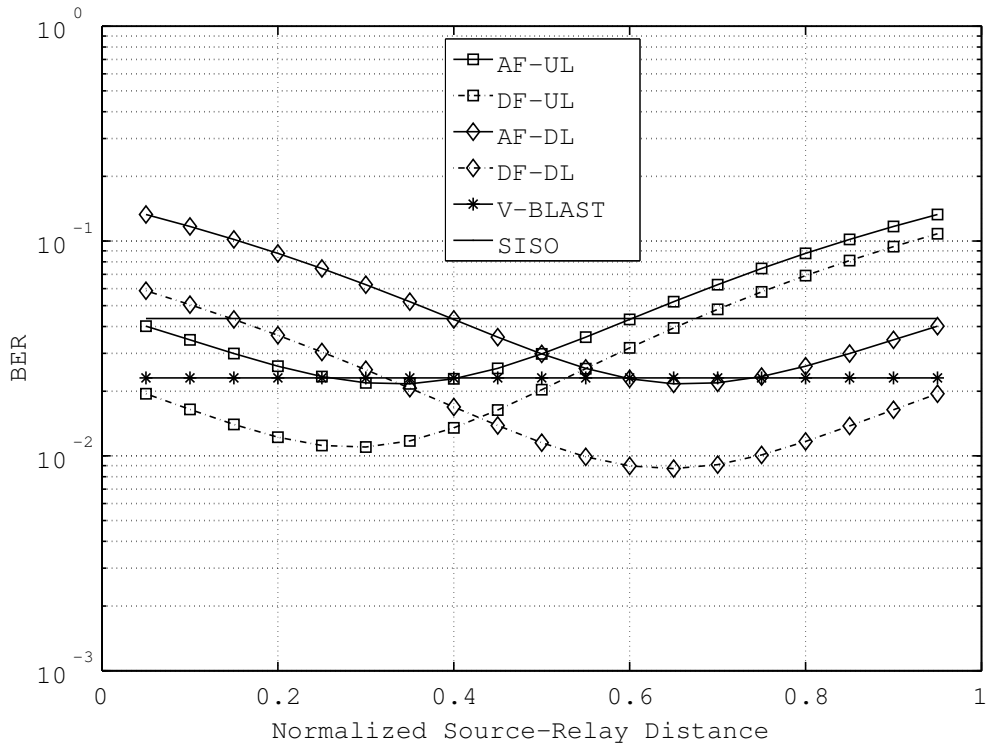


(a) Uniform power

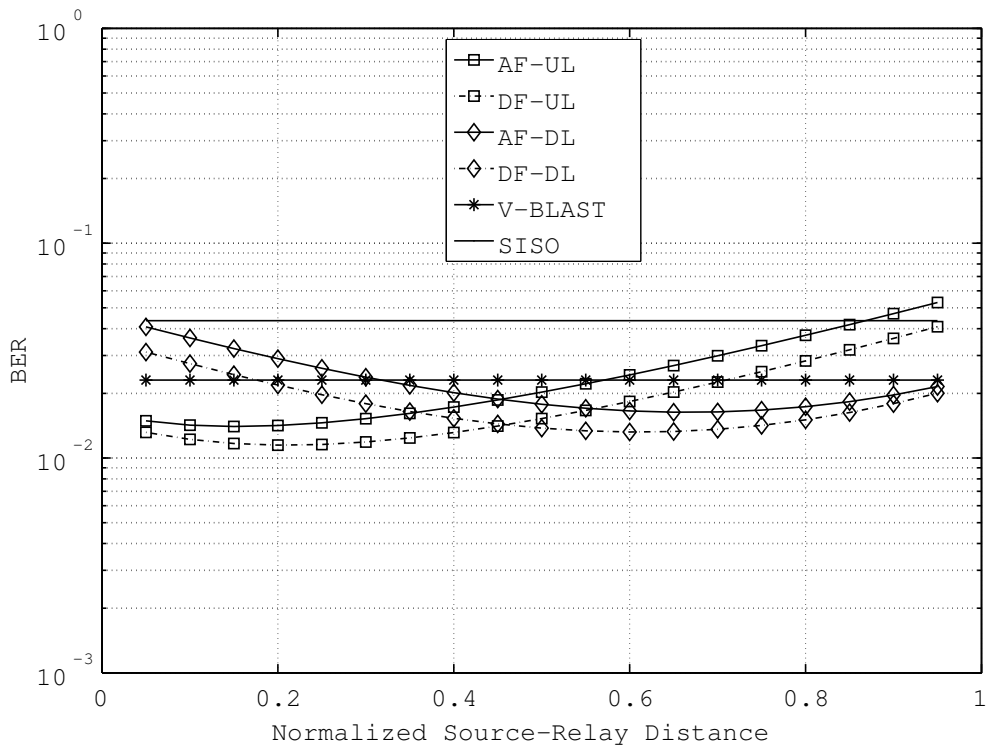


(b) Optimal power allocation

Figure 7.6 Relay location vs. BER performance, SNR = 0dB.

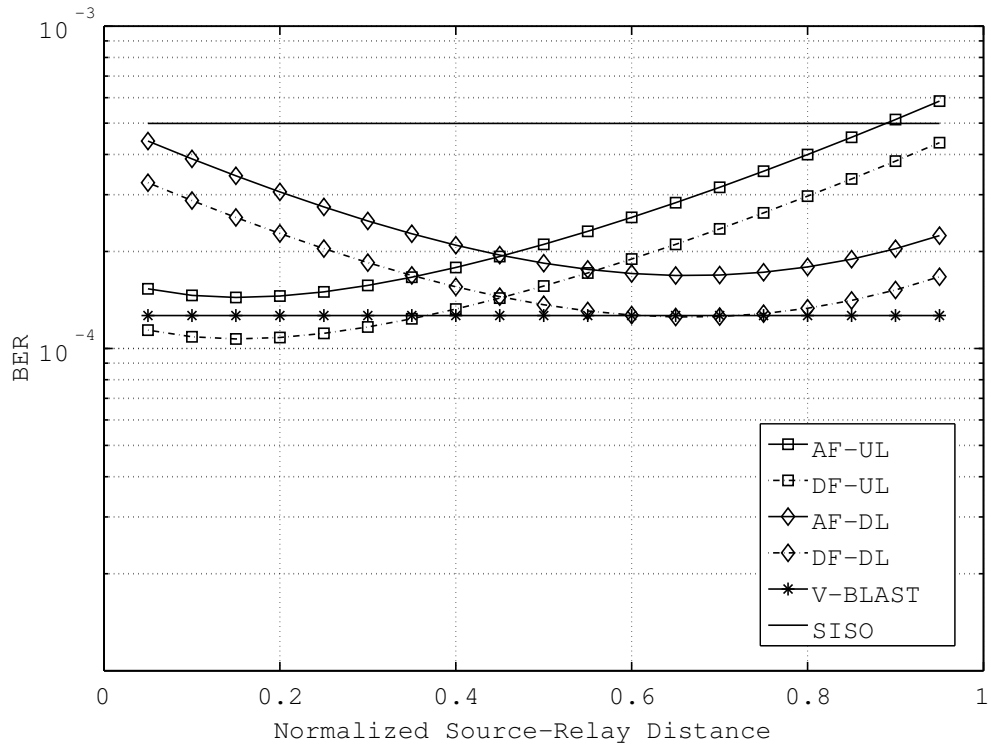


(a) Uniform power

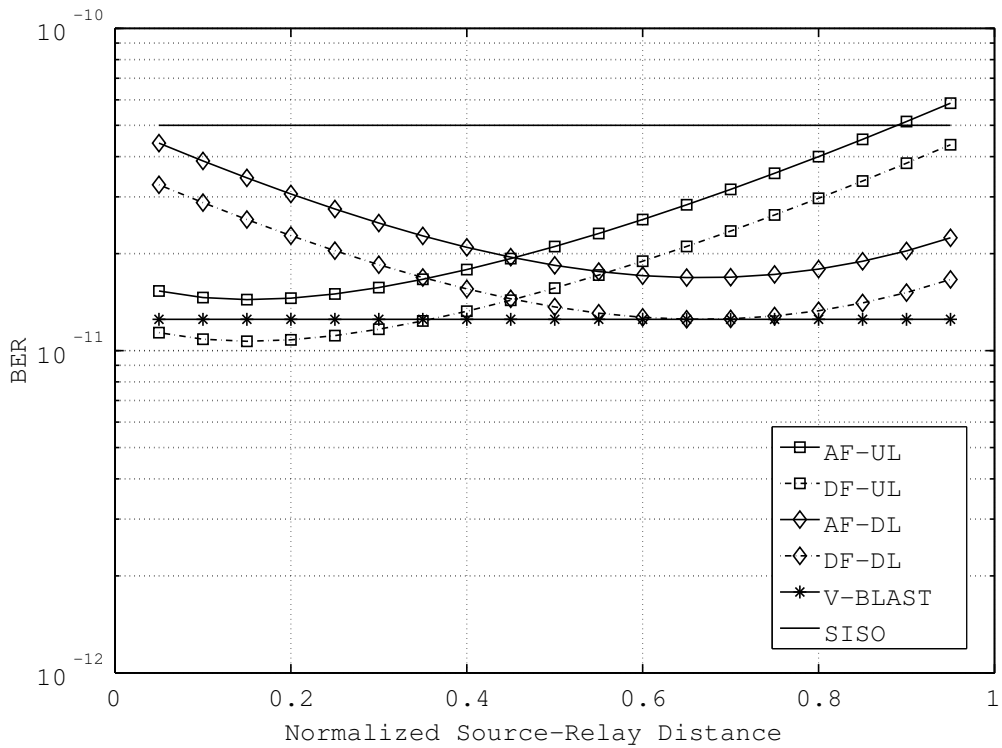


(b) Optimal power allocation

Figure 7.7 Relay location vs. BER performance, SNR = 10dB.



(a) SNR = 30dB



(b) SNR = 100dB.

Figure 7.8 Relay location vs. BER performance.

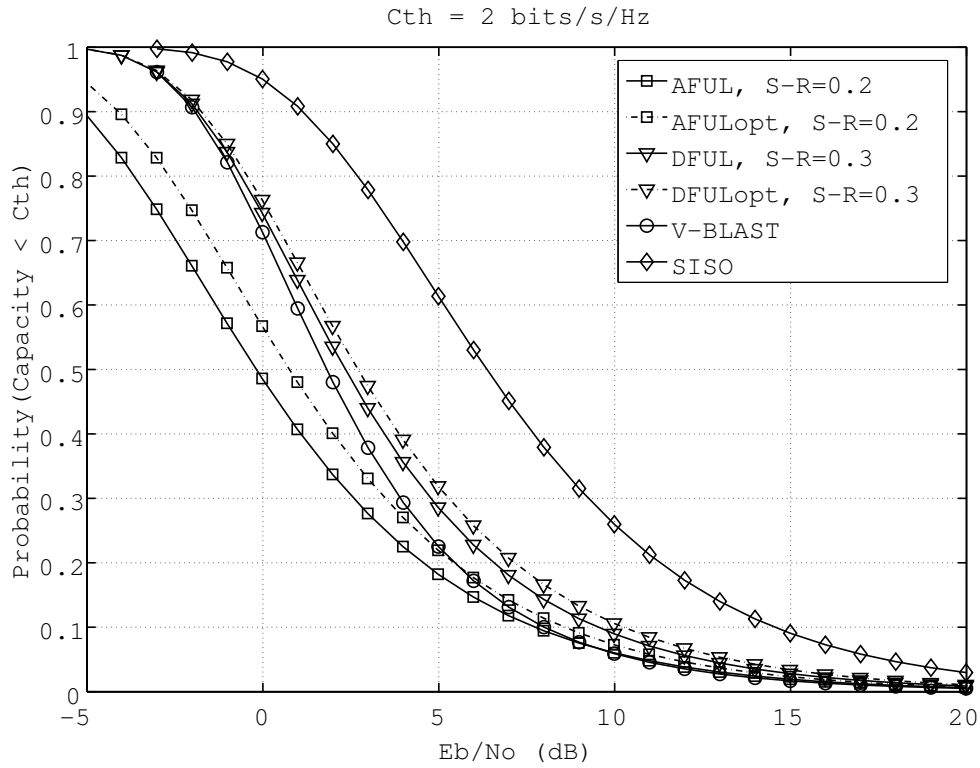
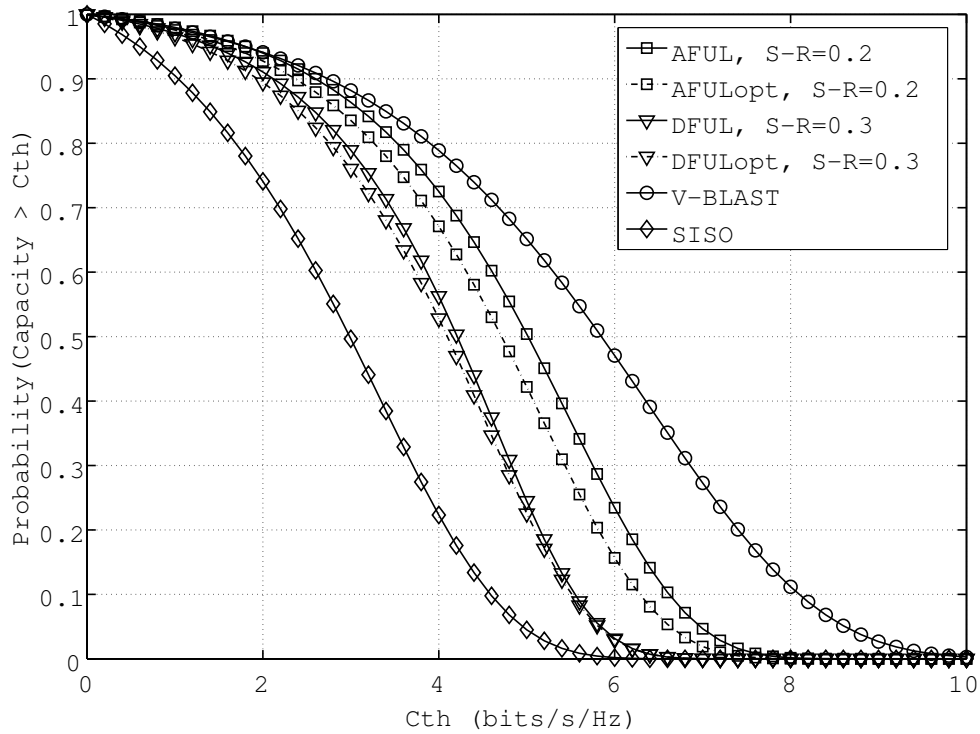
(a) Outage capacity vs. E_b/N_0 , $c_{th} = 2 \text{ bits/s/Hz}$ (b) Outage capacity vs. c_{th} , $E_b/N_0 = 10 \text{ dB}$,

Figure 7.9 Outage capacity performance of uplink CSM with optimal power allocation.

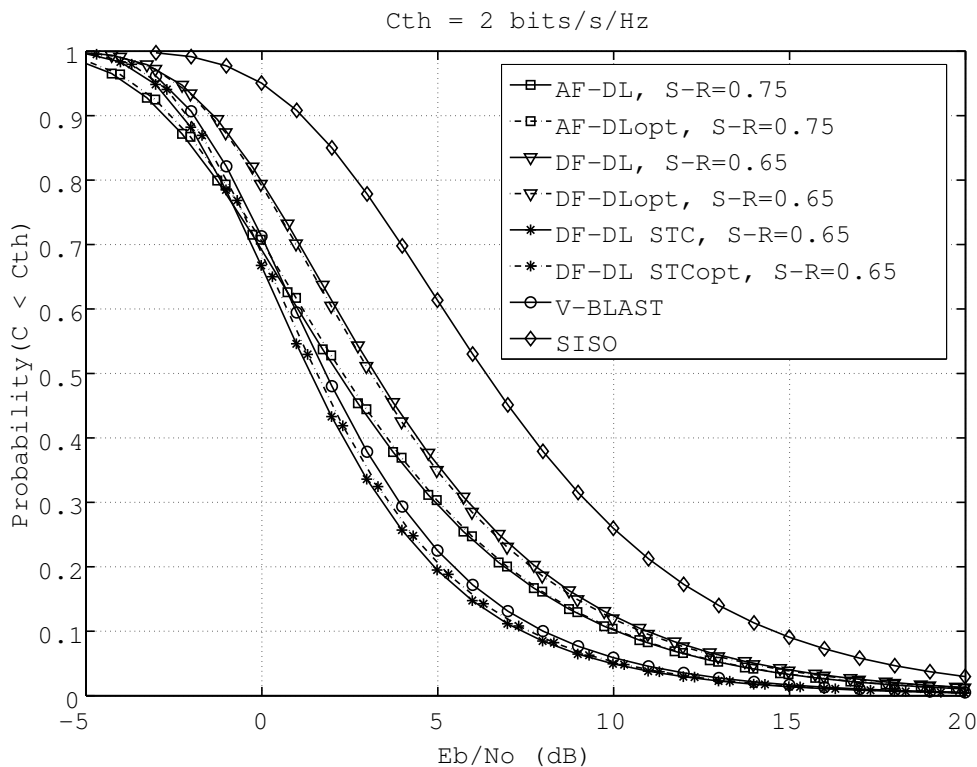
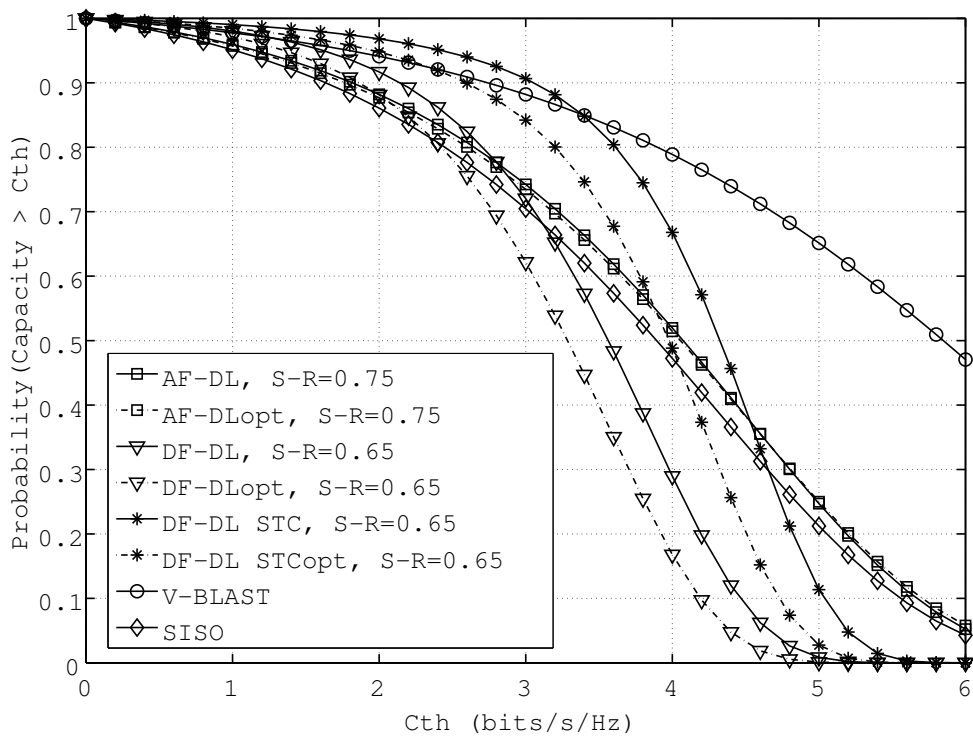
(a) Outage capacity vs. E_b/N_0 , $c_{th} = 2 \text{ bits/s/Hz}$ (b) Outage capacity vs. c_{th} , $E_b/N_0 = 10 \text{ dB}$,

Figure 7.10 Outage capacity performance of downlink CSM with optimal power allocation.

CHAPTER 8. CONCLUDING REMARKS

8.1 General Conclusion

We proposed several cooperative spatial multiplexing schemes for uplink/downlink transmissions in wireless relay networks. The end-to-end transmission consists of a source, relaying terminals, and destination sink. Depending on the scheme being employed, the data may be decoded (amplify-and-forward, non-regenerative relay) or just amplified (decode-and-forward, regenerative relay) at the relaying terminals before being forwarded to the destination. Core system model, including source, relay, and receiver designs are proposed and analyzed. The design goal, which is to realize MIMO system performance by utilizing only single-antenna wireless terminals, are proven by Monte-Carlo simulation results to have been met.

Using statistical inference, analysis of the systems are conducted in order to derive the theoretical outage probability and bit-error rate expressions. Confirmed and validated for its accuracy with Monte-Carlo simulations, the theoretical derivation conveniently serves as a powerful tool to analyze CSM system's performance without having to run hours, or maybe days, of numerical simulations. For example, although it doesn't solve the ever-challenging relay selection problem directly, the theoretical expressions are able to give an insight on the dynamic behavior of the system at different relay locations instantly. From which, a system designer can design the system to establish connections with relays which serves the transmission needs the best.

Another important performance benchmark is the Shannon capacity, which shows the maximum error-free transmission rate can be achieved by the system. Instead of calculating the instantaneous capacity, which sometimes does not mean a whole lot since the channel is random, we analyze the outage capacity probability of the system. This tool gives a much deeper

insight on the capacity performance of the end-to-end system because it tells us the probability whether the system will or will not support transmission rate over or below a particular threshold. Based on our results, we say that CSM system is, in general, less likely to go into capacity outage compared to SISO system.

Furthermore, with the help of Lagrange multiplier optimization method, optimal power allocation schemes for different CSM systems are also derived and proposed. These power allocation schemes minimize the outage probability such that indirectly, lower bit-error rate can also be achieved, thus maximizing the system performance. In some cases, the solutions to the Lagrange optimization problem need to be solved by lengthy numerical calculations only. In light of this problem, we also proposed a semi-optimal power allocation scheme which is more mathematically feasible to solve. Although the semi-optimal scheme is inferior to the optimal one, it still helps to increase the system performance over the uniform power allocation scheme. Surprisingly, while it increases BER and outage probability performance, we observe that the power scheme actually reduces the outage capacity performance. But overall, this reduction in outage capacity seems to be a reasonable price to pay for a more reliable transmission.

8.2 Real-world Implementation

The fact that the remarkable performance of the CSM systems can be achieved even with the power budget constrained to P , which is the power budget of a SISO system, shows that the current communications systems are far from optimized. Let us take an example with the current standard 3G WCDMA system. We assume that the base station receiver sensitivity is well above the handset specification such that it will have no problem in detecting signal from the users.

If we are to implement CSM based on this system based on 3GPP specs, we need to investigate whether the relay handsets are able to communicate with the source handsets, assuming they are of similar specs. 3GPP specifies a mobile handset reference sensitivity at $-106.7\text{dBm}/3.84\text{MHz}$ in terms of total signal power with a $\text{BER} \leq 0.001$. Furthermore, it specifies that the handset transmit power to be 125mW (21dBm) with antenna gain of 2dB .

With uniform power allocation and two relays, transmit power of one handset goes down to $P/3 = 41.67\text{mW}$ or 16dBm. Assuming Okumura-Hata propagation model, the path loss for source-relay distance of 300m is around 119dB which results in received power of -105dBm at the receiving handset. This is still well within the minimum sensitivity requirement of the 3G receiver (-106.7dBm), hence it is definitely possible to implement CSM in 3G WCDMA system. CSM is also applicable to WLAN environment as a specific ad-hoc networking scheme, or even to sensor networking particularly when higher reliability is needed at times.

Another interesting area to research is the application of the CSM in satellite communications. For earth to orbit, it's been applied since the early days of satellite communications in the form of relaying. The challenge is to analyze whether it can be applied to long-range communications (e.g. Mars Pathfinder, or any other deep space exploration projects). The author thinks that CSM may not be useful in this application because of the enormous distance of deep-space communications causes diversity signals as if they are one signal, i.e. the spatial separation between them becomes negligible, thus the diversity effect is canceled.

Theoretically, CSM sounds amazing. Unfortunately, in real world implementation, a device still needs basic operating power on top of the transmit/receive powers. Since CSM system requires the utilization of $M + N$ multiple wireless terminals (compared to only two devices in SISO), the aggregate operating power requirement alone adds up to $(M + N)/2$ times of SISO system. That plus transmit/receive powers, the overall power requirement may sound unreasonable for system designers, considering that low-power consumption systems are the trend of the century. Hence, the total power requirement of CSM is its weakest feature which, unfortunately, may hinder its deployment in the near future. Several solutions for this issue may include low power modulation schemes, improvements in transceiver design (low-power, wake-up receiver, etc), semiconductor and VLSI evolution, or even just a simple innovation in battery technology. In the worst case scenario, one can opt to apply CSM during low SNR condition only and revert back to SISO mode once SNR is of satisfactory level.

Another big issue will be the scale and complexity of the system; just by the descriptions presented in Chapter 3 and 4, we can already imagine the amount of overhead signaling needed.

That plus the multicast nature of the transmission really adds up to the complexity dimension. Hence, CSM realization is a multi-layer problem and a lot of interesting researches can be done towards solving it in the future.

8.3 Future Works

A lot of improvements can still be made to this dissertation work. Some of which includes:

- Theoretical analysis for general $1 \times M \times N$ uplink and $M \times N \times 1$ systems.
- Theoretical analysis for general M -ary PSK or other similar higher bit modulations.
- Theoretical analysis for practical systems with and without STC.
- Relay selection scheme based on instantaneous link condition.
- Low-power and efficient modulation schemes.

In general, one could build a much accurate theoretical analysis when one does not apply the approximation of (5.3) to the modified Bessel function in the outage probability expressions. The major complexity of the calculation is beyond the scope of this dissertation, thus we leave this challenging problem to the motivated readers as a future homework.

APPENDIX A. ADDITIONAL MATERIALS

A.1 Derivation of Decoding Scheme for Practical Space-time Coded Downlink Amplify-and-Forward Cooperative Spatial Multiplexing

The relays apply amplifying factor and space-time coding to the source-transmitted signal, such that the received signal at the destination at time slots $2K$ and $3K$ is given by:

$$y_{D_{2K}} = g_{D,R_1}\beta_1s_1 + g_{D,R_2}\beta_2s_2 + n_{D_{2K}} \quad (\text{A.1})$$

$$y_{D_{3K}} = -g_{D,R_1}\beta_{1K}\hat{s}_2^* + g_{D,R_2}\beta_{2K}\hat{s}_1^* + n_{D_{3K}} \quad (\text{A.2})$$

where $s_1 = y_{R_1}$, $s_2 = y_{R_2}$, and \hat{s}_1 & \hat{s}_2 is defined in (4.16) & (4.15) respectively. To recover the space-time coded signal, we use the combining scheme:

$$\tilde{s}_1 = g_{D,R_1}^*y_{D_{2K}} + g_{D,R_2}y_{D_{3K}}^* \quad (\text{A.3})$$

$$\tilde{s}_2 = g_{D,R_2}^*y_{D_{2K}} - g_{D,R_1}y_{D_{3K}}^* \quad (\text{A.4})$$

Applying (A.1), (A.2), (4.15), and (4.16) into (A.3) and (A.4), the combining scheme can be further derived into:

$$\begin{aligned} \tilde{s}_1 &= g_{D,R_1}^* [g_{D,R_1}\beta_1s_1 + g_{D,R_2}\beta_2s_2 + n_{D_{2K}}] \\ &\quad + g_{D,R_2} [-g_{D,R_1}^*\beta_{1K}(\beta_2s_2 + N_{R_{12}}) \\ &\quad + g_{D,R_2}^*\beta_{2K}(\beta_1s_1 + N_{R_{21}}) + n_{D_{3K}}] \end{aligned} \quad (\text{A.5})$$

$$\begin{aligned} \tilde{s}_2 &= g_{D,R_2}^* [g_{D,R_1}\beta_1s_1 + g_{D,R_2}\beta_2s_2 + n_{D_{2K}}] \\ &\quad - g_{D,R_1} [-g_{D,R_1}^*\beta_{1K}(\beta_2s_2 + N_{R_{12}}) \\ &\quad + g_{D,R_2}^*\beta_{2K}(\beta_1s_1 + N_{R_{21}}) + n_{D_{3K}}] \end{aligned} \quad (\text{A.6})$$

By simple mathematical derivation and realizing that the cumulative AWGN noises adds up to another AWGN noise with new variance, the expression simplifies nicely into:

$$\tilde{s}_1 = (|g_{D,R_1}|^2 + \beta_{2K}|g_{D,R_2}|^2)\beta_1 s_1 + N_{s_1} \quad (\text{A.7})$$

$$\tilde{s}_2 = (\beta_{1K}|g_{D,R_1}|^2 + |g_{D,R_2}|^2)\beta_2 s_2 + N_{s_2} \quad (\text{A.8})$$

By feeding \tilde{s}_1 and \tilde{s}_2 into the SIC decoder at the destination receiver, the spatial-multiplexed symbols transmitted from the source is recovered as \hat{x}_1 and \hat{x}_2 .

A.2 Theoretical BER Analysis of Uplink Amplify-and-Forward Cooperative Spatial Multiplexing

To solve the integral in the following outage probability expression given in (5.19)

$$F_{AF_1(x)} = \int_0^{\pi/2} F_g^2\left(\frac{x}{\sin^2 \varphi}\right) f_\varphi(\varphi) d\varphi \quad (\text{A.9})$$

we used [33, eq.B4] to transform (A.9) into

$$F_{AF_1(x)} = \int_0^1 F_g^2\left(\frac{x}{t}\right) dt = \int_1^\infty \frac{F_g^2(xt)}{t^2} dt \quad (\text{A.10})$$

By substituting the Bessel function approximation of (5.3) into (5.17) and rewriting (A.10), we get

$$F_{AF_1(x)} = \int_1^\infty \frac{1 - 2e^{-\mathcal{N}xt/2} + e^{-\mathcal{N}xt}}{t^2} dt \quad (\text{A.11})$$

where $\mathcal{N} = \beta_1 + \beta_2$. Then we use the definition of the integral exponential function definition in [37]

$$E_k(x) = \int_1^\infty \frac{e^{-xt}}{t^k} dt \quad (\text{A.12})$$

and the recursive rule

$$E_k(x) = \frac{1}{k-1} (e^{-x} - xE_{k-1}(x)), \quad k = 1, 2, 3, \dots \quad (\text{A.13})$$

to get to

$$\begin{aligned} F_{AF_1(x)} &= 1 - 2E_2\left(\frac{\mathcal{N}x}{2}\right) + E_2(\mathcal{N}x) \\ &= 1 - 2\left(e^{-\frac{\mathcal{N}x}{2}} - \frac{\mathcal{N}x}{2}E_1\left(\frac{\mathcal{N}x}{2}\right)\right) + (e^{-\mathcal{N}x} - \mathcal{N}xE_1(\mathcal{N}x)) \end{aligned} \quad (\text{A.14})$$

where $\mathcal{N} = \beta_1 + \beta_2$. Finally, we use [37, eq.6.5.15]

$$\Gamma(0, x) = E_1(x) \quad (\text{A.15})$$

and some simple algebra to arrive at

$$\begin{aligned} F_{AF_1}(x) &= 1 - 2e^{-\frac{x(\beta_1+\beta_2)}{4a}} + e^{-\frac{x(\beta_1+\beta_2)}{2a}} \\ &\quad + \frac{x(\beta_1+\beta_2)}{2a} \left[\Gamma\left(0, \frac{x(\beta_1+\beta_2)}{4a}\right) - \Gamma\left(0, \frac{x(\beta_1+\beta_2)}{2a}\right) \right] \end{aligned}$$

From here, the expression for BER can be found by solving

$$\begin{aligned} \overline{P_{e,1AF}} &= \int_0^\infty F_{AF_1}(x) \left(\frac{1}{2\sqrt{\pi x}} e^{-x} \right) dx \\ &= \int_0^\infty \left(1 - 2e^{-\frac{x(\beta_1+\beta_2)}{4a}} + e^{-\frac{x(\beta_1+\beta_2)}{2a}} \right. \\ &\quad \left. + \frac{x(\beta_1+\beta_2)}{2a} \left[\Gamma\left(0, \frac{x(\beta_1+\beta_2)}{4a}\right) - \Gamma\left(0, \frac{x(\beta_1+\beta_2)}{2a}\right) \right] \right) \left(\frac{1}{2\sqrt{\pi x}} e^{-x} \right) dx \end{aligned} \quad (\text{A.16})$$

The parts which contain the integration of incomplete Gamma functions can be solved by using [39, eq.6.455.1]

$$\begin{aligned} \int_0^\infty x^{\mu-1} e^{-\beta x} \Gamma(\nu, \alpha x) dx &= \frac{\alpha^\nu \Gamma(\mu + \nu)}{\mu(\alpha + \beta)^{\mu+\nu}} {}_2\mathcal{F}_1\left(1, \mu + \nu; \mu + 1; \frac{\beta}{\alpha + \beta}\right) \\ &\quad \text{Re}(\alpha + \beta) > 0 \quad \text{Re} \mu > 0 \quad \text{Re}(\mu + \nu) > 0 \end{aligned} \quad (\text{A.17})$$

where ${}_2\mathcal{F}_1(\cdot)$ is the Gauss hypergeometric function defined in [37, Ch.15]. Finally, with simple calculus and algebraic derivations, we arrive at the expression for first detection step BER of uplink AF system given in (5.51)

$$\begin{aligned} \overline{P_{e,1AF}} &= \frac{1}{2} - \sqrt{\frac{2}{\mathcal{O}_{\bar{\gamma}} + 2}} + \frac{1}{2} \sqrt{\frac{1}{\mathcal{O}_{\bar{\gamma}} + 1}} \\ &\quad + \frac{\Gamma(\frac{3}{2})}{3\sqrt{\pi}} \frac{\mathcal{O}_{\bar{\gamma}}}{(\mathcal{O}_{\bar{\gamma}} + 1)\sqrt{\mathcal{O}_{\bar{\gamma}} + 1}} \left[{}_2\mathcal{F}_1\left(1, \frac{3}{2}; \frac{5}{2}; \frac{2}{\mathcal{O}_{\bar{\gamma}} + 2}\right) - {}_2\mathcal{F}_1\left(1, \frac{3}{2}; \frac{5}{2}; \frac{1}{\mathcal{O}_{\bar{\gamma}} + 1}\right) \right] \end{aligned} \quad (\text{A.18})$$

Similarly, for the second detection step BER, we start with

$$\overline{P_{e,2AF}} = \int_0^\infty F_{AF_2}(x) \left(\frac{1}{2\sqrt{\pi x}} e^{-x} \right) dx$$

$$= \int_0^\infty \left(1 - \frac{x^2}{4a^2} \beta_1 \beta_2 e^{-\frac{x(\beta_1 + \beta_2)}{2a}} K_1^2 \left(\frac{x\sqrt{\beta_1 \beta_2}}{2a} \right) \right) \left(\frac{1}{2\sqrt{\pi x}} e^{-x} \right) dx \quad (\text{A.19})$$

Since the integration of Bessel function squared is not well defined, we use (5.3) to simplify the previous integration into a more mathematically tractable form and solve for

$$\begin{aligned} \overline{P_{e,2AF}} &= \int_0^\infty \left(1 - e^{-\frac{x(\beta_1 + \beta_2)}{2a}} \right) \left(\frac{1}{2\sqrt{\pi x}} e^{-x} \right) dx \\ &= \frac{1}{2} - \frac{1}{2} \sqrt{\frac{1}{2\mathcal{O}_{\bar{\gamma}} + 1}} \end{aligned} \quad (\text{A.20})$$

where

$$\mathcal{O}_{\bar{\gamma}} = \frac{E_s}{2E_r} \left(\frac{\bar{\gamma}'_{R_i,S} + \bar{\gamma}_{D_j,R_i}}{\bar{\gamma}'_{R_i,S} \bar{\gamma}_{D_j,R_i}} \right) \quad (\text{A.21})$$

BER derivation for downlink AF-CSM system follows the same methodology with only slightly different outage probability expressions to be multiplied by the derivative of the Q-function, followed by integration process similar to (A.16) and (A.19).

A.3 Derivation of CDF of the Harmonic Mean of Two Exponential RVs

For the readers convenience, we hereby lay out the proof of Theorem 1 (5.6) as was presented in [34].

Let X_1 and X_2 be two independent exponential RVs with distributions $X_i \sim \mathcal{E}(\beta_i)$, $i = 1, 2$. Now, define a new RV Z as

$$Z = \frac{1}{2} \left(\frac{1}{X_1} + \frac{1}{X_2} \right) \quad (\text{A.22})$$

which is just the reciprocal of the harmonic mean in (5.1). Under independence assumption, the MGF of Z can be written as the product of the MGF of $1/X_1$ and $1/X_2$. Using lemma 2 (5.5), MGF of Z is calculated as

$$\mathcal{M}_Z(s) = 2\sqrt{\beta_1 \beta_2} s K_1(2\sqrt{\beta_1 s}) K_1(2\sqrt{\beta_2 s}) \quad (\text{A.23})$$

. The CDF of $X = \mu_H(X_1, X_2)$ is given by

$$\begin{aligned}
 P_X(x) &= \Pr(X < x) = \Pr\left(\frac{1}{X} > \frac{1}{x}\right) \\
 &= \Pr\left(Z > \frac{1}{x}\right) = 1 - \Pr\left(Z < \frac{1}{x}\right) \\
 &= 1 - P_Z\left(\frac{1}{x}\right)
 \end{aligned} \tag{A.24}$$

where $P_Z(\cdot)$ is the CDF of Z . Applying the differentiation property of Laplace transform

$$P_Z(z) = \mathcal{L}^{-1}\left(\frac{\mathcal{M}_Z(s)}{s}\right) \tag{A.25}$$

where $\mathcal{L}^{-1}(\cdot)$ is the inverse Laplace transform operator. Combining everything into A.24, we get

$$P_X(x) = 1 - \mathcal{L}^{-1}\left(2\sqrt{\beta_1\beta_2}K_1(2\sqrt{\beta_1s})K_1(2\sqrt{\beta_2s})\right) \tag{A.26}$$

which can be evaluated to give (5.6).

BIBLIOGRAPHY

- [1] C.E. Shannon, "A mathematical theory of communication," *Bell Syst. Tech. J.*, vol.27, pp.379-423, 623-656, July-Oct. 1948.
- [2] G.J. Foschini and M.J. Gans, "On limits of wireless communications in a fading environment when using multiple antennas," *Wireless Personal Commun.*, vol. 6, pp.311-335, Mar. 1998.
- [3] M. Dohler, E. Lefranc, and H. Aghvami, "Space-time block codes for virtual antenna arrays," *Personal, Indoor and Mobile Radio Communications, 2002. The 13th IEEE International Symposium on*, pp.414 - 417 vol.1, Sept. 2002
- [4] J.H. Winters, "On the capacity of radio communication systems with diversity in a Rayleigh fading environment," *IEEE J. Select. Areas Commun.*, vol. SAC-5, p.871878, June 1987.
- [5] G.D. Golden, G.J. Foschini, R.A. Valenzuela, and P.W. Wolniansky, "Detection algorithm and initial laboratory results using the V-BLAST spacetime communication architecture," *Electron. Lett.*, vol. 35, no. 1, p.1415, 1999.
- [6] V. Tarokh, N. Seshadri, and A.R. Calderbank, "Space-time codes for high data rate wireless communication: Performance criterion and code construction," *IEEE Trans. Inf. Theory*, vol. 44, no. 2, pp.744-765, Mar. 1998.
- [7] J.N. Laneman and G.W. Wornell, *Cooperative Diversity in Wireless Networks: Algorithms and Architectures*, Ph.D. thesis, Massachusetts Institute of Technology, Cambridge, MA, Aug. 2002.

- [8] T. Hunter and A. Nosratinia, "Performance analysis of coded cooperation diversity," *Proc. of IEEE ICC*, Anchorage. 2003.
- [9] A. Sendonaris, E. Erkip, and B. Aazhang, "User cooperation diversity-Part I," to appear in *IEEE Tr. Communications*.
- [10] P.W. Wolniansky, G.J. Foschini, G.D. Golden, and R.A. Valenzuela, "V-BLAST: An architecture for realizing very high data rates over the rich scattering wireless channel," *Proc. of IEEE ISSSE-98*, Pisa, Italy, Sep. 1998.
- [11] Yijia Fan and J.S. Thompson, "MIMO configurations for relay channels: theory and practice," *IEEE Transactions on Wireless Communications*, to be published, 2007.
- [12] Yijia Fan and J.S. Thompson, "On the outage capacity of MIMO multihop networks," *IEEE GLOBECOM '05*, vol. 4, pp.2204-2208, Nov. 2005
- [13] H. Bolcskei, R.U. Nabar, O. Oyman, and A.J. Paulraj, "Capacity scaling laws in MIMO relay networks," *IEEE Transactions on Wireless Communications*, vol. 5, pp.1433-1444, June 2006
- [14] J.N. Laneman and D.N.C. Tse, "Cooperative diversity in wireless networks: efficient protocols and outage behavior," *IEEE Transactions on Information Theory*, vol. 50, No. 12, pp.3062-3080, Dec. 2004.
- [15] M.O. Hasna and M.-S. Alouini, "Performance analysis of two-hop relayed transmissions over Rayleigh-fading channels," *Proc. Vehicular Technology Conf.*, Birmingham, AL, pp. 1992-1996, 2002.
- [16] E.C. van der Meulen, "Three-terminal communication channels," *Adv. Appl. Prob.*, vol. 3, pp. 120-154, 1971.
- [17] H. Sato, "Information transmission through a channel with relay," *The Aloha System*, University of Hawaii, Honolulu, Tech. Rep. B76-7, Mar. 1976.

- [18] T. Cover and A.A. el Gamal, "Capacity theorems for the relay channel," *IEEE Trans. on Inform. Theory*, vol. IT-25, no. 5, pp. 572-584, Sept. 1979.
- [19] J.G. Proakis, *Digital Communications*, New York: McGraw-Hill, 4th edition, 2001.
- [20] B. Sklar, "Rayleigh fading channels in mobile digital communication systems part I: Characterization," *IEEE Communications Magazine*, July 1997.
- [21] S.M. Alamouti, "A simple transmit diversity techniques for wireless communications," *IEEE JSAC*, pp.1451-1458, 1998.
- [22] B. Sklar, *Digital Communications*, New Jersey: Prentice-Hall, 1st edition, 1988.
- [23] Matthew N.O. Sadiku, *Elements of Electromagnetics*, pp.647, New York:Oxford University Press, 1st edition, 1995.
- [24] G.J. Foschini, G.D. Golden, P.W. Wolniansky, and R.A. Valenzuela, "Simplified processing for wireless communication at high spectral efficiency," *IEEE J. Selec. Areas Commun.-Wireless Commun. Series*, vol.17, pp.1841-1852, 1999.
- [25] S.W. Kim, "Log-Likelihood Ratio based Detection Ordering for the V-BLAST", *IEEE Globecom*, pp.292-296, Dec. 2003.
- [26] B. Sklar, "Rayleigh fading channels in mobile digital communication systems part I: Characterization," *IEEE Communications Magazine*, July 1997.
- [27] S.W. Kim, "Cooperative spatial multiplexing in mobile ad hoc networks," *IEEE International Conference on Mobile Ad Hoc and Sensor System(MASS)*, Washington D.C., Nov. 2005.
- [28] A. Darmawan, "Cooperative spatial multiplexing system," *M.S. Thesis, Iowa State University*, Ames, IA, 2004.
- [29] A. Darmawan, S.W. Kim, and H. Morikawa, "LLR-based ordering in amplify-and-forward cooperative spatial multiplexing system," *IEEE WCNC 2007*, Hong Kong, Mar. 2007.

- [30] A. Darmawan, S.W. Kim, and H. Morikawa, "Amplify-and-forward scheme in cooperative spatial multiplexing," *IST Mobile Summit 2007*, Budapest, July 2007.
- [31] M.D. Springer, *The Algebra of Random Variables*, New York:Wiley, 1979.
- [32] A. Papoulis and S.U. Pillai, *Probability, Random Variables and Stochastic Processes*, 4th ed, New York:McGraw-Hill, 2002.
- [33] S. Loyka and F. Gagon, "Performance analysis of the V-BLAST algorithm: an analytical approach," *IEEE Transactions on Wireless Communications*, vol. 3, pp.1326-1337, July 2004.
- [34] M.O. Hasna and M.S. Alouini, "End-to-end performance of transmission systems with relays over Rayleigh-fading channels," *IEEE Transactions on Wireless Communications*, vol. 2, No.6, pp.1126-1131, Nov. 2003.
- [35] A. Ribeiro, X. Cai, and G.B. Giannakis, "Symbol error probabilities for general cooperative links," *IEEE Transactions on Wireless Communications*, vol. 4, no. 3, pp.1264-1273, May 2005.
- [36] C.B. Papadias and G.J. Foschini, "On the capacity of certain space-time coding schemes," *EURASIP Journal on App. Signal Proc.*, vol.5, pp.447-458, 2002.
- [37] M. Abramowitz and I.A. Stegun, *Handbook of Mathematical Functions With Formulas, Graphs, and Mathematical Tables*, 9th ed. New York: Dover, 1970.
- [38] J.G. Proakis, "Digital Communications," Boston, MA: McGraw Hill, 4th edition, 2001.
- [39] I.S. Gradshteyn and I.M. Ryzhik, *Table of Integrals, Series, and Products*, San Diego, CA: Academic Press, 7th edition, 2007.

ACKNOWLEDGEMENTS

This is it. I am alive. This is the pinnacle of my 27 years being a scholar since pre-school years. When people ask me what it feels like graduating from a doctoral study, I always answer: nothing and darkness. I feel *nothing* because, theoretically, this is the third time I graduate from college. *Darkness*, from now on I will really be sailing in uncharted water. It was a long fight to reach this point and it would have been impossible for me to do it alone.

First and foremost, I would like to thank God for making me who I am and giving me a wonderful and supportive family, while always guiding my steps during this journey called life. The next gratitude goes to my advisor, Dr. Hiroyuki Morikawa who opened the door to The University of Tokyo for me, and provided me with all resources needed to proceed with my research. Special thanks to Dr. Sang Wu Kim, my advisor during my master's study in Iowa State University, for introducing me with the concept of cooperative communications, which turned out to be a problem worth a Ph.D. dissertation.

Millions of thanks to my friends all around the world who supported me during the time when I needed help the most. When I was banging my head against the wall, they kept reminding me to take a break and enjoy life a bit (or two). Their moral support was one of the biggest factor I can still write this part of the dissertation. Like people say, friends are your treasures in life, and not until this point of time do I finally understand the meaning of those words. So, Mario, Yulita, Jeff, Andrew, Ok, Mikko, Foo, John, Pedro, Ronald, Denis, Ferdi, Esther, Kaoru, Kida, Takako, and others not mentioned here, my sincere gratitude for your friendships. I wish there will be a point in life where I can repay you all.

If someone ask me whether this doctoral study is worth four-and-a-half years of my life, even considering the opportunity costs I had foregone (like getting married, making six-figure

pay already somewhere, or live happily ever after, etc.), I would say “**YES**” in a heartbeat. I have to say that it is not a fight for everyone (many gave up along the way), but it is a *Mission:Possible*, given that you are physically and mentally ready to face academic and mortal problems which seem to be unsolvable (in the beginning). There will be times when your humanity (or sanity) are tested to the limits. You can consider it as if you are tempted to join *The Darkside*.

So what’s the glory in all this? Well, besides being able to scare off people when you hand them your name card, being in academic means that you are in full control of your time. This gives you the chance to reflect upon yourself and life in general, assess your own ability, gain deeper knowledge in the field, and most of all, wisdom. The process itself is one which lets your quantitative and qualitative analysis skills grow as you face tougher problems. Generally, I feel that doctoral course is more of a race against yourself, instead of competing with the people in your field; you try to challenge your own limit and you will grow as far as you let yourself to.

With glory, there always comes responsibility. Getting the degree is just the easy part. What comes next is the challenge to profess all the skills you gain and defend that you are actually worth to bear the degree. Whether you are *the* Ph.D. or *just another* Ph.D., it’s all up to yourself. Moreover, *where* and *how* would you use the skills, are other questions which will eventually appear. I advise the reader who are still pursuing his/her degree to really consider about and address these questions as early as possible.

Finally, I would like to close this dissertation with a very wise Japanese proverb: “*Once in a lifetime, you have to climb Mt. Fuji, but you are a fool if you do it twice*”. The same analogy is valid for doctoral study.